

CHARACTERIZATION AND THERAPEUTIC TARGETING OF CD133 IN HUMAN  
GLIOBLASTOMA

M.Sc. Thesis – S.K. Salim; McMaster University – Biochemistry & Biomedical Sciences

CHARACTERIZATION AND THERAPEUTIC TARGETING OF CD133 IN HUMAN  
GLIOBLASTOMA

By SABRA KHALID SALIM, HON. B.Sc.

A Thesis Submitted to the School of Graduate Studies in Partial Fulfilment of the  
Requirements for the Degree Master of Science

McMaster University © Copyright by Sabra Khalid Salim, July 2021

**DESCRIPTIVE NOTE**

MASTER OF SCIENCE (2021)

Biochemistry & Biomedical Sciences

McMaster University

Hamilton, Ontario

TITLE: Characterization and therapeutic targeting of CD133 in human glioblastoma

AUTHOR: Sabra Khalid Salim, Hon. B.Sc. (McMaster University)

SUPERVISOR: Dr. Sheila K. Singh

NUMBER OF PAGES: 128

## **LAY ABSTRACT**

Glioblastoma (GBM) is one of the most common malignant brain tumors in adults. Despite an aggressive therapy regimen, almost all patients relapse 7-9 months post-diagnosis. Therapy failure and poor patient outcome may be attributed to a small population of cells known as glioblastoma stem cells, or GSCs, that are able to escape therapy and seed disease recurrence. GSCs are most notably identified by the cell surface protein CD133, which has previously been shown to associate with pro-tumor properties including treatment resistance, tumor growth, maintenance, progression and metastasis. While expression of CD133 in cancer has been heavily characterized, little is currently known about its function. One such avenue to understand its mechanism of action in cancer, and more particularly GBM, is to define its interactions with other proteins. Protein-protein interactions play a pivotal part as the backbone of signalling pathways that drive tumor development and growth. Therefore, defining and mapping the CD133 interaction network may help us understand how this protein governs regulation of GSCs, and ultimately, GBM progression.

While the biology of CD133 has yet to be elucidated, targeting CD133 on GSCs has presented a promising therapeutic strategy for patients with GBM. Previously in the Singh Lab, we developed an engineered T-cell therapy, known as a CAR-T, that can recognize CD133 to induce tumor cell death. While this showed success in our animal models of human GBM, other considerations must be addressed on its path to clinical development. As of current, CAR-T therapies are generated from T-cells taken from cancer patients. This hosts a myriad of concerns including the quality of patient T-cells,

the time and cost to manufacture, and its availability for patients with rapidly progressing disease. To circumvent this issue, donor-derived CAR-T cells can be genetically engineered for safe usage in GBM patients as a readily available, “off-the-shelf” therapy.

To define the function of CD133, we have attempted to use a technique known as BioID, which tags the protein of interest with a smaller biotin ligase. This biotin ligase can subsequently tag proteins that come within the vicinity of CD133, that may later be identified by sequencing as potential interactors. As current use of BioID may not reliably mimic the interaction of CD133, we sought to genetically engineer human GBM lines with the BioID protein to more closely resemble tumor-relevant behaviours of CD133. To develop a donor-derived CAR-T therapy, we similarly used genetic engineering of T-cells to ensure specific targeting of tumor cells with CD133, while sparing healthy tissues. By using CD133 as a centralizing concept in this thesis, we ultimately hope to develop our biological understanding of CD133, while testing the therapeutic development of a donor-derived CAR-T therapy.

## **ABSTRACT**

CD133, a pentaspan glycoprotein, has long been known to represent aggressive, stem-like populations across various human malignancies. While its expression correlates with numerous clinical outcomes including disease progression, metastasis, recurrence, and poor overall survival in numerous cancers, little is currently known about its function. In the brain cancer glioblastoma (GBM), CD133-expressing cells have previously been shown to initiate tumours, evade therapy and interestingly, self-renew, a key property of cancer stem cells. With an implied signalling role in driving self-renewal, we aim to elucidate the role of CD133 in glioblastoma. To understand the role of CD133, we aim to study its protein-protein interactions using the proximity-dependent labelling technique known as miniTurboID. By tagging proteins of interest with a promiscuous biotin ligase at both protein termini, potential interactors can be biotinylated and identified by subsequent mass spectrometry. While miniTurboID has traditionally been performed by synthetic transgenes expressing the tagged proteins of interest in commercial cell lines, overexpression may not recapitulate its native function. Thus, using CRISPR technology, we aim to insert the miniTurboID ligase at both the N- and C-terminus of CD133 in patient-derived human GBM lines.

Although little is currently known about CD133 function, development of targeted therapies has presented a promising strategy in pre-clinical studies. In the Singh Lab, we previously developed a chimeric antigen receptor T-cell, or CAR-T, comprised of a T-cell expressing a synthetic receptor capable of recognizing a tumor-associated antigen and activating cytolytic-killing directed towards the target cell. Currently, CAR-T therapies

are autologous, or patient-derived, in nature which may host a myriad of concerns including patient-specific qualitative and quantitative T-cell dysfunction, inconsistent generation of CAR products, and availability to rapidly progressing patients. To circumvent this concern, “off-the-shelf”, donor-derived or allogeneic CAR-T products may be generated for use in GBM patients. However, in addition to CAR integration, allogeneic products must be additionally modified to eradicate expression of the endogenous TCR, as this would induce a phenomenon known as graft versus host disease, in which healthy tissues are targeted.

Thus, in this thesis, we show gene editing potential in human GBMs to perform an endogenous genomic knock-in of miniTurboID. With the identification of interacting proteins, defining the subsequent functionality of CD133 may elucidate oncogenic cellular programs, and highlight common nodes of interaction within divergent cell signaling pathways. To develop an allogeneic CAR-T product, we designed a two-step approach in which the CAR sequence was integrated into the TCR gene for simultaneous knock-out. We later show early pre-clinical efficacy in comparison to traditional autologous CAR-T in our patient-derived models of human GBM. Thus, by using CD133 as a centralizing concept in this thesis, we ultimately hope to develop our biological understanding of CD133, while testing the therapeutic development of a donor-derived CAR-T therapy.

## ACKNOWLEDGEMENTS

إِنَّ اللَّهَ مَعَ الصَّابِرِينَ ط يَا أَيُّهَا الَّذِينَ آمَنُوا اسْتَعِينُوا بِالصَّبْرِ وَالصَّلَاةِ

“Believers, seek help in patience and prayer, Allah is with those who are patient” (2:153).

Religion has been a guiding principle for me in my life. Oftentimes, I find myself coming back to this verse as a reminder that all hardships, whether personal or academic, should be approached with patience, perseverance, and tenacity. It has also reminded and humbled me to trust in something greater. With that, I owe where I am today to the Almighty for my trials and tribulations, but even more so for the innumerable blessings I have been provided.

First and foremost, I would like to sincerely thank Dr. Sheila Singh. Almost four years ago as an undergraduate student, Dr. Singh gave me the opportunity of a lifetime to join her team of innovative scientists to study brain cancer. While this has been an incredible learning experience for me scientifically, it is the support, guidance, and mentorship you consistently provided me that I will never forget. You are a powerhouse; an exceptional scientist, clinician, mother and friend to so many. I am in awe of all that you do and am reminded of how those around you cherish you. I am thankful and indebted to you for all that you have done for me in my career as a budding scientist. No words will ever describe how grateful I am, but I hope that I may one day show you how profound your impact has been on me.

I would also like to thank two of my biggest scientific mentors, Dr. Chitra Venugopal and Dr. Parvez Vora. I have few words that could adequately describe how thankful I am to both of you. I have made many mistakes along the way (of which I can name), but the two of you have shown me nothing but patience and kindness. Chitra, you have been my biggest support and friend. There is nothing that I cannot come to you with. Even when you are at your busiest, you always make time for me. For that, I cannot thank you enough. To Parvez, I owe all my technical skills. While I describe your mentorship style as “frightening”, I would not be able to accomplish this thesis without your support and patience. Thank you for always being a phone call away, and for putting all my hardships into perspective and reminding me of my foundations. I am grateful to have found friendship in you both.

To past and present Singh Lab members, I am eternally grateful for the support, scientific mentorship and friendship. I am lucky to call you all my friends and will always cherish the memories we have made. I will never forget the blood (literally), sweat, tears, and laughs we shared, and I hope that we can cross paths in the future to make more.

To my committee members, Dr. Jonathan Bramson and Dr. Yu Lu, thank you for all your scientific guidance and support throughout my thesis. I am grateful for both your

invaluable advice, suggestions and insights into the cumulation of this work. Without your scientific guidance, these works would not be where they are today. I would also like to thank our collaborators Dr. Jason Moffat, Jeffrey Wei, Dr. Vassil Dimitrov, Dr. Katie Chen, and the folks at Century for their contributions to this work. From molecular designing to troubleshooting, I am indebted to them for their guidance, time and efforts. In addition, I would like to thank my funding agencies MITACS and CIHR for the invaluable financial support provided to me. Of most significance is the Brain Tumor Foundation of Canada (BTFC) which has provided me with support since my undergraduate career. Not only has the BTFC assisted young scientists like myself in establishing scientific careers in brain cancer, the BTFC is an essential service, hub and support group to physicians, allies and brain cancer patients alike. From the BTFC, I would like to particularly thank Susan Ruypers who has provided me with so many opportunities to engage and learn from other scientists, and patients living with brain cancer. Patients are the backbone of this research, and thus I am eternally grateful to them and the BTFC and will continue in the fight against these diseases.

Finally, I would like to thank my wonderful family. To my baba, mama, nana, Sabrin, Tariq, Ezza and friends, I would not be here without their love and guidance. I am indebted to them for their patience with me, picking me up from the lab late at night, supporting me during the tough times, and reminding me to keep moving forward. In particular, to my baba and mama -you have both sacrificed so much for me and Sabrin to be where we are today. If I tried to count your favours, I would spend an eternity trying. I love you both with every fibre of my being and I hope to spend the rest of my life showing you how grateful and lucky I am to be your daughter. I hope that I make you proud.

I would like to dedicate this thesis to my family, and to the patients who have selflessly supported and donated their specimens to our research. In particular, I would like to thank Cindy Graham and her family. I wish that we could have crossed paths on more positive times, but I am grateful to have met you. Few people can show the strength and bravery that I witnessed in Cindy, during the short time that I have known the Graham family. Research and its hardships can often feel futile, but it is you who has inspired me to keep moving forward and fighting GBM to one day find a cure. It has been my greatest honour to have known you.

## LIST OF FIGURES AND TABLES

### CHAPTER 2 Figures

**Figure 1:** Human GBMs display differential localization of CD133

**Figure 2:** CRISPR-mediated genomic targeting of CD133 in human GBMs by electroporation of ribonucleoprotein (RNP) complexes

**Figure 3:** Next-generation sequencing amplicons, and adeno-associated viral infection generate knock-in of BioID at CD133 loci

Supplementary Figure 1

### CHAPTER 3 Figures

**Figure 4:** Editing in primary T-cells reveals efficient TCR knockout by RNP electroporation.

**Figure 5:** CART133 knock-in successfully generated alloCART133 and requires TCR<sup>+</sup> cell depletion.

**Figure 6:** AlloCART133 shows anti-tumor efficacy *in vitro* and *in vivo* in patient-derived GBM xenografts.

Supplementary Figure 2

Supplementary Figure 3

Supplementary Figure 4

## LIST OF SYMBOLS AND ABBREVIATIONS

CNS	Central Nervous System
CT	Computed Tomography
GBM	Glioblastoma
MRI	Magnetic Resonance Imaging
IDH	Isocitrate Dehydrogenase
PFS	Progression-free survival
OS	Overall Survival
SoC	Standard of Care
CAR	Chimeric Antigen Receptor
HLA	Human leukocyte antigen
RNP	Ribonucleoprotein
CRISPR	Clustered Regularly Interspaced Palindromic Repeats
mAb	Monoclonal antibody
scFv	Single chain variable fragment
EGFR	Epidermal growth factor receptor
CSF	Cerebrospinal fluid
ctDNA	Circulating tumor DNA
ITH	Intratumoral heterogeneity
GSC	Glioblastoma stem cells
CSC	Cancer stem cell
BTIC	Brain tumor initiating cell
TAM	Tumor-associated macrophages
TIL	Tumor-infiltrating lymphocytes
MDSC	Myeloid-derived suppressor cells
IFN	Interferon
TNF	Tumor necrosis factor
IL	Interleukin
RTK	Receptor tyrosine kinase
TME	Tumor microenvironment
PD-1	Programmed cell death 1
NK	Natural Killer
CD133	Cluster of differentiation 133
AML	Acute myeloid leukemia
Wnt	Wingless-related integration site
rGBM	Recurrent glioblastoma
pGBM	Primary glioblastoma
ICI	Immune checkpoint inhibitory
MHC	Major histocompatibility complex
HSPC	Hematopoietic stem and progenitor cells
TCR	T-cell receptor
KO	Knock-out
KiKo	Knock-in, Knock-out

B2M	Beta-2 Microglobulin
TRAC	T-cell Receptor Alpha Locus
GvHD	Graft-versus-Host Disease
WHO	World Health Organization
Cas	CRISPR-associated protein
AAV	Adeno-associated virus
FACS	Fluorescence activated cell sorting

## **DECLARATION OF ACADEMIC ACHIEVEMENT**

During my graduate studies, I contributed to 7 research papers, 1 book chapter, and presented and chaired at local and international conferences. The work described in this thesis is a result of the combined effort of myself, Dr. Vaseem Shaikh, Dr. Chitra Venugopal, and Dr. Sheila K. Singh. In this thesis, I contributed to the experimental design, execution, interpretation of data, and writing of all sections. Dr. Sheila K. Singh supervised all research projects and aided in data interpretation, alongside Dr. Chitra Venugopal. The T-cell work in this thesis is built off the work performed by Dr. Parvez Vora in the establishment of the first CAR-T against CD133 in human GBM. Guide and HDR design were completed by Dr. Jason Moffat, Jeffrey Wei and Dr. Vassil Dimitrov of the Moffat lab. CAR sequence was designed by Dr. Parvez Vora and the Century team. *In vivo* and *in vitro* treatment was performed with the help of Dr. Vaseem Shaikh.

,

## **TABLE OF CONTENTS**

<b>DESCRIPTIVE NOTE</b>	<b>4</b>
<b>LAY ABSTRACT</b>	<b>5</b>
<b>ABSTRACT</b>	<b>7</b>
<b>ACKNOWLEDGEMENTS</b>	<b>9</b>
<b>LIST OF FIGURES AND TABLES</b>	<b>11</b>
<b>LIST OF SYMBOLS AND ABBREVIATIONS</b>	<b>12</b>
<b>DECLARATION OF ACADEMIC ACHIEVEMENT</b>	<b>14</b>
<b>1.1 Glioblastoma</b>	<b>18</b>
1.1.1 Epidemiology	18
1.1.2 Clinical and Histopathological Features	18
1.1.3 Molecular Classification and Diagnosis	19
1.1.4 Treatment and Prognosis	20
<b>1.2 Molecular Characterization of GBM</b>	<b>23</b>
1.2.1 Genomic and Mutational Profile	23
1.2.2 The DNA Methylome and Epigenomic Regulation	25
1.2.3 Transcriptomic Landscape and Subgrouping	26
<b>1.3 Intratumoral heterogeneity (ITH)</b>	<b>28</b>
1.3.1 Spatiotemporal Heterogeneity	29
1.3.2 Functional Heterogeneity	33
1.3.3 The Tumor Microenvironment	35
<b>1.4 Cancer Stem Cells</b>	<b>37</b>
1.4.1 GSC Markers	39
1.4.2 CD133 in therapy resistance	41
1.5.1 Biochemical Properties of CD133	42
1.5.2 CD133-regulated signalling pathways	43
<b>1.6 Targeted and Immunotherapeutic Approaches</b>	<b>47</b>
1.6.1 Monoclonal Antibodies (mAbs)	47
1.6.2 Chimeric Antigen Receptor T-cells (CAR-Ts)	49
<b>1.7 Challenges to Immunotherapy</b>	<b>51</b>
1.7.1 Target Heterogeneity and CAR design	51
1.7.2 Mode of CAR-T delivery	53
1.7.3 Extrinsic and Intrinsic T-cell Deficits in GBM	54
1.7.4 Allogeneic CAR-T Therapy	55

<b>1.8</b>	<b>Statement of Intent</b>	<b>58</b>
<b>CHAPTER 2: ELUCIDATING THE CD133 PROTEIN-PROTEIN INTERACTOME BY ENDOGENOUS GENOMIC KNOCK-IN OF BIOID</b>		<b>59</b>
<b>2.1</b>	<b>Protein-protein interactions and proximity-dependent labelling</b>	<b>59</b>
<b>2.2</b>	<b>Transgenic and endogenous assessment</b>	<b>60</b>
<b>2.3</b>	<b>Materials and Methods</b>	<b>61</b>
2.3.1	Dissociation and culturing of Primary GBM tissue	61
2.3.2	Propagation of Brain Tumor Stem Cells (BTSCs)	62
2.3.3	Fluorescence Activated Cell Sorting (FACS) and Analysis	62
2.3.4	Western Immunoblotting	62
2.3.5	Immunofluorescence	63
2.3.6	Subcellular Fractionation	63
2.3.7	Nested PCR and preparation for Next-generation sequencing	64
2.3.8	AAV Generation, Purification and Quantification	64
2.3.9	Electroporation and infection of human GBMs	65
<b>2.4</b>	<b>Results</b>	<b>66</b>
2.4.1	CD133 is differentially localized and expressed in human GBMs	66
2.4.2	Genomic editing of primary cells by dual modification	67
2.4.3	Genomic cleavage and repair template design	68
2.4.4	Electroporation of RNP targeting terminal ends of PROM1	70
2.4.5	AAV infection of human GBMs	71
2.4.6	Short-term next steps	72
<b>FIGURE 1. HUMAN GBMS DISPLAY DIFFERENTIAL LOCALIZATION OF CD133.</b>		<b>73</b>
<b>FIGURE 2. CRISPR-MEDIATED GENOMIC TARGETING OF CD133 IN HUMAN GBMS BY ELECTROPORATION OF RIBONUCLEOPROTEIN (RNP) COMPLEXES.</b>		<b>74</b>
<b>FIGURE 3. NEXT-GENERATION SEQUENCING AMPLICONS, AND ADENO-ASSOCIATED VIRAL INFECTION GENERATE KNOCK-IN OF BIOID AT CD133 LOCI.</b>		<b>75</b>
<b>SUPPLEMENTARY FIGURE 1.</b>		<b>77</b>
<b>TABLES</b>		<b>77</b>
<b>CHAPTER 3: GENERATION AND VALIDATION OF ALLOGENEIC CAR-T THERAPY AGAINST CD133</b>		<b>78</b>
<b>3.1.</b>	<b>Materials and Methods</b>	<b>78</b>
3.1.1.	T-cell Expansion	78
		16

3.1.2.	Generation of lentiviral-transduced “autologous” CAR-Ts	78
3.1.3.	Generation of allogeneic CART133	78
3.1.4	Activation/Exhaustion and Cytokine Release Assays	79
3.1.4.	Luciferase-Based Cytotoxicity Assay	79
3.1.5.	In vivo Orthotopic Injections and H&E Staining of Xenograft Tumors	80
3.1.6.	Statistical Analysis	80
<b>3.2.</b>	<b>Results</b>	<b>81</b>
3.2.3.	KiKo design for the generation of alloCART133	81
3.2.1	Efficient knock-out of TCR by RNP electroporation	82
3.2.2	CAR Integration by AAV Infection and TCR <sup>+</sup> Cell Depletion	83
3.2.3	Generation of an alloCART133 expansion protocol	85
3.2.4	In vitro treatment of alloCART133 shows comparable efficacy to CART133	88
3.2.5	In vivo treatment of alloCART133 shows moderate tumor control	89
3.2.6	Short-term next steps	90
<b>FIGURE 4. EDITING IN PRIMARY T-CELLS REVEALS EFFICIENT TCR KNOCKOUT BY RNP ELECTROPORATION.</b>		<b>92</b>
<b>FIGURE 5: CART133 KNOCK-IN SUCCESSFULLY GENERATED ALLOCART133 AND REQUIRES TCR<sup>+</sup> CELL DEPLETION.</b>		<b>93</b>
<b>FIGURE 6: ALLOCART133 SHOWS ANTI-TUMOR EFFICACY IN VITRO AND IN VIVO IN PATIENT-DERIVED GBM XENOGRAFTS.</b>		<b>95</b>
<b>SUPPLEMENTARY FIGURE 2.</b>		<b>97</b>
<b>SUPPLEMENTARY FIGURE 3.</b>		<b>98</b>
<b>SUPPLEMENTARY FIGURE 4.</b>		<b>99</b>
<b>CHAPTER 4: CONCLUSIONS AND FUTURE DIRECTIONS</b>		<b>100</b>
<b>4.1</b>	<b>Discussion</b>	<b>100</b>
4.1.1	Endogenous genomic knock-in of BioID	101
4.1.2	Generation of alloCART133 shows early pre-clinical efficacy	103
<b>4.2</b>	<b>Future Directions</b>	<b>104</b>
<b>REFERENCES</b>		<b>107</b>
<b>APPENDIX: ACADEMIC ACHIEVEMENTS</b>		<b>127</b>

## **CHAPTER 1: Introduction**

### **1.1 Glioblastoma**

#### *1.1.1 Epidemiology*

Glioblastoma (GBM) is the most common primary malignant brain tumour in adults, accounting for 14.5% of all brain and CNS neoplasms, and 57.7% of all gliomas (Ostrom et al., 2020). In Canada, GBMs affect 4.50 per 100,000 persons annually, with increasing incidence over the past thirty years. GBMs are primarily diagnosed in older males, with a median age of 65, reaching peak incidence of 15.30 persons per 100,000 between 75-84 years (Ostrom et al., 2020).

#### *1.1.2 Clinical and Histopathological Features*

As a tumor often found in the cerebrum, patients with GBM often present with focal neurological deficits including motor weakness, seizures, speech difficulties and headaches depending on tumor localization (Sanli, Turkoglu, Dolgun, & Sekerci, 2010). Upon symptom presentation, patients undergo radiological imaging by computed tomography (CT) or magnetic resonance imaging (MRI) (Alexander & Cloughesy, 2017). Typical CT imaging features of GBMs reveal a heterogeneous and infiltrative disease with irregular-enhancing margins, a hypodense center representing necrosis, and peritumoral, vasogenic-type edema (Abd-Elghany et al., 2019; Rees, Smirniotopoulos, Jones, & Wong, 1996). Most GBMs present as focal disease, however, 2-20% of patients present with multifocal, satellite areas of enhancement and regional necrosis (Alexander & Cloughesy, 2017; Hassaneen et al., 2011; Patil et al., 2012). While differential imaging features may provide insight into prognostic and/or molecular features, diagnosis of GBM

is primarily confirmed by histological and molecular analysis of resected or biopsied tissue (David N. Louis et al., 2016; Wangaryattawanich et al., 2015). The World Health Organization (WHO) classifies gliomas into four grades based on histological features of nuclear atypia, microvascular proliferation, high mitotic activity and necrosis (Aldape, Zadeh, Mansouri, Reifenberger, & von Deimling, 2015; D'Alessio, Proietti, Sica, & Scicchitano, 2019; D. N. Louis et al., 2007). While several histomorphological patterns exist, all GBMs meet these histological criteria and are thus characterized as WHO Grade IV tumors (Gupta & Dwivedi, 2017). Although the WHO classification scheme has proven reliable, histological heterogeneity of tumors and the lack of association with tumor aggressiveness, treatment response and progression-free survival (PFS) presents a diagnostic challenge. However, molecular and cytogenetic information in concert with histological assessment has reproducibly assisted in the classification and diagnosis of diffuse gliomas such as GBM (Vigneswaran, Neill, & Hadjipanayis, 2015).

### *1.1.3 Molecular Classification and Diagnosis*

Molecular classification of GBM has been defined by the detection of chromosomal aberrations (1p/19q co-deletions) and isocitrate dehydrogenase (IDH) 1 or 2 mutational statuses. Although GBMs are characterized by the absence of 1p/19q translocation events, previously, IDH-mutational status was used to further stratify GBM into one of two subtypes; primary or *de novo* GBM, or secondary GBM (Vigneswaran et al., 2015; H. Yan et al., 2009). Accounting for 90% of all GBMs, primary GBMs developed rapidly without previous evidence of malignant neoplastic disease, while secondary GBMs progressed from lower grade gliomas (Ohgaki & Kleihues, 2013). Although histologically

indistinguishable, primary and secondary GBMs differ in biological, phenotypic, and clinical properties as a result of differential IDH mutational status, of which primary GBM is IDH-wildtype (Ohgaki & Kleihues, 2013). However, as of the new 2021 WHO classification schema, GBM diagnosis is limited only to IDH-wildtype specimens, with secondary GBMs now simply characterized as IDH-mutant Grade IV astrocytomas (D. N. Louis et al., 2021).

#### *1.1.4 Treatment and Prognosis*

Historically, GBM was treated by maximally safe surgical resection, followed by adjuvant radiotherapy. Cytoreductive surgery has remained as a first line therapy to reduce mass effect and enhance overall survival for the treatment of GBM. Extent of resection (EOR) has previously been demonstrated to independently predict survival (Sanai, Polley, McDermott, Parsa, & Berger, 2011). Following surgical management, radiation has been the most important adjuvant treatment modality in extending survival in patients (Hau et al., 2016). To increase survival benefit, the addition of various chemotherapeutic agents to the standard therapy had later been investigated. Since the early 1980s, assessment of combination treatment with various chemotherapeutic agents including carmustine, cisplatin and procarbazine yielded little success (Chang et al., 1983; Green et al., 1983; Grossman et al., 2003; Shapiro et al., 1989; Stupp et al., 2005). However, in 2002, a phase II trial demonstrated that concomitant use of temozolomide, a novel oral alkylating agent, with radiotherapy was safe, efficacious and well tolerated for primary GBM (Stupp et al., 2002). These results prompted the assessment of a randomized phase III trial comparing the efficacy of radiotherapy alone versus

concomitant radiotherapy and TMZ. Unlike previous chemotherapeutic agents, concomitant TMZ significantly increased median overall survival (OS) by 2.5 months, and two-year survival by 16.1%, thus redefining the SoC for patients with GBM (Stupp et al., 2005). This new multimodal regimen would thus consist of surgical resection, 60 grays (Gys) of fractionated focal irradiation (2 Gy daily for five days per week over a six-week period) with 75 mg/m<sup>2</sup> of oral TMZ daily, followed by six maintenance cycles of oral TMZ (150-200 mg/m<sup>2</sup> for five days every 28 days) (Stupp et al., 2005). However, despite this aggressive SoC, median OS has remained at 14.6 months. Some advances have been made in surgical procedures and techniques such as the introduction of fluorescence-guided surgery, neuronavigation, functional mapping and intraoperative MRI to minimize morbidity (Young, Jamshidi, Davis, & Sherman, 2015). Other minor advancements include maintenance therapy adjuncts such as tumor-treating fields (TTFields), consisting of anti-mitotic, low-intensity, alternating electrical currents which increased OS and PFS in a randomized clinical trial (Stupp et al., 2017). However, since the advent of TMZ, no major treatment advances have drastically improved patient outcome (Fernandes et al., 2017).

#### *1.1.5 Prognostic Markers and Risk Stratification*

Despite little change in patient outcome over the past decade, molecular biomarkers and risk stratification have attempted to improve prognosis by guiding therapeutic intervention and clinical management of disease (Sheng et al., 2020). Biomarkers may also predict therapeutic response and guide personalized approaches. One such marker is O<sup>6</sup>-methylguanine-DNA methyltransferase (*MGMT*), which encodes

for a DNA repair enzyme and is predictive for response to alkylating agent chemotherapy such as TMZ. Treatment with TMZ drives methylation of purine bases of DNA, primarily at O6-guanine sites, creating mispairing of DNA bases. This lesion becomes cytotoxic upon activation of DNA mismatch repair (MMR) by futile base-excisions, leading to apoptosis (J. Zhang, Stevens, & Bradshaw, 2012). However, methyl adducts can be removed by MGMT, generating resistance to TMZ. Expression of MGMT can be marked by profiling of methylation status of its promoter, in which methylation induces transcriptional repression. Thus, methylation of the *MGMT* promoter has presented as a positive prognostic factor for response to TMZ in GBM in numerous studies (median OS, methylated = 21.7 months, unmethylated = 13.8 months) (Hegi et al., 2005). While stratifying GBM patients based on *MGMT* status to receive TMZ shows potential for treatment decision-making, lack of attractive therapeutic alternatives for *MGMT*-unmethylated patients makes this approach less practical for current clinical use (Wick et al., 2014).

In the context of IDH-wildtype GBM, other molecular markers have shown clinical and prognostic significance including amplification of epidermal growth factor receptor (*EGFR*), telomerase reverse transcriptase promoter (*TERT*<sub>p</sub>) methylation, global methylation phenotype, and copy number variation (CNV) (Ceccarelli et al., 2016; Eckel-Passow et al., 2015; Mirchia & Richardson, 2020). However, independent significance remains poor, requiring a thorough understanding of the molecular alterations underlying GBM progression, and the identification of novel, robust biomarkers.

## 1.2 Molecular Characterization of GBM

### 1.2.1 Genomic and Mutational Profile

In assessing the genomic landscape, GBM exhibits DNA copy number alterations (CNA), aberrant gene expression and DNA methylation, as well as pathway dysregulation. Molecular studies from the early 2000s identified important genetic events in the pathogenesis of GBM. In 2004, a population-based study on *de novo* GBM identified the most frequent genetic alterations; loss of heterozygosity (LOH) of 10q (69%), amplification of epidermal growth factor receptor (*EGFR*) (34%), tumor protein 53 (*TP53*) mutations (31%), *p16<sup>INK4a</sup>* homozygous deletion (31%) and phosphatase and tensin homolog (*PTEN*) mutations (24%) (Ohgaki et al., 2004). Later in 2008, The Cancer Genome Atlas conducted a pilot project to comprehensively characterize genomic alterations in human GBM in 206 *de novo* GBM specimens. Mapping of somatic nucleotide substitutions, homozygous deletions and focal amplifications and copy number alterations (CNAs) revealed frequent aberrations in receptor tyrosine kinase (RTK) signalling, and the *TP53* and retinoblastoma tumor suppressor pathways. Analysis of CNA data alone revealed 70%, 66% and 59% of somatic alterations in RB, *TP53* and RTK pathways respectively (Cancer Genome Atlas Research, 2008). Mutational analysis of mitogenic RTK signalling revealed that 86% of GBM samples harboured at least one genetic event in core pathways including Ras and phosphoinositide 3-kinase (PI3K). These included mutations and or amplifications in *ERBB2*, platelet-derived growth factor receptor A (*PDGFRA*), *MET*, neurofibromatosis 1 (*NFI*), phosphatase and tensin

homolog (*PTEN*) and *EGFR*. Genomic alterations in at least 2 of the 4 RTK groups in 11% of specimens additionally indicated co-activation and cooperation of these independent signalling pathways, leading to oncogenic proliferation and survival. Of the 87% of specimens that revealed *TP53* alterations, 14% of deletions or mutations were observed in cyclin-dependent kinase inhibitor 2A (*CDKN2A*), 11% in *MDM2* and 4% in *MDM4*. *CDKN2A* alterations, namely genomic deletions, were also observed in the RB pathway along with *CDKN2B* and cyclin dependent kinase 4 (*CDK4*) (Brennan et al., 2013; Cancer Genome Atlas Research, 2008). However, mutations in the transcriptional corepressor *RBI* were mutually exclusive, suggesting multiple genomic mechanisms to RB signalling and subsequent cell cycle progression. Other independent analyses of the genomic landscape of GBM corroborated the identification of relevant alterations in these three pathways (Brennan et al., 2013; Cancer Genome Atlas Research, 2008; Parsons et al., 2008). Thus, these findings in *de novo* GBM specimens suggested that the three “truncal” pathways were a core requirement for GBM pathogenesis (Cancer Genome Atlas Research, 2008).

Other oncogenic mutations have been reported in GBM, namely chromosomal translocation and structural rearrangement, gene fusions and promoter mutations events. In addition to the identification of LOH of chromosome 10q, gain of chromosome 19/20, gain of chromosome 7 and heterozygous and/or homozygous loss of chromosome 9p are frequently observed and coexist (Crespo et al., 2011). Less frequent intrachromosomal translocation events such as those in chromosome 4 lead to oncogenic fusion events of fibroblast growth factor receptor 3 (*FGFR3*) and transforming acidic coiled-coil 3

(*TACC3*) in smaller subsets of GBM (3.1%) (D. Singh et al., 2012). Somatic mutations in regulatory regions may also play a role in gliomagenesis, such as promoter mutations in *TERT*, and less frequently in the ubiquitin ligase *TRIM28* and the calcium channel gamma subunit *CACNG6* (Ceccarelli et al., 2016).

### 1.2.2 *The DNA Methylome and Epigenomic Regulation*

Regulation of gene expression by epigenetic processes are hallmark processes in the development of cancers. Similarly, epigenomic regulation of GBMs are observed and work in synergy with genomic alterations to give rise to tumorigenic properties (Jones & Baylin, 2007). In addition to mutations detected in oncogene promoters, promoter-associated DNA methylation alterations induce changes in transcriptional activity of regulatory genes. Analysis of DNA methylation patterns in 272 GBM tumors identified three methylation patterns, of which the first cluster revealed a highly concordant pattern of methylated loci. Termed the glioma-CpG island methylator phenotype (G-CIMP), GBM specimens with this phenotype showed differential clinical and molecular characteristics associated with hypermethylation, and thus transcriptional silencing, of tumor invasion and extracellular matrix genes (Noushmehr et al., 2010). By 2012, a study of 210 GBM samples identified six methylation subtypes of GBM, including G-CIMP, with distinct global methylation patterns, clinical features, tumor localization, genomic alternations, CNAs and gene expression profiles (Sturm et al., 2012). Other epigenomic events have also been implicated in GBM including histone modification, chromatin remodelling, and non-coding RNA regulation (Lu, Akinduro, & Daniels, 2020; Sturm et al., 2012; Y. Zhang et al., 2017). However, despite extensive profiling and molecular

stratification, standardization and clinical utility of epigenomics as a diagnostic measure have been limited in GBM, and more broadly across diverse brain tumours (Capper et al., 2018).

### *1.2.3 Transcriptomic Landscape and Subgrouping*

Analysis of the genomic and epigenomic landscape provided insight into the underlying biological mechanisms of GBM pathogenesis. However, gene expression profiling in the mid 2000s highlighted previously underappreciated molecular heterogeneity in GBMs and presented as a putative tool for more robust prediction of survival (Freije et al., 2004). One of the earliest studies of molecular stratification of high-grade gliomas, including GBM, identified four hierarchical clustering groups of tumours termed 1A, 1B, 2A and 2B from a set of 595 genes. Membership in hierarchical cluster 1A strongly predicted favourable prognosis and was characterized by overexpression of genes involved in neurogenesis. Membership in hierarchical clusters 1B, 2A and 2B revealed poorer prognoses and were characterized by overexpression of genes involved in synaptic transmission, mitoses and extracellular matrix components and regulators, respectively. While this prognostication was promising, stratification revealed membership of lower grade gliomas (WHO Grade III) in group 1B. The lack of strong prognostic differences in clusters with predominantly GBM membership (1B, 2A and 2B) suggested the need for a GBM-specific classification system. Thus, a study in 2006 developed an independent molecular classification consisting of three tumor subclasses; proneural (*PN*), proliferative (*Prolif*) and mesenchymal (*Mes*), recognized by their dominant molecular features. While WHO Grade III gliomas were included in the

identification of these classes, a significant proportion of GBM lesions were classified into each of the three molecular categories (31% *PN*, 20% *Prolif* and 49% *Mes*) (Phillips et al., 2006). The *PN* subtype revealed strong association with normal brain tissue and the process of neurogenesis, while the *Prolif* and *Mes* subtypes resembled highly proliferative tissues and tissues of mesenchymal origin, respectively. Between the three subtypes, the *PN* subtype revealed markedly better prognoses. In 2010, the TCGA expanded on this classification system by identification of two additional subtypes in an independent analysis of 200 GBM patient samples. This newer classification comprises four subtypes termed Proneural (TCGA-PN), Neural (TCGA-NE), Classical (TCGA-CL) and Mesenchymal (TCGA-MES). The newly defined TCGA-CL subtype was found to be characterized by chromosome 7 amplification paired with chromosome 10 loss (93% of samples), high-level *EGFR* amplification (95% of samples), and homozygous deletion of *Ink4a/ARF* locus (95% of samples). CL GBMs were also characterized by lack of additional abnormalities in *TP53*, *NF1*, *PDGFRA* or *IDH1*. This study confirmed the presence of a TCGA-MES and TCGA-PN subtype now characterized by high frequency of *NF1* mutations/deletions and alterations in *PDGFRA/IDH1*, respectively. The TCGA-NE subtype was typified by expression of neuronal markers; however, this subtype was later removed due to the identification of normal neural lineage contamination (Verhaak et al., 2010; Q. Wang et al., 2017). However, in assessing the clinical relevance of this subtype, few differences were observed except for the TCGA-PN subtype in which apparent prognoses was confounded by relatively favourable outcomes of *IDH*-mutant

GBMs that were frequently classified under this molecular category (Verhaak et al., 2010; Q. Wang et al., 2017).

As newer technologies have emerged to comprehensively interrogate genomic and transcriptomic architecture, Neftel et al. attempted to redefine transcriptional subtypes using single-cell RNA sequencing (scRNA-seq). Integrative analysis of 28 tumors by scRNAseq in combination with bulk genetic and expression data of 401 TCGA specimens defined six meta-modules or recurrent programs; mesenchymal-like (MES-like) 1, MES-like 2, astrocytic-like (AC-like), oligodendroglial-like (OPC-like), and neural progenitor-like (NPC-like) 1 and 2. MES-like 1 and 2 were characterized by mesenchymal-related gene expression, in which MES-like 1 showed strong association with hypoxia-response genes. The other four meta-modules were characterized by neurodevelopmental genes characteristic of neuronal or glial lineages or progenitor cells, but with distortions from normal developmental programs (Neftel et al., 2019). While this classification was even more comprehensive than its predecessors, the lack of relevant clinical annotation suggested limited utility for prognostication using transcriptomic stratification. However, these studies highlighted the significant amount of sample to sample or intertumoral heterogeneity of GBMs.

### **1.3 Intratumoral heterogeneity (ITH)**

Through molecular stratification, intertumoral heterogeneity of GBMs was thoroughly characterized. However, prognostic value may have been limited due to an additional confounding factor known as intratumoral heterogeneity (ITH). Numerous studies in GBM have revealed spatial and temporal heterogeneity within a single tumor at

the genomic, transcriptomic, cellular and functional levels. Thus, while bulk expression programs such as the TCGA subtypes may have been informative to the array of alterations across GBMs, the layered diversity of states in GBM may have hindered prognostication.

### 1.3.1 *Spatiotemporal Heterogeneity*

Early studies in GBM suggested the presence of ITH at the spatial or regional level. Previous studies in GBM relied on a single regional biopsy from a surgical specimen, and pooled tumor-lysate approaches that may have inadvertently underappreciated lower frequency alterations (Francis et al., 2014; Qazi et al., 2017). However, multiregional analyses of tumor specimens at the genomic level highlighted regional variability in genotypic aberrations. In 2003, fluorescence *in situ* hybridization (FISH) analyses of 14 surgical specimens detected low level *EGFR* amplifications in *TP53-mutant* tumors. Initially believed to be mutually exclusive genomic events, regional analysis of samples highlighted genomic spatial heterogeneity. Even more so, in tumors with detectable *EGFR* amplifications, non-uniform, topologically-graded distribution of cells was observed (Okada et al., 2003). Genetic spatial heterogeneity was later expanded on in which multiple other RTKs revealed heterogeneous mosaic amplification in single tumor specimens (Snuderl et al., 2011). The detection of spatially distinct genomic events within a single surgically-resected specimen later suggested that spatial heterogeneity may be a more widespread phenomenon. Thus, in 2013, Sottoriva *et al.* attempted to assess genomic, spatial ITH by objective surgical multisampling to derive spatially distinct tumor fragments from eleven GBM patients. While some genetic aberrations were

consistent across samples from the same patient, CNAs were heterogeneously detected in tumor fragments (Sottoriva et al., 2013). Later work by Kim *et al.* again revealed genomic spatial ITH by profiling of 38 specimens, in which those with distal recurrent tumor foci had highly divergent genomic profiles in comparison to their local counterparts (J. Kim et al., 2015). Unsurprisingly, the indication of spatial genomic ITH suggested that this diversity would be detected in other levels of the tumor. Indeed, resultant transcriptomic heterogeneity has been extensively profiled in GBM. Irrespective of spatial organization, GBMs show significant transcriptional diversity. In the same surgical sampling study, matched specimens were assessed for transcriptomic subtypes, revealing that fragments from the same tumor mass were classified into different GBM subtypes. With the advent of higher resolution technologies, single-cell RNA sequencing of five freshly resected GBMs additionally revealed significantly high transcriptional diversity within single tumors by comparison to healthy brain controls (Patel et al., 2014). Similar to the previous study, tumors were also scored on bulk RNA (population-level) profile which identified the associated transcriptional subtype of each sample. However, when bulk analysis was compared to single-cell transcriptional subtype, individual cells revealed a heterogeneous mixture of subtypes within a single tumor. Higher intratumoral subtype heterogeneity in different tumors with the same population-level subtype also corresponded to decreased survival, emphasizing the clinical relevance of ITH not previously appreciated in molecular stratification efforts (Patel et al., 2014). In consequence of spatial genomic heterogeneity, spatial transcriptomic heterogeneity has also been investigated in GBM. While previous studies have assessed a broad array of

tumor tissue, a recent study performed transcriptomic analysis of distinct anatomical regions of GBM: the leading edge, infiltrating tumor, cellular tumor, pseudopalisading cells and necrosis, and microvascular proliferation regions. Samples from these regions were microdissected from 41 tumors and analysed by RNAseq following ISH.

Differential gene expression profiling revealed that samples from different anatomical regions within the same tumor had distinct expression profiles (Puchalski et al., 2018).

Beyond these biologically-distinct, anatomical regions, a recent study assessed spatial transcriptomics of 24 GBM specimens identifying a total of 139 patient-specific clusters, again highlighting inter- and intratumoral spatial heterogeneity (Ravi et al., 2021).

In addition to spatial heterogeneity, GBMs show temporal evolution and heterogeneity. ITH at a temporal level may result from various selective pressures such as therapy that continually drive dynamic glioma evolution. Prior to molecularly interrogating temporally-spaced GBM specimens, temporal heterogeneity was inferred by phylogenetic reconstruction of copy number profiles and whole genome sequencing (H. Kim et al., 2015; Sottoriva et al., 2013). However, later work utilizing sequential tumor biopsies uncovered and confirmed a considerable degree of temporal evolution at the genomic level of GBMs, with only 25-75% of shared genetic alterations between initial and recurrent tumors from the same patient (Barthel et al., 2019; Johnson et al., 2014; J. Kim et al., 2015; Touat et al., 2020). While certain genetic alterations believed to occur at the earliest stages of GBM development, known as “truncal” mutations, remained such as chromosome 7 gains and chromosome 10 losses, GBMs can exhibit can acquire treatment-induced hypermutation, or selection against clones present at the initial tumor

(Barthel et al., 2019; Touat et al., 2020; J. Wang et al., 2016). Due to the scarcity of temporally-distinct tumor tissues, temporal evolution has also been tracked by matched collections of CSF containing circulating tumor DNA (ctDNA) from GBM patients. Of patients with detectable ctDNA, divergence of genetic profiles from the initial resected tumor to the ctDNA increased with larger time interval between collection. Interestingly, genomic profiles in GBM corroborated with previous studies in which “truncal” alterations persisted, with convergent and branched evolution of acquired genomic alterations in core glioma pathways such as growth receptor pathways (Miller et al., 2019). At the transcriptomic level, transcriptomic temporal heterogeneity has also been frequently observed and studied in GBM. On a bulk RNA level, over 66% of GBM patients have been observed to undergo transcriptional subtype switching, with a bias towards the more aggressive, mesenchymal subtype (Phillips et al., 2006; J. Wang et al., 2016; Q. Wang et al., 2017) Subtype switching has also been documented on a single-cell resolution by cellular DNA barcoding in which heritable genetic barcodes were seen among cells of different transcriptional states, unambiguously illustrating temporal transcriptomic plasticity (Neftel et al., 2019). By independently demonstrating temporal and spatial heterogeneity independently, it is apparent that the two phenomena combine to generate an extensive degree of ITH in GBM. Together, these studies also present ITH as a clinical and molecular factor for poor prognosis, and therapy evasion and resistance not previously accounted for.

### 1.3.2 *Functional Heterogeneity*

Studies of spatiotemporal dynamics in GBM presented ITH as an underpinning of treatment resistance and tumor recurrence. From an evolutionary perspective, the ongoing selection of cell populations with differential molecular characteristics may give rise to a tumor landscape driven by various biological programs (Qazi et al., 2017). This may in turn allow tumors to exhibit functional heterogeneity in which a single specimen hosts diverse sensitivities to therapeutic agents targeting single pathways or phenotypes. Early studies of functional heterogeneity attempted to address feeble clinical responses to RTK-inhibitor monotherapy. Characterization of RTK expression revealed that single GBMs coactivate multiple RTKs, thereby limiting efficacy of therapies targeting single RTKs. *In vitro* treatment of various RTK targeting compounds including EGFR inhibitor (erlotinib), hepatocyte growth factor receptor inhibitor (c-MET) (SU11274) and PDGFR/c- KIT/abl kinase inhibitor (imatinib) were insufficient as monotherapies and were only effective when combined. This study thus highlighted that ITH of RTK expression could confer resistance to single therapies by activation of redundant mechanisms (Stommel et al., 2007). While this pointed to ITH as a mechanism of treatment resistance, the study of bulk GBM specimens did not directly link genomic heterogeneity to functional heterogeneity. Thus, in 2015, Meyer *et al.* performed single-cell derived clonal genomic and functional analyses of GBM specimens. Upon generating 44 individual single cell cultures, functional characterization revealed differential growth, differentiation potential, and chemotherapeutic response, including TMZ from a single tumor. Integrated genomic and transcriptomic analysis confirmed genomic heterogeneity

of clones and tied differential drug response to gene expression profiles, highlighting pathways including ion channels, neurotransmitter signaling, and synaptic membrane genes in resistant clones (Meyer et al., 2015). In addition to suggesting that clones with differential resistance profiles could coexist within a single specimen, this study shed light on the molecular contributions of ITH to functional differences in tumors that drive treatment resistance and relapse. In 2017, Reinartz *et al.* expanded on the assessment of functional heterogeneity in GBM and again demonstrated differential clonal sensitivity to various chemotherapeutic agents, but also identified therapy-induced shifts that rendered primary therapies less effective, revealing the significance of temporal ITH on differential drug response (Reinartz et al., 2017). While clonal analysis was informative, assessment of drug sensitivity on focal surgical specimens underestimated the extent of functional heterogeneity. Thus, to more extensively define functional heterogeneity, recent works have additionally defined the contributions of spatial heterogeneity by treatment of several focal tumor biopsies from single tumors. High-throughput screening of 461 compounds from a wide range of drug classes including apoptotic modulators, conventional chemotherapies and inhibitors of histone deacetylases, heat shock proteins, proteasomes and kinases revealed heterogeneous response tied to individual biological traits. By maximizing clonal diversity in GBM specimens, this study addressed how drug sensitivity is distributed across disease (Skaga et al., 2019). In the context of phenotypic similarity, functional screening using CRISPR-Cas9 technology in GBM has highlighted the role of genomic heterogeneity on functional heterogeneity in drug resistance. TMZ resistance and sensitivity was revealed by be governed by a core set of genes in the MMR

pathway. However, different samples revealed genotype-specific dependencies despite varying degrees of phenotypic similarity in TMZ-resistance (MacLeod et al., 2019).

Together, these studies highlight the functional consequence of bulk and spatiotemporal molecular ITH, and present ITH has a source of therapy resistance leading to disease relapse.

### *1.3.3 The Tumor Microenvironment*

Beyond the neoplastic cell compartment, GBM heterogeneity is further complicated by extrinsic factors that comprise the dynamic immunosuppressive tumor microenvironment (TME). The TME consists of residing and infiltrating immune cells that create a complex milieu to promote tumor invasion, plasticity and growth (Q. Wang et al., 2017). The GBM TME has been revealed to host endothelial cells, tumor-infiltrating lymphocytes, tumor-associated microglia and macrophages (TAMs), and myeloid-derived suppressor cells (MDSCs) that dampen anti-tumor immunity, in which innate and adaptive immune responses lead to tumor control, as well as generate treatment-resistance (Razavi et al., 2016).

Endothelial cells (ECs) are stromal cells that generate excessive and aberrant vasculature in a process known as angiogenesis to promote GBM growth. GBM-associated ECs additionally produce paracrine factors that support other components of the TME and can transform into mesenchymal-like cells that are highly proliferative, migratory and chemoresistant (M. Huang et al., 2020). Together with pericytes and smooth muscle cells, dividing endothelial cells result in the formation of collapsible, defective and permeable blood vessels to generate foci with low oxygen or hypoxia

(Monteiro, Hill, Pilkington, & Madureira, 2017). Hypoxic regions within GBM are hostile environments that drive necrosis, resistance to treatment, and neoplastic cell invasion and motility (Colwell et al., 2017). Even more, hypoxic regions often obstruct anti-tumor immunity by exerting immune suppression on various effector cells. Effector cells, namely cytotoxic T-cells marked by CD8, have previously been shown to mount an anti-tumor response in many cancers (O'Donnell, Teng, & Smyth, 2019). However, GBMs show known immune evasion mechanisms driven by cell-mediated and molecular microenvironmental modulation. Subsets of TILs and TAMs, along with MDSCs, drive cell-mediated immunosuppression in the TME. T-regulatory cells (Tregs) are a subset of CD4 or T-Helper cells that are recruited to the TME by chemotaxis. These cells inhibit anti-tumor T-cell activity by blocking production of effector cytokines including interferon-gamma (IFN- $\gamma$ ), and IL-12, IL-10 and transforming growth factor beta (TGF- $\beta$ ) (H. Wang et al., 2021). While cytotoxic T-cells may infiltrate GBMs in the TME, the cumulation of immunosuppressive signals induce dysfunction that impairs tumor targeting. Other cell populations in the TME that drive immunosuppression are TAMs. TAMs can be divided into two populations; resident microglia, or bone marrow-derived macrophages which along with T-cells infiltrate the TME by entry through a disrupted and dysregulated blood-brain-barrier (BBB), glymphatic drains in the dural sinuses, and/or through skull and vertebral bone marrow reservoirs (Arvanitis, Ferraro, & Jain, 2020; Cugurra et al., 2021; Louveau et al., 2015). In addition to releasing immunosuppressive and pro-tumorigenic cytokines into the TME, TAMs induce cytotoxic T-cell dysfunction and apoptosis by expression of markers including

programmed cell death ligand 1 (PD-L1), cytotoxic T-lymphocyte-associated protein 4 (CTLA-4), FasL, and CD73 (Goswami et al., 2020; Razavi et al., 2016). Recent scRNAseq deciphering the composition of TAMs additionally showed that they are heterogeneous and represent various functional states (Ochocka et al., 2021). The TME also contains myeloid-derived suppressor cells, a population of bone marrow-derived immature myeloid cells. Like TAMs, MDSCs hinder the activity of T and natural killer (NK) cells, again inhibiting anti-tumor immunity (Bayik et al., 2020). While the TME adds to the extensive ITH observed in GBM, bidirectional paracrine signalling between tumor cells and the TME further drives ITH (Gangoso et al., 2021; Hara et al., 2021; Q. Wang et al., 2017). Together, the multifaceted nature of ITH makes GBM a highly complex, plastic and aggressive disease.

#### **1.4 Cancer Stem Cells**

While characterization of ITH in GBM has been informative, defining the source of heterogeneity presented as a rational development towards targeting the root of GBM. Studies in liquid malignancies such as leukemia linked ITH to a clonal population of neoplastic cells with distinct stem-like properties broadly known as cancer stem cells (CSC) (Lapidot et al., 1994). Under this model of cancer, a small population of cells are endowed with stem cell properties of proliferation, self-renewal and multi-lineage differentiation potential, as well as distinct tumor-initiation capacity. By homeostatic control of self-renewal and differentiation, CSCs can generate a heterogeneous pool of progeny comprising ITH (Dalerba, Cho, & Clarke, 2007 2007). Investigation in brain tumors including GBM identified a population of CSCs that showed properties of

stemness *in vitro* and *in vivo* (Galli et al., 2004; S. K. Singh et al., 2003; S. K. Singh et al., 2004). Variably termed brain tumor initiating cells (BTICs), brain tumor stem cells (BTSCs) or glioma stem cells (GSCs), these cells were isolated based on studies performed in normal neural stem cells (NSCs) which displayed self-renewal capacity by formation of neurospheres, a cluster of cells arising from a single stem cell (Reynolds & Weiss, 1992). Similarly, GSCs showed *in vitro* neurosphere formation when isolated from human brain tumors, including GBM (S. K. Singh et al., 2003). While this study confirmed the presence of stem-like properties of cells derived from brain tumors, later work sought to define true measure of CSCs, self-renewal *in vivo* and recapitulation of the original tumor. Serial retransplantation of isolated GSC populations generated tumors *in vivo* indicating self-renewal and gave rise to multilineage neoplastic cells thus confirming that these were in fact CSCs (S. K. Singh et al., 2004). Since the identification of GSCs, these cells have been shown to give rise to other cellular subpopulations including endothelial cells (Ricci-Vitiani et al., 2010). As GSCs were postulated to be at the apex of the tumor hierarchy and responsible for tumor initiation, numerous studies have attempted to uncover the cell-of-origin of GBM, and the transforming events that lead to a GSC phenotype (Alcantara Llaguno et al., 2015; Friedmann-Morvinski et al., 2012; Jacques et al., 2010; C. Liu et al., 2011). Most recently, GBM was suggested to arise from astrocyte-like NSCs in the subventricular zone (SVZ) that contains low-level driver mutations previously implicated in gliomagenesis (J. H. Lee et al., 2018). While these studies postulated a unidirectional hierarchy, more recent studies have suggested that GSCs are dynamic and encompass a complex array of microstates that are defined

and maintained by environmental influences (Prager, Bhargava, Mahadev, Hubert, & Rich, 2020; Hubert, & Rich, 2020). Despite dynamic changes, GSCs may represent a conserved program with the highest entropy in the GBM cellular hierarchy solely capable of driving and maintaining tumor growth (Couturier et al., 2020; Lan et al., 2017; Richards et al., 2021; Suva et al., 2014).

#### 1.4.1 GSC Markers

Identification of GSCs has led to numerous studies to define a bonafide marker for isolation and therapeutic targeting. Prospective sorting of tumor cells by the cell surface protein CD133, a normal NSC (Uchida et al., 2000) and hematopoietic stem and progenitor cell (HSPC) marker (Miraglia et al., 1997), preferentially gave rise to clonally-derived neurospheres and recapitulated the phenotype of the tumor from which they were derived both *in vitro* and *in vivo* (S. K. Singh et al., 2003; S. K. Singh et al., 2004). However, the use of CD133 as a canonical GSC marker has been confounded with newer evidence suggesting that CD133<sup>-</sup> cells also exhibit tumorigenic capacity (Beier et al., 2007; Joo et al., 2008). This suggested that CD133 would not definitely demarcate GSC populations under a reductionist, binary and functional understanding of CSCs into ‘stem’ and ‘non-stem’ populations. However, the cancer stem cell hypothesis has morphed into a more nuanced understanding in which stemness may be a contextual and dynamic property. Tumor cells may thus transition between GSC and non-GSC states in response to autocrine or microenvironmental cues (Prager et al., 2020 & Rich, 2019). In 2010, a report by Chen *et al*, identified three clonogenic cell types- two of which were CD133<sup>-</sup> (Type I and III) and one CD133<sup>+</sup> (Type II). Type I and Type II cells produced secondary

clones that expressed CD133 while Type III produced strictly CD133<sup>-</sup> clones.

Interestingly, while all types were able to produce neurospheres in cultures *in vitro* and tumors *in vivo*, Type I and Type II which generated CD133<sup>+</sup> clones produced more heterogeneous progeny, had increased growth kinetics and were able to generate tumors *in vivo*. While this data presents populations of self-renewing CD133<sup>-</sup> cells that could be masked by differentiated populations of CD133<sup>-</sup>, only CD133<sup>+</sup> cells reliably exhibited a stem phenotype (Chen et al., 2010). Additionally, these works suggested that Type I and Type II cells represent inter-convertible phenotypic states of the same cell population. Thus, CD133<sup>+</sup> expression may still mark a dynamic GSC phenotype that may be acquired or lost, but maintained within tumors (Brescia et al., 2013).

The significance of CD133 in marking GSC populations has additionally been revealed in the attempt to identify other reliable markers. Other markers have often been revealed to be co-expressed with CD133 and may represent subsets of GSCs in tumor niches. One such marker is integrin alpha 6, an extracellular matrix receptor, which was found to be highly expressed in the GSC population, particularly within the perivascular niche. While integrin alpha 6-expressing cells had tumorigenic potential, cells that co-expressed CD133 had the highest tumor-initiating capacity when co-segregated with integrin alpha 6 expression (Lathia et al., 2010). Similarly, discovery of another putative GSC marker, A2B5, a glial progenitor marker, revealed 100% tumor formation when co-expressed with CD133 versus 92% engraftment of A2B5<sup>+</sup>CD133<sup>-</sup> cells, indicating the significance of CD133 as a GSC marker (Ogden et al., 2008). Assessment of an additional GSC marker, CD15, or stage specific embryonic antigen 1 (SSEA-1) revealed

that CD133 expression more reliably predicted expression of other stem markers including SOX2, BMI1, OLIG2, and EZH2 (Son, Woolard, Nam, Lee, & Fine, 2009; Lee, & Fine, 2009). Interrogation of the neuronal cell adhesion molecule L1CAM showed similar results in which L1CAM appeared to be a subset of CD133<sup>+</sup> GSCs rather than as independent marker (Bao et al., 2008). Together, these studies highlight that other markers may identify CSCs without underscoring the significance of CD133 in GBM.

#### *1.4.2 CD133 in therapy resistance*

As GSCs represent a biologically relevant subpopulation, investigation into its clinical relevance was necessary to define. Thus, multiple studies sought to establish the clinical utility of CD133 as a prognostic biomarker in GBM. CD133-expression has been shown to be predictive of pattern (local vs distal) and timing of recurrence, time to malignant progression from low-grade gliomas, and poor OS in GBM (Venugopal et al., 2015; Zeppernick et al., 2008). As CD133 broadly marked poor outcome, other works sought to define the link between clinical factors and function in gliomagenesis. Thus, the role of CD133-expression in mediating therapy resistance was investigated. CD133<sup>+</sup> cells derived from human xenograft and patient specimens have previously shown increased radioresistance and repopulation after ionizing radiation therapy in comparison to their CD133<sup>-</sup> counterparts. This was mediated by activation of DNA damage response, particularly of checkpoint activation, that would allow CD133<sup>+</sup> cells to preferentially survive radiation-induced apoptosis. (Bao et al., 2006). CD133<sup>+</sup> cells, or GSCs, were thus revealed to be primed to evade radiotherapy. As SoC combines chemotherapy, CD133<sup>+</sup> cells were later assessed for their drug resistance capabilities. Indeed, CD133<sup>+</sup> cells

showed significant resistance to four conventional chemotherapeutic agents, including TMZ. While mechanisms of drug resistance were not thoroughly studied, chemoresistance was suggested to be mediated by higher expression of an ATP-binding cassette transporter protein known as BCRP1, a drug transporter protein and/or MGMT on CD133<sup>+</sup> cells (G. Liu et al., 2006). As GSCs have previously been shown to evade chemotherapy to propagate new tumor cells into recurrence through quiescence, these studies suggested that CD133-expressing cells could survive and persist through treatment and re-emerge to initiate tumor relapse, as observed in a similar paradigm of AML (Shlush et al., 2014). While the clinical significance of CD133 has been defined for GBM, the molecular mechanisms that govern preferential therapy resistance and stemness have not been defined. Thus, while many groups have shown the utility of CD133, little is known about the underlying biological mechanisms that mediate associated phenotypes.

## **1.5 Biological Function and Regulation of CD133**

### *1.5.1 Biochemical Properties of CD133*

*PROM1* gene is located on chromosome 4 in humans and is differentially regulated at the genomic, transcriptomic and protein levels (GeneCard: GC04M015912). The *PROM1* gene has been shown to contain at least five TATA-less alternative promoters (P1-P5) that are expressed in a tissue-dependent manner (Shmelkov et al., 2004; Sompallae et al., 2013). Of interest is expression under P2, the third most distally located promoter, which drives CD133 expression in brain and ovarian tissues. Transcription has also been shown to be regulated by promoter methylation, as observed by the presence of a CpG island encompassing promoters P1-3 of CD133 which is

regulated by MYC and SP1 (Gopisetty, Xu, Sampath, Colman, & Puduvalli, 2013; Colman, & Puduvalli, 2013; Sompallae et al., 2013; Tabu et al., 2008). At the transcriptional level, 27 exons have been identified in *PROM1*, of which seven variants are produced by alternative splicing (Fargeas et al., 2004). Transcripts encode for a pentaspan protein with three cytoplasmic domains, five helical transmembrane domains, and three extracellular loops (UniProtKB: 04390). Post-translationally, CD133 can additionally be modified by glycosylation and acetylation events. Golgi intermediate compartment residing acetyltransferases NAT8B and NAT8 physically interact with CD133 to acetylate the protein on three lysine residues predicted to reside on the first extracellular loop (Mak et al., 2014). CD133 additionally shows eight putative asparagine (N)-linked glycosylation sites, and one phosphoserine site at the protein's C-terminus (UniProtKB: 04390) (Rigbolt et al., 2011)

### *1.5.2 CD133-regulated signalling pathways*

As of current, little is known about the function of CD133. Insight into its function in the context of ontogeny has been limited to the discovery of a frame-shift mutation in prominin-1, the *CD133* gene, leading to an autosomal-recessive, retinal degenerative disease (Maw et al., 2000). While this implicated CD133 in early retinal development, little has been identified of its function in the context of oncology, and more particularly in GBM.

Early work in GBM attempted to identify transcriptomic profiles associated with CD133 expression in GBM. To explore these underlying molecular characteristics, our lab previously identified a CD133 gene expression signature based on CD133 co-expressed

and anti-co-expressed genes from three independent brain tumor gene expression datasets (GSE7696 [n=84], GSE13041 [n=191], GSE4290 [n=180]) representing 455 gliomas. The CD133 signature comprised probe sets from the top and bottom 5% of all probes based on similarity in expression to CD133. Using gene set enrichment analysis (GSEA), cancer stem cell genes as well as in embryonic stem cell signatures were observed to be significantly enriched in the CD133 signature (Venugopal et al., 2015). Similar work from the Tian group identified an independent CD133 gene expression signature by transcriptomic profiling of sorted CD133<sup>+</sup> and CD133<sup>-</sup> cells from human GBM consisting of 214 differentially expressed genes resembling human embryonic stem cells (X. Yan et al., 2011).

Generation of molecular networks comprising protein products encoded by CD133 co-expressed genes identified 4 modules with distinct biological processes: cell proliferation pathways (PLK1 and Aurora B Kinase), RNA processing and metabolism, protein translation and export, and DNA repair (Fanconi anemia pathway). To further identify CD133 associated self-renewal machinery, connectivity mapping of the CD133-dependent gene signature identified anti-helminthic drug Pyrvinium, which was capable of attenuating CD133-mediated proliferation, self-renewal, and tumor formation in GBMs. Previous studies suggested that pyrvinium exerts anti-neoplastic effects by attenuation of developmental signaling pathways such as sonic hedgehog (SHH), and AKT signaling (Venerando, Girardi, Ruzzene, & Pinna, 2013 & Pinna, 2013). Thus, gene expression analysis of Wnt protein AXIN, a target of the canonical Wnt protein  $\beta$ -catenin, revealed decreased expression in pyrvinium-treated samples. Global GSEA additionally

linked CD133 with other signaling pathways that govern self-renewal and proliferation, namely *Bmi1* and *Jak2*. Most notably, this study implicated CD133 in the canonical Wnt/ $\beta$ -catenin axes, which is associated with features of stemness (Fodde & Brabletz, 2007; Venugopal et al., 2015). Identification of Wnt association in this study corroborated with earlier work in which CD133 was shown to directly promote  $\beta$ -catenin signaling in cancer cells. In particular, CD133, HDAC6, and  $\beta$ -catenin were revealed to form a ternary complex to contextually stabilize  $\beta$ -catenin through HDAC6 activity and maintain self-renewal capacity. Other mechanistic insights have revealed CD133 interaction through the PI3K/AKT signalling axis (Mak et al., 2012). In 2013, Wei *et al.* identified a direct interaction between a phosphorylated c-terminal tyrosine residue (Y828) and p85, a PI3K regulatory subunit (Wei et al., 2013). Functionally, the biological consequence of this interaction revealed the necessity of Y828 phosphorylation in self-renewal. Recent work has also revealed a unique CD133-AKT-Wnt axis in GBM. In this study, CD133 overexpression identified a marked increase in pAKT, pGSK-3 and  $\beta$ -catenin while treatment with Wnt inhibitors reduced expression of pAKT and surface CD133 expression. Clinical relevance of this pathway was also confirmed in which Wnt-active GBM cells exhibited increased tumorigenicity in human xenograft models of GBM (Manoranjan et al., 2020). While historically AKT signalling has not been associated with Wnt signalling, this study highlighted activation of the Wnt pathway by non-canonical receptors and upstream activators, namely CD133. Though CD133 activity has repeatedly shown interaction with these signalling nodes, the direct interacting mechanisms that define these axes have yet to be thoroughly understood.

Other functional insights of CD133 may be derived from its interaction with membrane cholesterol in plasma membrane protrusions (Corbeil et al., 2009 & Huttner, 2010). In previous studies, treatment with the cholesterol-sequestering drug methyl- $\beta$ -cyclodextrin attenuates the self-renewal of embryonic stem cells (ES) and HSPCs (M. Y. Lee, Ryu, Lee, Park, & Han, 2010 Park, & Han, 2010; Yamazaki et al., 2006) which are known to express CD133 (Kania et al., 2005; Miraglia et al., 1997). This may suggest that CD133 may play a role in contributing to self-renewal organization of membrane topology. In identifying common signalling nodes, the interaction with CD133 and PI3K, which also plays a role in phospholipid docking (P. Liu, Cheng, Roberts, & Zhao, 2009 & Zhao, 2009), could also mediate lipid fluidity. Differential CD133 regulation and localization has also been recently shown to activate various cell signalling programs in a contextual fashion. CD133 expression has been shown to be regulated at a transcriptional level by initiation at tissue-specific promoters, post-transcriptional level by alternative splicing, and differential glycosylation at eight putative sites which may regulate subcellular localization. While no direct mechanism has been implicated in CD133 localization, GBMs have been shown to heterogeneously distribute CD133 to the plasma membrane and/or intracellularly. Interestingly, localization to the plasma membrane and association with stemness phenotypes was more predicted by detection of a the glycosylation dependent epitope of CD133 known as AC133, related to the second extracellular loop (Campos et al., 2011). While this study interrogated regulation of CD133 in GBM, later work identified differential and contextual biological function associated with localization. Intracellular CD133 was observed to home to a pericentrosomal region, and inhibit autophagy to

suppress cell differentiation. In contrast, cell surface CD133 required phosphorylation and activated PI3K/AKT signalling in preferential growth conditions in various human cancer cells (Izumi et al., 2019). Together, these works have identified an array of potential signalling networks regulated by CD133 across various oncogenic contexts. However, understanding and clearly defining a holistic function of CD133 has yet to be performed in GBM. In identifying the molecular mechanisms that govern a CD133 phenotype, we may elucidate novel oncogenic cellular programs, and highlight common nodes of interaction within divergent cell signaling pathways.

## **1.6 Targeted and Immunotherapeutic Approaches**

While the biological understanding of CD133 remains elusive, the association with negative clinical outcomes highlights an avenue to target GBM. However, assessment of therapeutic modalities over the past decade has revealed little progress in the development of novel therapeutics (Ozdemir-Kaynak, Qutub, & Yesil-Celiktas, 2018 2018). While GSCs have been implicated as a functionally relevant subpopulation of cells, early targeted therapeutic strategies have instead attempted to address phenotypic outputs. However, targeted strategies have presented as an option in attacking specific cell-mediated vulnerabilities necessary for tumor growth, maintenance and progression.

### *1.6.1 Monoclonal Antibodies (mAbs)*

Some of the earliest targeted therapies consisted of monoclonal antibodies (mAbs) due to their high specificity and affinity to targets on brain tumors. Some of the first mAbs assessed in GBM were directed towards curbing the vascularization of the tumor, due to the importance of angiogenesis in GBM growth. Vascular endothelial growth

factor A (VEGF-A), an important mitogen for vascularization and angiogenesis, constituted a good target for inhibiting the growth of blood vessels to control tumor growth. Thus, bevacizumab, a humanized mAb against VEGF-A, was given accelerated FDA approval for testing in recurrent GBM (rGBM). Several antiangiogenic therapies were tested in GBM previously but showed little efficacy in comparison to bevacizumab that was capable of extending PFS (Lombardi et al., 2017). However, a systematic Cochrane review did not find sufficient evidence for its use in primary or recurrent GBM (Ameratunga et al., 2018)(Chamberlain, 2008; Chamberlain & Raizer, 2009; Friedman et al., 2009). Thus, other mAbs have been generated and tested for use in GBM targeting various biologically-relevant proteins on tumor cells including nimotuzumab and cetuximab, (anti-EGFR)/EGFRvIII(Mateo et al., 1997) IMC-3G3 (anti-PDGFR)(Shah, Loizos, Youssoufian, Schwartz, & Rowinsky, 2010). However, assessment in clinical trials has yielded little success as either monotherapeutic approaches or in combination with SoC (Du et al., 2019; Hasselbalch et al., 2010)

MAbs have also been developed to promote anti-tumor immunity by targeting proteins that suppress immune response from the TME. Broadly known as immune checkpoints molecules, these surface proteins mediate inactivation of T-cells when bound to ligands expressed on GBM cells or immunosuppressive immune cells in the TME. Thus, the development of immune checkpoint inhibitors (ICIs) sought to block this immunosuppressive mechanism to boost T-cell mediated anti-tumor effects (Pardoll, 2012). One of the most well characterized immune checkpoints is the receptor-ligand pair programmed cell death 1 (PD-1) and programmed cell death ligand 1 (PD-L1). Thus,

investigation of PD-1 blocking ICIs nivolumab and pembrolizumab in GBM due to their success in other solid tumors (Pardoll, 2012). While pre-clinical assessment was promising (Zeng et al., 2013), phase III trials of nivolumab (CheckMate 143, 498, 548) and phase Ib/II pembrolizumab (KEYNOTE-028, NCT02337491, NCT02313272) failed to meet primary endpoints as single agents or with SoC (Lombardi et al., 2020; Reardon et al., 2020; Sahebjam et al., 2021; X. Wang et al., 2019). Other ICIs targeting checkpoints such as cytotoxic T-lymphocyte-associated protein 4 (CTLA-4) and CD80/86 (ipilimumab; NCT02311920, NCT02829931), CD47 and signal regulatory protein alpha (SIRP $\alpha$ )(Willingham et al., 2012), TIM-3 and galectin-9 (LGALS9)(Z. Liu et al., 2016), LAG-3 and fibrinogen like 1 (FGL1)(Lim et al., 2020; J. Wang et al., 2019) CD276, and CD73 and A2A adenosine receptor (A2AR)(Goswami et al., 2020) have all been assessed either pre-clinically or through clinical trials in GBM (J. Huang et al., 2017; Lombardi et al., 2020; Ott et al., 2020). While newer studies have attempted to address the lack of success of ICI in GBM such as timing of therapy (neoadjuvation), as well as use of molecular stratification of potential responders (Ito, Nakashima, & Chiocca, 2019) additional challenges for treatment in GBM remain including limited tumor entry due to the BBB, poor tumor distribution and ITH (Sousa, Moura, Moreira, Martins, & Sarmiento, 2018). Even more so, inhibition of cell signaling mechanisms may have been insufficient in inducing cytotoxic effects necessary for tumor control.

### *1.6.2 Chimeric Antigen Receptor T-cells (CAR-Ts)*

To address the need for cytotoxic therapies, the study of engineered cell-based immunotherapies in liquid cancers showed great promise for assessment in solid cancers

(Mohanty et al., 2019). One such strategy, known as chimeric antigen receptor (CAR) T-cells (CAR-Ts), consists of the adoptive transfer of T-cells genetically modified to express a tumor-targeting receptor. The CAR is composed of an extracellular ligand-binding domain that recognizes a tumor-associated or -enriched antigen (TAA), a transmembrane domain, and one or more intracellular signaling domains to activate T-cells through an major histocompatibility complex (MHC)-independent manner. This generates a cytotoxic response mediated by degranulation of perforin and granzyme proteins that induce apoptosis of the target cell (Bagley, Desai, Linette, June, & O'Rourke, 2018 June, & O'Rourke, 2018). First documented for use in acute lymphoblastic leukemia (ALL), the CAR was specifically designed to recognize CD19, a marker associated with B-cell malignancies. Now as an FDA-approved drug, CD19 CAR-T cells have demonstrated robust activity and clinical response (Maude, Teachey, Porter, & Grupp, 2015 & Grupp, 2015). Although clinical progress in GBMs has been slow, recent CAR-T therapies have emerged targeting widely characterized TAAs in solid tumors such as human epidermal growth factor receptor 2 (HER2)(N. Ahmed et al., 2017), IL-13 receptor alpha 2 (IL13-R $\alpha$ 2)(Brown et al., 2016), and a splice variant of epidermal growth factor receptor EGFR (EGFRvIII) expressed on 24-67% of GBMs (Heimberger et al., 2005; O'Rourke et al., 2017). These early studies have demonstrated feasibility and safety of administering CAR-T therapies to patients with GBM, particularly regarding the lack of cytokine release syndrome (CRS) and neurotoxicity frequently observed in the use of CAR-Ts in other liquid and solid malignancies (Brudno & Kochenderfer, 2016). Targeting CD133 through this modality thus presented as a

promising approach. Thus, we successfully developed a second-generation anti-CD133 CAR-T therapy (CART133) using donor-derived T-cells (Vora et al., 2020). *In vitro* assessment of CART133 showed significant cytotoxic capacity at low effector-target ratios, T-cell activation and cytokine release when co-cultured with CD133<sup>HIGH</sup> GBMs, in comparison to a CAR control. In our preclinical models, just two intracranial doses of one million CAR-T cells resulted in almost complete elimination of tumor burden and a significant survival advantage over control mice. As previously mentioned, CD133 is most notably expressed on HSPCs (Miraglia et al., 1997). Thus, we additionally assessed the safety profile of CART133 utilizing a humanized model of hematopoiesis in which we showed that intracranial and intravenous CART133 treatment is both therapeutically efficacious and safe in the context of on-target, off-tumor effects (Vora et al., 2020).

## **1.7 Challenges to Immunotherapy**

While CD133 has shown to be a promising therapeutic target in our pre-clinical models, additional pre-clinical and clinical considerations must be noted before implementation in patients. In looking at the efficacy of the CAR-Ts assessed in GBM (ex: anti- IL13-R $\alpha$ 2, HER2, EGFRvIII), patients have had modest clinical benefit. This may be due to target selection, CAR design, site of treatment injection, and/or tumor factors such as the immunosuppressive microenvironment (Migliorini et al., 2018).

### *1.7.1 Target Heterogeneity and CAR design*

As of current, the clinical CAR-T landscape for GBM has shown little benefit. Treatment with IL-13R $\alpha$ 2-directed, first-generation CAR-Ts in a pilot trial revealed only transient response with no durable clinical outcomes (Brown et al., 2015). This was

believed due to the lack of strong CAR design. Thus, a modified, second-generation CAR was developed with a CD137 costimulatory domain to improve T-cell persistence. While full reports have not been revealed, results in a case study again showed initial anti-tumor regression for a period of 7.5 months prior to the development of multifocal disease (Brown et al., 2016). These data suggested that target selection and heterogeneity may have been a leading factor in the lack of clinical success of the IL-13R $\alpha$ 2 CAR-T. Indeed, assessment of pre- and post-therapeutic tissues revealed loss of IL-13R $\alpha$ 2 expression, but also heterogeneity leading to recurrence of antigen-negative disease (Brown et al., 2015). The assessment of CAR-Ts against other antigens such as EGFRvIII, and human epidermal growth factor 2 (HER2) for GBM have additionally revealed poor results with no clinical benefit as single targets (N. Ahmed et al., 2017). While other single targets are in early exploration, pre-clinical assessment of multi-targeting CAR-Ts have shown more promise and may address the issues of target heterogeneity (Bielamowicz et al., 2018).

As CAR-Ts move towards clinical assessment, numerous other strategies are also being actively tested in pre-clinical models including modifications of the CAR design to improve anti-tumor efficacy. Functional modifications have been assessed pre-clinically such as the overexpression of the canonical AP-1 factor c-Jun to generate CAR-Ts resistant to exhaustion (Lynn et al., 2019). Other novel works have focused on improving CAR design including the development of logic-gated CAR-Ts such as the synthetic Notch (synNotch) receptor CAR-T, which consists of an engineered receptor that activates a transcriptional output upon binding to its cognate antigen, and induces expression of a CAR against a TAA. This design would increase specificity of the CAR,

address tumor heterogeneity by multiplexing, and promote better durability by regulation of CAR expression (Choe et al., 2021). CAR-Ts that deliver therapeutic payloads such as bi-specific T-cell engagers (BiTEs) upon binding to EGFR to aid in anti-tumor immunity by recruitment of bystander T-cells, and target tumor heterogeneity and antigen escape (Choi, Yu, Castano, Bouffard, et al., 2019 Bouffard, et al., 2019). Ultimately, these strategies will be helpful in developing highly efficacious CAR-T therapies for clinical use.

### *1.7.2 Mode of CAR-T delivery*

The solid tumor microenvironment exerts major challenges for CAR-T therapy, particularly in regards to T-cell infiltration. As a result, newer studies have attempted to assess various modes of CAR-T delivery, namely peripheral infusion in comparison to locoregional delivery. Peripheral infusion, or intravenous infusion, of EGFRvIII CAR-Ts revealed trafficking to regions of active GBM, and thus infiltration into the CNS (O'Rourke et al., 2017). While this was promising, the assessment of locoregional delivery presented a more targeted approach. Thus, intracavitary and intratumoral delivery of CAR-Ts were investigated and revealed tolerability and an acceptable safety profile with limited, transient adverse effects (Brown et al., 2015). In one particular patient, intracavitary infusions were able to control local tumor regression after infusion. However, multifocal disease regression prompted researchers to investigate intraventricular infusion into the CSF in hopes of improving distal trafficking. Ten additional infusions by catheter were able to regress all CNS lesions, including spinal tumors, suggesting that differential delivery routes may be more beneficial in the treatment of diffuse tumors such as GBM (Brown et al.,

2016). Thus, these works have revealed the necessity of evaluating multiple facets to improve the apparent efficacy of CAR-T treatment modalities.

### *1.7.3 Extrinsic and Intrinsic T-cell Deficits in GBM*

Although factors pertaining to improving CAR receptor function and treatment have been studied, little has been done to assess the basal quality of patient-derived T-cell products used to generate CAR-Ts. Although tumor immunosuppression has long been known to generate T-cell dysfunction locally in tumor-infiltrating lymphocytes (TILs), a growing body of evidence suggests that immune cell dysfunction is systemic (Brooks, Roszman, Mahaley, & Woosley, 1977; Chongsathidkiet et al., 2018; Dix, Brooks, Roszman, & Morford, 1999; K. Woroniecka et al., 2018; Woroniecka, Rhodin, Chongsathidkiet, Keith, & Fecci, 2018). Peripheral T-cell pools show qualitative and quantitative deficits despite confinement of the tumor to the intracranial compartment. Quantitatively, GBM patients show lymphopenia by lack of T-cell sequestration out of the bone marrow and T-cell deficient lymphoid organs. This is mediated by tumor-imposed loss of sphingosine-1-phosphate (S1P1), which governs T-cell trafficking, from the T-cell surface (Chongsathidkiet et al., 2018). Qualitatively, T-cells from GBM patients show anergy, senescence and exhaustion (Brooks et al., 1977; K. I. Woroniecka et al., 2018). In particular, peripheral T-cells have previously been observed to show expression of exhaustion/senescence markers PD-1, KLGR1 and CD57, as well as functional deficits marked by T-cell hyporesponsiveness irrespective of treatment with the immunosuppressive corticosteroid dexamethasone (Mirzaei, Sarkar, & Yong, 2017;

Mohme et al., 2018). Even more so, the use of radiation, TMZ and glucocorticoids for treatment has been shown to induce significant amount of immunosuppression in patients with GBM (Grossman et al., 2011). Pre-clinical evaluation of CAR-Ts, which are generated from healthy donors, would thus not adequately predict the efficacy of patient-derived CAR-Ts used in clinical trials (Fraietta et al., 2018). Current assessment of patient-derived, or autologous CAR-Ts have been limited to post-clinical trial studies, in which a patient is treated and the CAR product is assessed post-therapeutically. However, it may ultimately be beneficial to assess the efficacy of a patient-derived CAR-T, in a pre-clinical autologous setting, *a priori* to identify predictive value for efficacy in the clinic.

#### 1.7.4 *Allogeneic CAR-T Therapy*

While modifying autologous CARs may be a difficult approach, the above concerns can be circumvented by use of donor-derived or allogeneic CAR-Ts. Autologous CAR-Ts host a myriad of concerns including inconsistency between infusion products of patients, and the time to generation for patients who need immediate care. Other questions pertain to the dubious quality of patient-derived T-cells after previous lines of treatment such as chemoradiotherapy (Depil, Duchateau, Grupp, Mufti, & Poirot, 2020). Allogeneic CAR-Ts thus present a readily-available, “off-the-shelf” therapy. Without modification, donor T-cells can induce a phenomenon known as graft-*versus*-host-disease (GvHD) in which human leukocyte antigen (HLA)-mismatch causes donor T-cells to attack recipient tissue. This is primarily accomplished through recognition by the heterodimeric T-cell receptor (TCR), of which 95% in humans consist of a polymorphic  $\alpha$  (alpha) and  $\beta$  (Briellmaier-Liebetanz, Wagner, & Werres) chain (Li et al., 2015). Conventional TCRs recognize

peptide-loaded major histocompatibility complexes (pMHCs) and can initiate a response if the antigen-presenting cell is deemed foreign or abnormal (Shiromizu & Jancic, 2018). Various approaches have been taken to generate safe, allogeneic adoptive T-cell therapies including the use of T-cells with  $\gamma\delta$  TCRs which maintain a pre-activated state and respond in an MHC-unrestricted fashion (Zou et al., 2017). Other T-cell pools include umbilical cord-blood derived T-cells which are antigen-naïve and would thus reduce the risk of generating GvHD (Kwoczek et al., 2018). While these T-cell pools can be hard to obtain due to their low abundance, genetic perturbation of conventional  $\alpha\beta$  T-cells can abrogate detection of foreign tissues. On the other hand, tissue rejection must also be considered through recipient recognition of donor tissue. When combined with the introduction of the CAR-targeting construct, these genetic modifications can generate “stealth” CAR-T cells that do not induce GvHD, remain unrecognized by the host, as well as attack the tumor. Early studies in T-cell engineering utilized clustered regularly interspaced short palindromic repeats (CRISPR) gene editing using the CRISPR-associated protein 9 (Cas9) to knock-out the TCR in T-cells targeting cancer-testis antigens NY-ESO-1 and LAGE-1. Cells were also knocked-out for *PDCDI*, the PD-1 gene and tested in three patients with advanced, refractory myeloma or metastatic sarcoma. This pilot study revealed that these edited cells were capable of demonstrating anti-tumor immunity and safety in multiple patients. Even more so, these preliminary results demonstrated the safety and feasibility of multiplex gene editing in human T-cells (Stadtmauer et al., 2020). As this study did not assess CAR-T cells, subsequent studies attempted to assess allogeneic CAR development. Thus, the pre-clinical development of double TCR and PD1 knockout CARs followed for

leukemia, particularly against CD22. However, in this work, a one-step generation of modular CAR-T cells was used in which the CAR sequence was knocked into the TCR locus, generating a CAR under endogenous control of the TCR promoter, which has previously shown improved CAR phenotypes (Eyquem et al., 2017). While this was logistically simpler, the regulation of the CAR by the TCR promoter generated TCR-KO CD22-specific CAR-Ts with optimal phenotypes (Dai et al., 2019). Traditional autologous CARs have previously been shown to undergo tonic signalling, a phenomenon in which the CAR constitutively or chronically activates in the absence of antigen, leading to rapid T-cell exhaustion and CAR-T dysfunction (Long et al., 2015). Even more so, accelerated differentiation and exhaustion have been observed with excessive signalling of innate TCRs. Thus, this study and others disrupted the TCR, and other biologically-relevant loci, by use of a knock-in, knock-out (KiKo) system, in which the TCR is knocked-out and the CAR sequence inserted or knocked-in by homology-directed repair (HDR), leaving the CAR under control of the endogenous TCR promoter. Across multiple studies, the generation of an allogeneic CAR product by KiKo has demonstrated potent effector function, dynamic transcriptional regulation of CAR expression, and reduced levels of exhaustion as assessed by expression of PD-1, TIGIT, TIM-3 AND LAG-3 . (Dai et al., 2019). Work by *Dai et al.* additionally assessed a double KiKo strategy at *PCDC1* with an anti-CD19 CAR sequence, presenting an efficacious strategy for multiplexing allogeneic CAR-Ts. Other allogeneic CAR-Ts have also combined knock-out of  *$\beta_2$ -microglobulin* ( *$\beta_2M/B_2M$* ), which encodes for a the  $\beta$  chain of the HLA Class I molecules to prevent host elimination of the T-cell product for CARs against CD19 and prostate stem cell antigen

(PSCA)(Ren et al., 2017). Currently, allogeneic CAR-Ts are being assessed in clinical trials for liquid cancers such as multiple myeloma and B-cell malignancies (Dai et al., 2019; Eyquem et al., 2017) (ex: NCT02799550, NCT04093596). While some progress is being made for other solid tumors such as colorectal cancers (NCT03692429), allogeneic CAR-Ts for use in brain cancer such as GBM remain in early pre-clinical stages and against previously characterized antigens with poor clinical response such as EGFRvIII (Choi, Yu, Castano, Darr, et al., 2019). Thus, while allogeneic CAR-Ts present an improvement in the accessibility and manufacturing of T-cell therapeutic products, the generation of CARs against more potent and clinically-relevant targets, such as CD133, is currently required for GBM.

## **1.8 Statement of Intent**

With an implied signalling role, CD133 is integral in the regulation of oncogenic phenotypes across solid cancers, including GBM. Despite its clinical and biological significance, little is currently known about its function in promoting associated phenotypic outputs. Though the mechanism of CD133 has yet to be defined, immunotherapeutic targeting by CAR-T in our lab has previously presented as a promising strategy. However, on the path towards clinical development, the generation and assessment of an allogeneic CAR-T product may circumvent current issues associated with the traditional, autologous CAR-Ts. Thus, in this thesis, we hypothesized that defining the role of CD133 in human GBMs by study of protein-protein interactions, may uncover novel and robust cell signalling pathways critical to the progression and maintenance of GBM. Even more so, we hypothesized that the development of an

allogeneic CAR-T against CD133 by genomic engineering would address clinical concerns, and present an avenue for optimization of current T-cell based therapies in GBM.

## **CHAPTER 2: Elucidating the CD133 protein-protein interactome by endogenous genomic knock-in of BioID**

### **2.1 Protein-protein interactions and proximity-dependent labelling**

To uncover novel signalling of CD133, we aim to explore and define its protein-protein interactions (PPIs). PPIs form the backbone of signal transduction pathways and networks known as interactomes, across diverse physiological processes (Li et al., 2017). Even more so, aberrant PPIs such as those in cancer may present as tumor-specific targets, particularly for cancers with low mutational burdens like GBM (Loregian & Palu, 2005; H. Lu et al., 2020; Touat et al., 2020). Mapping the interactome to reveal the organization of the proteome into functional units may allow us to understand complex oncogenic phenotypes and processes (Kim & Roux, 2016). Thus, identifying putative PPIs of biologically relevant proteins such as CD133 may ultimately uncover novel stem-related signalling pathways amenable to targeting.

Historically, various approaches have been used to identify PPIs. However, conventional methods to study protein behaviours were inherently limited in their ability to identify PPIs. These methods included the yeast-2-hybrid (Y2H) system, pull-down assays and far western blots which could either only identify high-affinity/stable PPIs , limit isolation to non-physiological conditions and have high rates of false positivity (Kim & Roux, 2016; May & Roux, 2019). However, the advent of proximity dependent

labelling (PL) addressed some of the initial weaknesses of PPI discovery. One such technique, known as BioID, presents as a promising discovery platform for identification of broad association PPIs under physiological conditions (May & Roux, 2019). First reported in 2012, BioID harnesses a promiscuous, mutant biotin ligase (BirA\*) derived from *E.coli* which is fused to a protein of interest, or bait protein, and expressed in cells of interest. Upon supplementation of biotin, potential protein interactors to the bait protein, or prey, are biotinylated. As biotinylation is a rare post-translational modification, standard biotin-affinity capture can be used to isolate these interactors for identification by mass spectrometry. Similar PL techniques have been developed using other engineered enzymes such as engineered ascorbate peroxidase 2 (APEX2) and horseradish peroxidase (HRP). However, molecular products generated in these techniques are toxic to cells. Thus, biotin ligases present as optimal biochemical platforms to identify PPIs, such as those of CD133.

## **2.2 Transgenic and endogenous assessment**

Currently, most BioID studies rely on overexpression systems of ectopic bait proteins exogenously tagged to a biotin ligase (Vandemoortele et al., 2019; Varnaite & MacNeill, 2016). However, these systems can create known artefacts including subcellular mislocalization, complex and protein formation, and downstream regulation (Gibson, Seiler, & Veitia, 2013). In an effort to overcome these limitations, inducible systems have been utilized to control ectopic bait expression such as the Flp recombinase system (Flp-In T-Rex) which can be tuned to match endogenous levels. However, this technique has primarily been performed in 293 cells, and is technically laborious. Other

methods have attempted to perform an endogenous genomic knock-in of BioID at specific genomic loci to generate a BioID-tagged bait protein. Endogenous BioID screens are more likely to generate biologically relevant hits and build meaningful interactomes with less noise contributed by false-positive hits accumulated in an overexpression system (Moreira et al., 2018; Vandemoortele et al., 2019). However, this has been performed in a complex two-step fashion in which the BioID module is added, and an accompanying selection vector is removed using a CRE recombinase system, followed by single cell clonal analysis in commercial cell lines (Vandemoortele et al., 2019). Thus, the need to generate a highly efficient and simplified endogenous BioID tagging technique is required for application in the discovery of native PPIs.

## **2.3 Materials and Methods**

### *2.3.1 Dissociation and culturing of Primary GBM tissue*

Human GBM samples are obtained from consenting patients, in accordance to protocols approved by the Hamilton Health Sciences/McMaster Health Sciences Research Ethics Board. Brain tumor samples are dissociated in PBS containing 0.2 Wünsch unit/mL Liberase Blendzyme 3 (Roche), and incubated in a shaker at 37°C for 15 min. The dissociated tissue is filtered through a 70µm cell strainer and collected by centrifugation (1200 rpm, 3 min). Red blood cells are lysed using ammonium chloride solution (STEMCELL Technologies). GBM cells are resuspended in Neurocult complete (NCC) media, a chemically defined serum-free neural stem cell medium (STEMCELL Technologies), supplemented with human recombinant epidermal growth factor (20 ng/mL; STEMCELL Technologies), basic fibroblast growth factor (20 ng/mL;

STEMCELL Technologies), heparin (2 µg/mL 0.2% Heparin Sodium Salt in PBS; STEMCELL technologies), antibiotic-antimycotic (1X; Wisent), and plated on ultra-low attachment plates (Corning) and cultured as neurospheres.

### 2.3.2 *Propagation of Brain Tumor Stem Cells (BTSCs)*

Neurospheres derived from minimally-cultured human GBM samples will be plated on Polyornithine-Laminin (P/L) coated plates for adherent growth. Adherent cells are re-plated in low-binding plates and cultured as tumorspheres, which are maintained as spheres upon serial passaging *in vitro*. These cells retain their self-renewal potential and are capable of *in vivo* tumor formation. Cells are incubated at 37°C and 5% CO<sub>2</sub>.

### 2.3.3 *Fluorescence Activated Cell Sorting (FACS) and Analysis*

Cells of interest (GBMs) in single cell suspensions are resuspended in PBS+2mM EDTA. Cells will be stained with antibody of choice for 15 mins at room temperature. Samples will be run on a MoFlo XDP Cell Sorter (Beckman Coulter). Dead cells are excluded using the viability dye 7AAD (1:10; Beckman Coulter). Compensation will be performed using mouse IgG CompBeads (BD). Under the context of sorting, small aliquots of each sample will be re-analysed to determine the purity of the sorted populations. Cells are allowed to equilibrate at 37°C for a few hours prior to use in experiments.

### 2.3.4 *Western Immunoblotting*

Total denatured protein (20 µg) is separated using 10% sodium dodecyl sulphate–polyacrylamide gel electrophoresis and transferred to polyvinylidene fluoride membrane. The membrane is probed with primary antibodies against the protein of interest, as well as a loading control; often anti-GAPDH antibody (Abcam #ab8245, 37 kDa) or anti-β-

tubulin antibody (Abcam #ab6046, 50 kDa). For fractionation, anti-Na<sup>+</sup>/K<sup>+</sup> ATPase (Abcam #ab76020, 113 kDa) and anti-GAPDH to test for membrane and cytosolic purity, respectively. The secondary antibody is horseradish peroxidase conjugated goat anti-mouse IgG (Bio-Rad #1721011) or goat anti-rabbit IgG (Sigma #A0545). Bands are visualized using Luminata™ Forte Western HRP Substrate (Millipore) and chemidoc. Western immunoblots are later quantified with Image J software and protein levels are normalized to the loading control.

### 2.3.5 Immunofluorescence

Cells grown on chamber slides will be washed with 1X PBS solution three times, and then fixed with 10% formalin for 20 minutes at room temperature. Cells will then be permeabilized by treatment with 1% NP-40 in PBS solution for 10 minutes and then incubated with blocking solution (15% bovine serum albumin (BSA) in 1X TBS) for 1 hour. Cells will then be stained with the primary antibody of choice overnight at 4°C in humidified chamber or at room temperature for one hour. Antibodies will be washed 3X for 10 minutes in TBS-Tween solution. Slides will then be stained with secondary antibody in the same blocking solution for 45 minutes in a humidified chamber at room temperature. Slides will then be washed 3X with 0.05% TBS-Tween and once more for 5 minutes in 1X TBS. DAPI will be added to slides along with coverslips and allowed to dry overnight in fume hood for imaging.

### 2.3.6 Subcellular Fractionation

Cells in suspension are fractionated using the Mem-PER™ Plus Membrane Protein Extraction Kit from ThermoFisher Scientific. Briefly,  $1 \times 10^7$  cells were washed with 3

mL of Cell Wash Solution and centrifuged at  $300 \times g$  for 5 minutes, two times. The supernatant was discarded and cells were resuspended in 0.5 mL of Permeabilization Buffer in Eppendorf tube and incubated at  $4^{\circ}\text{C}$  for 10 minutes with constant mixing. The mixture was then spun down for 15 minutes at  $16,000 \times g$  and the supernatant collected containing cytosolic proteins. The pellet was subsequently resuspended in 0.25 mL of Solubilization Buffer and incubated at  $4^{\circ}\text{C}$  for 30 minutes with constant mixing. This mixture was then spun down for 15 minutes at  $16,000 \times g$  and the supernatant was collected containing membrane and membrane-associated proteins for subsequent western immunoblotting.

#### *2.3.7 Nested PCR and preparation for Next-generation sequencing*

To characterize genomic cut sites post-electroporation, cells were grown for a minimum of 48 h in NCC media. To generate crude genomic DNA (gDNA) lysates, approximately  $1\text{M}$  cells were lysed in Food Safety buffer (Thermo Fisher Scientific) diluted 1:3 v/v in  $\text{H}_2\text{O}$  containing Proteinase K. The sgRNA-binding region of gDNA was amplified by PCR using Illumina adapter-containing primers that bind approximately 75 base pairs upstream and downstream of the respective PAM sequence. Thereafter, Illumina indices were added to the ends of the genomic amplicons with 8 additional PCR cycles.

#### *2.3.8 AAV Generation, Purification and Quantification*

AAV was prepared using HEK 293T cells to generate AAV2/6 virus. Cells were transfected with transfer plasmid (pAAV-BioID), Replication/Capsid plasmid (Rep/Cap), and an adenovirus helper virus (pHelper) at predefined amounts following the AddGene adeno-associated viral transfection protocol using polyethylenimine (PEI). Cells were left

in DMEM-10% FBS for 96 hours following transfection, and then harvested from plates by incubation of 200 mM EDTA at a dilution of 1/80 in cell media for 10 minutes at room temperature. AAV Virus was purified from cells using the Takara serotype-independent purification kit (AAVpro® Purification Kit Midi [All Serotypes]). To assess genome-copy titer, AAV virus samples were quantified by use of qPCR following the AddGene AAV Titration by qPCR. Using SYBR Green Technology protocol, single AAV copies were amplified at various dilutions using primer sequences annealing to the AAV2 ITR sequences (FWD ITR primer, 5' GGAACCCCTAGTGATGGAGTT, REV ITR primer, 5'-CGGCCTCAGTGAGCGA). Standards were generated using ITR-containing plasmid DNA for approximate quantification. Viral purity was assessed by SDS-Page upon titer quantification. Briefly, 1E10 gc were separated using 10% sodium dodecyl sulphate–polyacrylamide gel electrophoresis. Gels were subsequently stained using silver staining (Pierce™ Silver Stain Kit, ThermoFisher Cat# 24612) to identify bands specific to the three AAV Capsid proteins; VP1, VP2 and VP3. Detection of any additional bands were used to indicate impurity of sample.

### *2.3.9 Electroporation and infection of human GBMs*

Genomic cuts were performed by electroporation of complexed Alt-R® SpCas9 Nuclease V3 (IDT complexed with either an N or C-terminus targeting guide at a 3:1 guide to protein ratio for 15 minutes at room temperature. Using Lonza Amaxa System Kits, 1M GBM cells were resuspended in the provided electroporation buffer and gently mixed with complexed RNP. The mixture was moved to an electroporation cuvette where the E-013 electroporation programs (Nucleofector Iib, Lonza Biosciences) was used. For sole

assessment of genomic cleavage, cells were gently resuspended in NCC media and incubated in 6-well dishes for four days prior to flow cytometric characterization. For knock-in, cells were plated at a density of 200,000 cells in 50 $\mu$ L of respective media with AAV at an MOI of 1E6 gc/cell. Cells will then be cultured for 2-7 days prior to flow cytometric characterization.

## **2.4 Results**

### *2.4.1 CD133 is differentially localized and expressed in human GBMs*

To identify PPIs of CD133, we sought to select primary human GBM specimens that highly expressed the protein. Flow cytometric analysis of five human GBM lines derived from patient tissues revealed variable surface expression of CD133 (**Figure 1A, Table 1**). However, previous data from our lab indicated that CD133 may not be solely expressed on the cell surface and may localize in the cytosol. To investigate differential localization, we performed membrane and cytosolic fractionation of these GBM cell cultures followed by western immunoblotting of each fraction in comparison to whole cell lysates. Indeed, we observed variability in localization, of which the most interesting was BT241, a recurrent GBM specimen with little cell surface CD133. BT241 again revealed little to no observable detection of membranous CD133, but a prominent band in the soluble cytosolic fraction. Samples with detectable cell surface CD133 by flow cytometry were corroborated by immunoblotting as observed in the membrane fractions (**Figure 1B**). Subcellular were confirmed for purity by co-staining with the sodium-potassium Na<sup>+</sup>/K<sup>+</sup> ATPase, and cytosolic glycolytic enzyme, glyceraldehyde 3-phosphate

dehydrogenase (GAPDH) as membrane and cytosolic markers, respectively

**(Supplementary Figure 1A-B).**

Thus, to holistically define the contextual PPIs associated with localization and putatively function, we decided to move forward with BT241 (Cytosol, CD133<sup>HIGH</sup>) and BT935 (Membrane, CD133<sup>HIGH</sup>). To confirm localization, we additionally optimized and performed immunofluorescent staining in which we observed strong membranous staining of CD133 in BT935, and strong cytosolic staining in BT241 when co-stained with nuclear and mitochondrial antibodies to identify subcellular compartments (**Figure 1C**). Thus, these preliminary findings provided a rationale to proceed with BioID screening in BT935 and BT241.

#### *2.4.2 Genomic editing of primary cells by dual modification*

In accordance with previously published works in primary cells, one promising method of genomic editing by HDR utilizes a two-step approach (Dai et al., 2019). To create site-specific cleavage, cells are electroporated with a ribonucleoprotein (RNP) complex composed of a CRISPR protein and small guide RNA. Upon cleavage, a repair template is delivered to cells by varying methods of transfection including electroporation, chemical transfection, and viral delivery. For our purposes, transgene delivery by adeno-associated virus (Skaga et al.) presented as the most efficacious approach due to reduced toxicity, efficient transgene delivery and genomic non-integration. Thus, the following works were designed based on a dual delivery approach consisting of electroporation of RNP and AAV infection to mediate HDR in our target cells for knock-in of the biotin ligase sequence into *PROM1* (**Figure 2A**).

### 2.4.3 Genomic cleavage and repair template design

To perform endogenous genomic knock-in of the biotin ligase (hereafter miniTurboID), we sought to define appropriate genomic loci for tagging at the C-terminus and N-terminus of the CD133 protein. As previously mentioned, the CD133 gene, *PROM1*, is regulated at multiple levels, of which gene expression and post-transcriptional regulation required thorough analyses to ensure tagging of the miniTurboID protein. *In silico* analysis of *PROM1* genomic and transcriptomic and regulation identified seven isoforms generated by alternative splicing (**Table 2**) (Fargeas, Huttner, & Corbeil, 2007). The first isoform, (O43490-1/AC133-1/S2) is the canonical isoform and is expressed in adult brain tissues (Corbeil et al., 2009). At the peptide level, this produces an 865 amino acid (aa) peptide with a 19aa signal peptide sequence which is subsequently cleaved upon translocation into the ER. Thus, we determined that the N-terminus insertion site would thus be directly after the signal peptide sequence, and thus in the first exon (chr4:160575849). Additionally, as this exon is retained across all isoforms, the miniTurboID would be retained upon post-transcriptional modification irrespective of alternative splicing. To insert the miniTurboID at the C-terminus of the protein, we identified the stop codon (chr4:15971070) in exon 27 that is retained in all isoforms, except for isoform 3. Upon designation of these genomic loci, we proceeded to design site-specific guides that would generate genomic cleavage. Of the CRISPR protein variants, usage of Cas9 was most feasible as our genomic regions of interest were GC rich, and thus compatible with respect to the Cas9 protospacer adjacent motif (PAM) (5'-NGG-3'). This would allow for more flexibility in guide design. To select appropriate guides that would target the N- and C-terminus sites of interest, we used the

online tool CHOPCOP to identify CRISPR-Cas9 single guide RNA sequences (Labun et al., 2019). These guides were selected based on their expected cutting efficiency and off-target scores. The following sequences were thus selected:

**N-Terminus:** 5'-GCGGGAACTCCTTTTCAGGAGGG

**C-Terminus:** 5'-TCAGCTATCAATGTTGTGATGGG

To induce homology-directed repair of a template containing the biotin ligase sequence, we had to design repair templates that would link the BioID sequence to the N- or C-terminus of CD133. However, prior to design, we investigated the use of various biotin ligase proteins. MiniTurboID, a successor of the initial BirA\* ligase, presented as an optimal protein due to its small size (28 KDa), high catalytic activity, and rapid biotinylation (Branon et al., 2018). We thus designed repair templates with 200 bp long homology-arms that would allow for insertion of the miniTurboID protein at the N- or C-terminus loci (**Supplementary Figure 1C**). These experimental arms would directly tag the miniTurboID protein to CD133 at its N-terminus, extracellular domain or the C-terminus intracellular domain. To ensure that biotinylation specific events were as a result of proximity-dependent labelling and not noise, we additionally designed controls for each experimental arm. These controls included a T2A ribosomal skipping sequence that would separate the miniTurboID from CD133 to identify background biotinylation. The N-terminus controls however additionally required the consideration of the signal peptide sequence that would be cleaved upon peptide processing. Thus, we added a synthetic signal peptide to ensure appropriate ER-directed translocation, folding and localization of CD133 uninterrupted by genomic editing (**Supplementary Figure 1C**). While these controls

would effectively be sufficient, we also designed an additional N-terminus control as ribosomal skipping and generation of a free miniTurboID could be secreted from the cell and lead to excess noise during downstream analysis. We thus generated a control that replicated the first control, but contained a miniTurboID sequence with a KDEL mutation, that would allow for ER retention of the protein (**Supplementary Figure 1C**). To allow for detection of integration, we added an enhanced GFP tagged to the miniTurboID. While this would present as a useful reporter system, tagging of the miniTurboID would allow for assessment of localization of the miniTurboID sequence prior to downstream validation.

#### *2.4.4 Electroporation of RNP targeting terminal ends of PROM1*

To transfect a CD133-targeting RNP complex, we first had to optimize electroporation parameters for GBM cells. In looking to the literature, few studies have performed RNP-based editing in primary cells. Thus, electroporation parameters required testing to ensure uptake of the RNP complex. Using a GFP plasmid, we tested five electroporation programs using the Nucleofector II device with 1 million BT241 GBM cells, of the E-013 program showed highest infection, and lowest cell death as measured by GFP signal and 7AAD staining, respectively (**Figure 2B**). In addition to BT241, this electroporation program successfully transfected BT935 (**Figure 2C**). We next sought to assess the N- and C-terminus guide efficacies by complexing guides with various protein quantities (2  $\mu$ g, 5  $\mu$ g, 10  $\mu$ g) at a 3:1 guide to protein ratio. Upon electroporation of 1 million GBM cells, we performed FACS analysis to assess changes in CD133 expression four days post-electroporation. While the guides were not intended to knock-out CD133, site-specific cleavage in the absence of repair template would induce non-homologous end

joining (NHEJ) of *PROM1* leading to detectable mutations and putatively a non-functional protein. Thus, as expected, N-terminus cut proved successful in BT935 at all RNP quantities, with the most potent reduction in CD133 at 10 µg of protein (**Figure 2D**). In BT241, N-terminus targeting did not yield a decrease in total positive cells, however, a population shift was observed at 2 µg of Cas9 protein, indicating putative targeting of *PROM1* (**Figure 2E**). Assessment of the C-terminus cut in BT241 additionally revealed a decrease in CD133 expression at 2 µg of Cas9 protein (**Figure 2F**). While this was indicative of *PROM1* targeting, deep sequencing was required to assess indel frequency and guide specificity at the N and C terminus loci. We then sought to perform next generation sequencing (NGS) of wildtype samples and their RNP-cleaved counterparts.

To prepare for NGS, BT241 and BT935 electroporated with an N- or C-terminus targeting RNP were pelleted for crude genomic extraction using a previously reported method (Gwynne et al., 2020). To amplify genomic regions with putative indels, we utilized a nested PCR approach in which genomic amplicons were amplified and subsequently indexed for identification during sequencing. Primer pairs were designed approximately 100bp upstream and downstream of the cut site to include large frameshift and/or deletions generated by a cut. Using gradient PCR, we optimized annealing temperatures and successfully generated genomic amplicons from all samples for N-terminus cuts (**Figure 3A-B**).

#### 2.4.5 AAV infection of human GBMs

Based on the aforementioned workflow to insert the miniTurboID into *PROM1*, we next sought to assess the infectivity of human GBMs with AAV. Various AAV serotypes

may be utilized with tropism for various tissue types. AAV6, has previously shown to transduce various CNS cell types including glia. However, pseudoserotypes, which encapsulate the genome of one serotype with the capsid of another have previously shown higher transduction efficiency and altered tropism. Thus, we interrogated the tropism of the pseudoserotype AAV2/6 in our samples. We transduced 1M cells of BT241 and BT935 with AAV2/6-GFP at varying multiplicity of infections (MOI). FACS analysis of samples three days post-transduction revealed GFP expression in both BT241 and BT935 at an MOI of 1E4 and above, of which 90% transduction was observed at an MOI of 1E6. Thus, AAV2/6 revealed tropism for human GBM samples at an optimal MOI of 1E6 (**Figure 3B-C**)

#### *2.4.6 Short-term next steps*

In the short-term, we hope to perform the genomic integration of BioID in human GBM specimens. Upon confirmation of guide targeting efficiency by NGS, GBMs will be electroporated with N- or C-terminus targeting RNP, and infected with AAV carrying BioID repair templates for HDR-mediated insertion. Cells will be confirmed for integration by expression of EGFP, and subsequently sorted and validated for BioID expression, localization and biotinylation function.

**Figure 1**

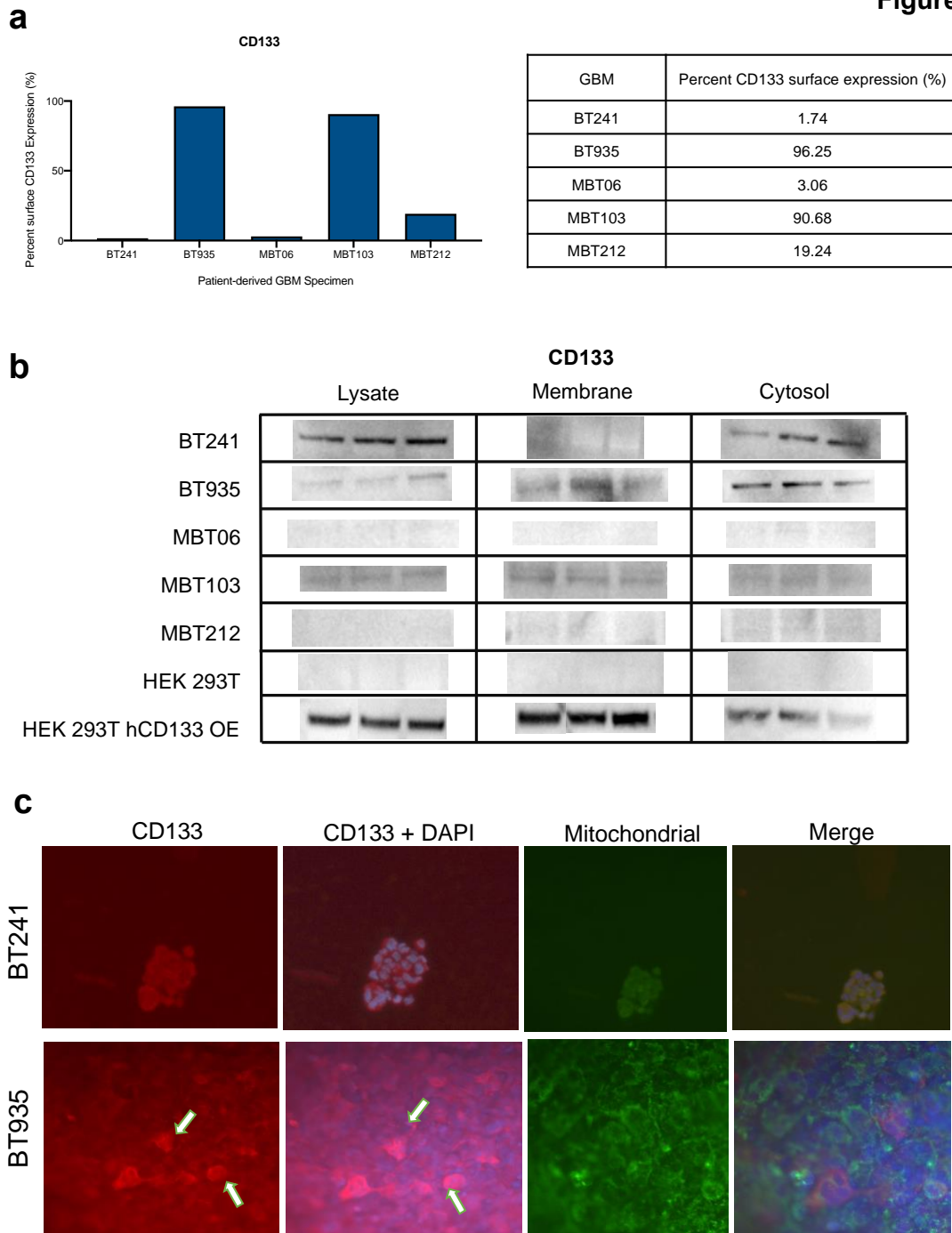


**Figure 1. Human GBMs display differential localization of CD133. a)** GBMs express varying amounts of cell surface CD133 by FACS characterization. **b)** Subcellular (membranous and cytosolic) fractionation of human GBMs reveals differential CD133

localization across specimens. **c**) Immunofluorescence of BT241 (top) and BT935 (bottom) confirms CD133 localization.

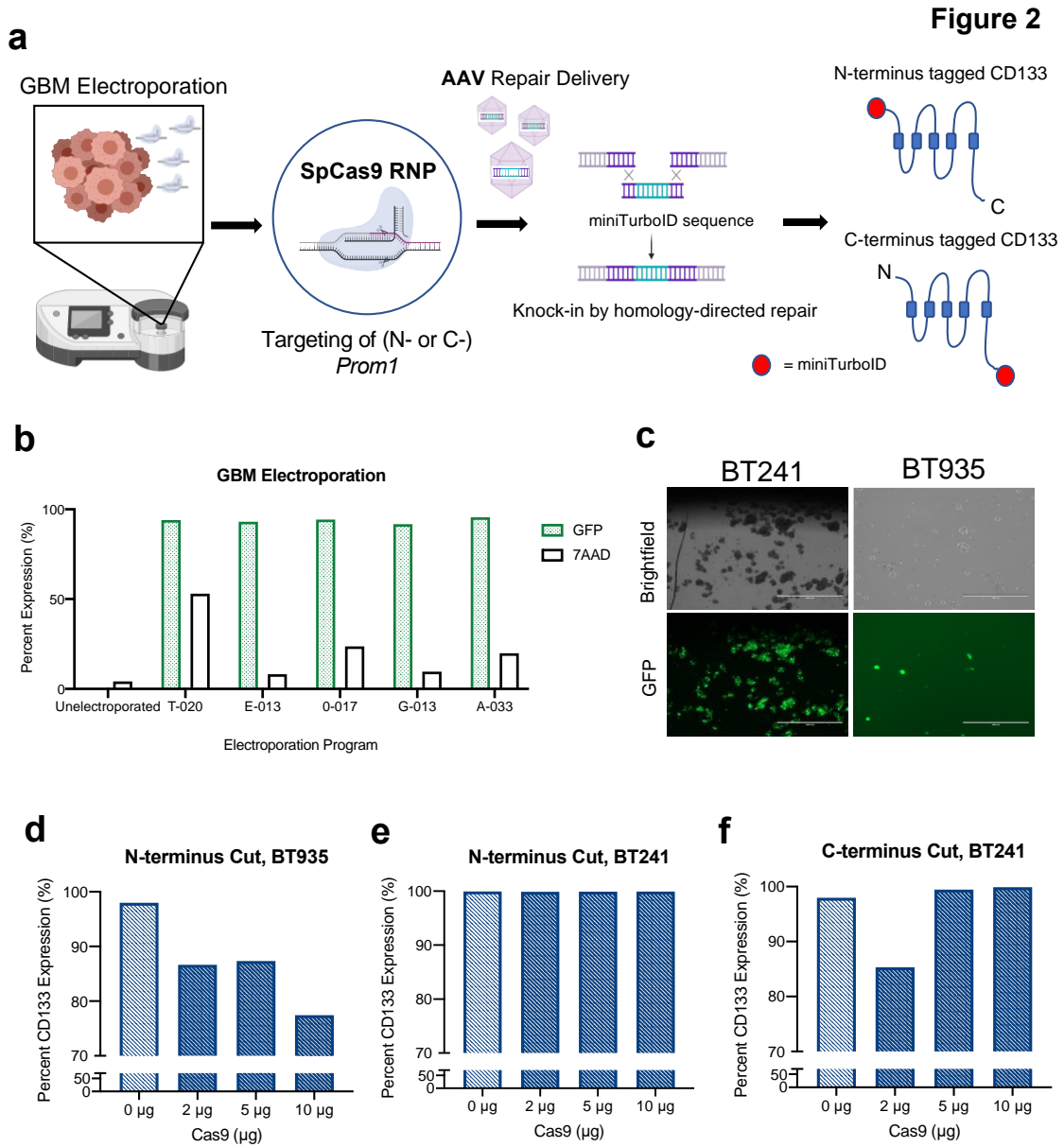


**Figure 2. CRISPR-mediated genomic targeting of CD133 in human GBMs by electroporation of ribonucleoprotein (RNP) complexes.** (a) Schematic on the editing strategy for BioID knock-in in human GBMs for generation of N- and C-terminus tagged CD133. Electroporation of N- or C-terminus-targeting Cas9 RNP in human GBMs generates a site specific cut that is repaired with miniTurboID repair template delivered via AAV. (b) Electroporation of plasmid GFP in BT241 (left) and (c) BT241 and BT935 (right, micrographs) reveals successful infection and low toxicity as measured by GFP

expression and 7AAD staining. (d-f) Electroporation of 2, 5 and 10  $\mu\text{g}$  of *PROM1*-targeting RNP reduces CD133 expression.

**Figure 3**

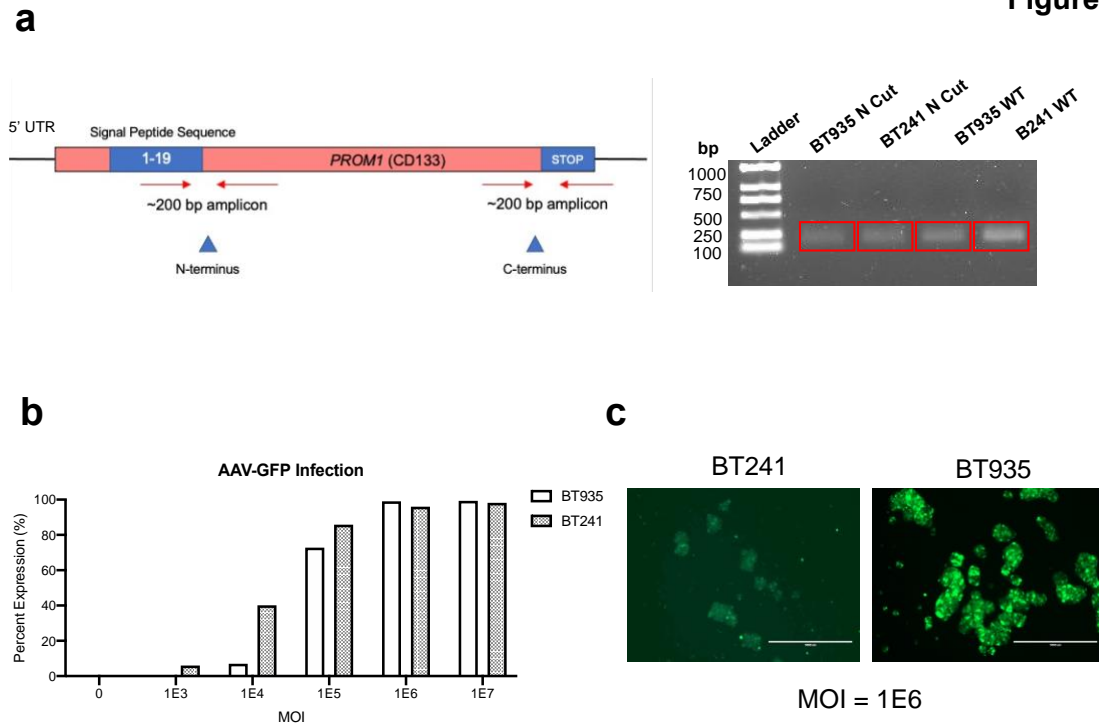
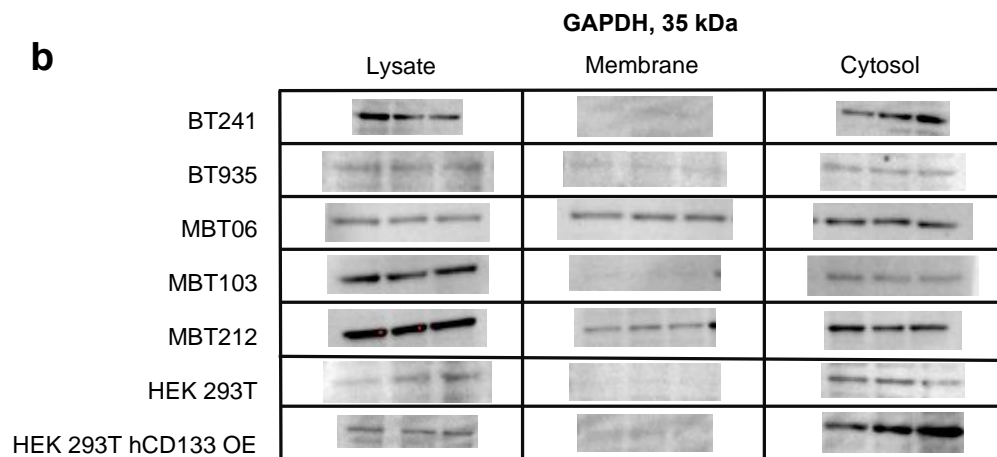
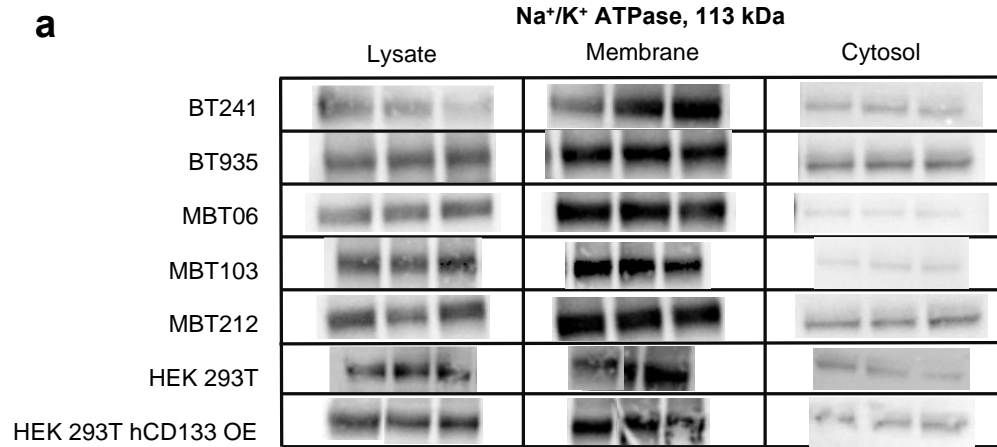


**Figure 3. Next-generation sequencing amplicons, and adeno-associated viral infection generate knock-in of BioID at CD133 loci.** (a) Schematic on the designing of primers for genomic amplification of expected RNP cleavage sites in *PROM1* (right) and N-terminus genomic amplicons (left). Primers were designed to anneal 75bp above the expected cut sites to generate 200 bp sized genomic amplicons for next generation sequencing (b-c) AAV2/6 shows tropism for human GBMs by infection of GFP with an optimal MOI of 1E6.

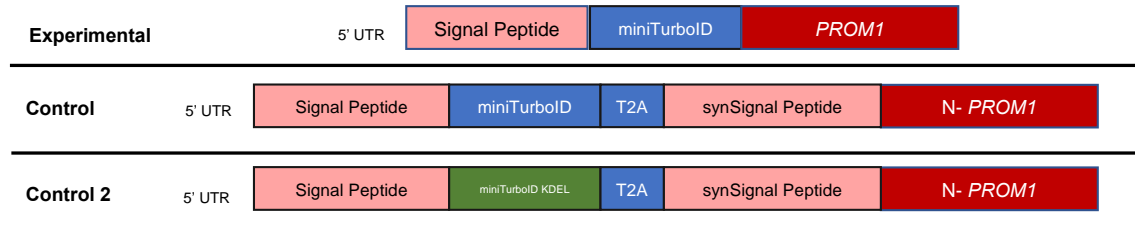
**Supplementary Figure 1**



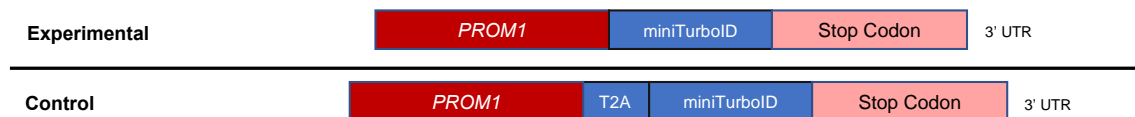
**Supplementary Figure 1 continued**

**C**

***N-terminal***



***C-terminal***



**Supplementary Figure 1. (a)** Sodium-potassium ATPase membrane marker and **(b)** GAPDH cytosolic marker staining of subcellular fractions in **Figure 1. (c)** Repair template design for N- and C-terminus knock-in of BioID into *PROM1*.

**Tables**

**Table 1**

Sample	Diagnosis	Age at Diagnosis	Sex	Survival time from diagnosis (months)
BT241	GBM	68	F	23
BT935	GBM	53	F	7
MBT06	GBM	50	F	Alive
MBT103	GBM	52	F	
MBT212	GBM	68	M	13

**Table 2**

Isoform	Alternative Name	Identifier	Positional Changes Relative to S2
Isoform 1	AC133-1; S2	O43490-1	N/A
Isoform 2	AC133-2; S1	O43490-2	92-100: Missing
Isoform 3	S3	O43490-3	93-101: Missing; 831-839: VETIPMKNM -> SSWVTSVQC; 840-865: Missing
Isoform 4	S10	O43490-4	93-101: Missing; 839-861: Missing
Isoform 5	S7	O43490-5	93-101: Missing; 831-861: Missing
Isoform 6	S11	O43490-6	831-861: Missing
Isoform 7	S12	O43490-7	839-861: Missing

## **CHAPTER 3: Generation and validation of allogeneic CAR-T therapy against CD133**

In this chapter, we aimed to generate an allogeneic CAR-T therapy targeted against CD133 in human GBM.

### **3.1. Materials and Methods**

#### *3.1.1. T-cell Expansion*

Human peripheral blood mononuclear cells (PBMCs) were acquired from consenting healthy blood donors using SepMate™ (STEMCELL technologies) as approved by the Health Science Research Ethics Board. Upon immunomagnetic enrichment of CD3<sup>+</sup> cells using the SepMate™ Human T Cell Isolation Kit, isolated T-cells were seeded into a 24-well dish in XSFM T-cell media supplemented with recombinant human (rh) IL-2 (100 IU/mL), rhIL-15 (5 ng/mL) and rhIL-7 (1ng/mL) at  $1.2 \times 10^6$  per well. Cells were activated with 90 µL of human T-cell TransAct™ in 900 µL of supplemented XSFM and expanded for 14 days prior to experimentation.

#### *3.1.2. Generation of lentiviral-transduced “autologous” CAR-Ts*

Twenty four hours after activation, T-cells were transduced with a CAR-lentivirus at a multiplicity of infection (MOI) of 2. CAR-T cell cultures were then expanded using fresh, supplemented XSFM media supplemented for 7 days prior to FACS characterization, followed by an additional 7 days of expansion prior to experimentation.

#### *3.1.3. Generation of allogeneic CART133*

Knockouts were performed by electroporation of complexed Alt-R® As Cas12a with the TRAC-targeting guide at a 3:1 guide to protein molar ratio for 15 minutes at room

temperature. Using Lonza Amaxa System Kits, 3M T-cells were resuspended in the provided electroporation buffer and gently mixed with complexed RNP. The mixture was removed to an electroporation cuvette where the T-023 electroporation programs (Nucleofector IIb, Lonza Biosciences) was used. For sole assessment of knock-out, cells were gently resuspended in their respective media and incubated in a 12-well dish for four days prior to flow cytometric characterization. For knock-in, cells were plated at a density of 200,000 cells in 50 $\mu$ L of respective media with AAV at an MOI of 1E6 gc/cell. Cells were then be cultured for 2-7 days prior to flow cytometric characterization, and for 14 days prior to experimentation.

#### *3.1.4 Activation/Exhaustion and Cytokine Release Assays*

CAR-T cells were co-incubated with GBM cells at an effector: target (E:T) ratio of 1:1 for 24 hours to assess activation. Cells were analyzed for expression of activation markers CD25 and CD69, and the exhaustion marker CD69 by FACS. BD Cytometric Bead Array Kit will be used for flow cytometric quantification of cytokines independently for CAR-T co-cultures, and blood plasma, according to manufacturer's description. Briefly, in each tube 50  $\mu$ L of either Cytokine Standards dilution or supernatant, 50  $\mu$ L of Cytokine Capture Beads and 50  $\mu$ L of PE Detection Reagent will be added. After three hours of hour incubation at room temperature, the beads will be washed and acquired on a MoFlo XDP flow cytometer (Beckman Coulter), setup using Cytometer Setup Beads.

#### *3.1.4. Luciferase-Based Cytotoxicity Assay*

Luciferase-expressing GBM cells were plated in triplicates at a concentration of  $3.0 \times 10^4$  cells per well. Effector cells were then added at the E:T ratios 4:1, 2:1, 1:1 and 0:1 in a final

volume of 200  $\mu$ L of XSFM media and 75  $\mu$ g/mL of D-luciferin potassium salt, . Bioluminescence intensity (BLI) was measured as relative luminescence units (RLU) by an Omega luminometer for 10 seconds. Cells were treated with 1% Nonidet P-40 (NP40) lysis buffer as a measure of maximal lysis. Target cells incubated without effector cells were used to measure spontaneous death RLU. The readings from triplicates were averaged and percent lysis was calculated with the following equation:

$$\% \text{ Specific lysis} = 100 \times (\text{spontaneous death RLU} - \text{test RLU}) / (\text{spontaneous death RLU} - \text{maximal killing RLU}).$$

### 3.1.5. *In vivo Orthotopic Injections and H&E Staining of Xenograft Tumors*

Animal studies were performed according to guidelines under Animal Use Protocols of McMaster University Central Animal Facility (AUP #19-01-01). Intracranial injections were performed as previously described using 200K-1M cells of primary GBMs in 8-12 week old NSG mice (Chokshi, Savage, Venugopal, & Singh, 2020). For tumor volume evaluation, animals are sacrificed when mice reach endpoint, and perfused with 10% formalin. Brains will be extracted and sliced at 2 mm thickness using a brain-slicing matrix for paraffin embedding and H&E staining. Images are captured using an Aperio SlideScanner and analyzed using ImageScope v11.1.2.760 software (Aperio). For survival studies, all the mice will be kept until they reach endpoint and number of days of survival will be noted for *Kaplan-Meier* Analysis.

### 3.1.6. *Statistical Analysis*

Respective data is represented as mean $\pm$ SEM, *n* values are listed in figure legends. Student's t-test analyses, two-way ANOVA with Bonferroni post-hoc tests, and Log-rank

(Mantel-Cox Test) analysis were performed using GraphPad Prism 5.  $P < 0.05$  is considered statistically significant.

## 3.2. Results

### 3.2.3. *KiKo* design for the generation of *alloCART133*

To generate an allogeneic CART133 (*alloCART133*), we looked to previously published works for editing strategies. One such strategy published by the Chen group utilized a knock-in, knock-out (KiKo) technique in which the TCR was knocked-out by RNP, and the CAR sequence was inserted by HDR at the same loci. This strategy has been previously reported to reduce tonic CAR signalling, as well as regulate expression and downregulation of the CAR, and thus regulate T-cell differentiation and exhaustion (Eyquem et al., 2017; Long et al., 2015). To generate the *alloCART133*, we utilized the two-step approach previously highlighted in Chapter 2, in which the genomic locus of interest is first targeted by RNP, and subsequently repaired by HDR leading to insertion of an exogenous repair template delivered by AAV. Thus, we designed a Cas12a (Cpf1) guide RNA (gRNA) targeting the first exon of the TCR alpha locus (*TRAC*) (**Figure 4A**).

**TRAC1 Guide:** GAGTCTCTCAGCTGGTACAGG

HDR templates containing a second-generation CAR sequence with a CD8 $\alpha$  hinge, CD28 co-stimulatory domain, CD3 $\zeta$  signaling domain, truncated EGFR (EGFRt) tag, and small chain variable fragment (scFv) targeting CD133 (CART133). These HDR templates utilized the same sequence used to generate the traditional, lentiviral-transduced CD133-targeting CAR (CART133). However, this template lacked an

exogenous promoter, and was flanked with 200 bp homology arms for integration at the *TRAC* cut site, in an AAV2 backbone (pAAV2).

### 3.2.1 *Efficient knock-out of TCR by RNP electroporation*

We next sought to assess TCR KO efficacy by T-cell electroporation. To determine optimal electroporation parameters, we electroporated a GFP plasmid into isolated human T-cells on Day 3 post-activation using a previously optimized electroporation program (T-023, Nucleofector II). After four days of expansion, we performed FACS analysis and observed 33% infection as measured by GFP expression, confirming uptake of plasmid using these electroporation parameters (**Figure 4B-C**). We next sought to assess whether electroporation of TCR-targeting RNP could generate efficient knock-out in human T-cells. However, unlike plasmid electroporation, consideration of complexing parameters and day of T-cell expansion required investigation. In accordance with previously published work, we conducted a preliminary study in which we would electroporate T-cells on Day 3 post-activation. As the accessory TCR molecule CD3 is the primary mode of activation in our culturing techniques, early TCR KO could putatively affect the extent of T-cell expansion post-editing. Thus, editing on Day 3 would allow T-cells to acquire an activated phenotype and continue to expand despite TCR KO. For RNP complexing, we first attempted complexing *TRAC* guide and Cpf1 protein at a 3:1 guide to protein ratio for 15 minutes at room temperature. While theoretically one mole of guide and one mole of protein would generate a functional RNP, adding additional guide would ensure complexing of all available protein. Using these set parameters, we sought to test RNP-targeting efficacy by electroporation 2 µg, 5 µg or 10 µg of complexed RNP per million

T-cells, in accordance with manufacturer recommendations. An additional non-targeting control guide (AsNeg1) was complexed with Cpf1 to confirm guide specificity and ensure electroporation did not affect TCR expression alone. After expanding electroporated cells for additional four days, we observed a 90% reduction in TCR expression by FACS analysis with as low as 2  $\mu$ g of RNP (**Figure 4D, Supplementary Figure 2A**). While there was some reduction in viability by electroporation, this effect was minimal, and healthy edited cells continued to expand. Thus, while complexing and T-cell characteristics were fixed parameters, editing was highly efficacious, leading us to proceed with the above parameters for generating a cut in the *TRAC* locus.

### 3.2.2 *CAR Integration by AAV Infection and TCR<sup>+</sup> Cell Depletion*

Prior to use of AAV, we first sought to assess various strategies for delivery including plasmid co-electroporation, isolated repair co-electroporation, and AAV. Repair delivery by plasmid and RNP co-electroporation at 15  $\mu$ g, 10  $\mu$ g, and 5  $\mu$ g, and repair template/RNP co-electroporation proved toxic and insufficient for knock-in in T-cells by FACS analysis (**Supplementary Figure 2B-E**). This may have been as a result of co-electroporation of large sized DNA fragments along with RNP, or due to impurity of DNA product. This could have been mitigated by assessing double electroporation (RNP and then repair), and purification of DNA fragments. While these strategies have previously been successfully used, we believed that AAV was the optimal approach for repair template delivery to avoid toxicities associated with the prior approach (Webber et al., 2019). The AAV strategy was additionally promising as a much higher quantity of repair DNA could be infected to increase the likelihood of an HDR event.

In looking to the literature, knock-in events in primary T-cells were observed upon AAV infection at an MOI of  $1E6$  AAV genome copies, approximately 2-4 hours after RNP electroporation (Dai et al., 2019; Eyquem et al., 2017). Thus, we first attempted to infect T-cells at various MOIs ( $1E5$ ,  $1E6$  and  $1E7$ ) three hours post-electroporation for successful CAR integration. After five days of expansion, FACS analysis revealed a lack of successful integration as measured by EGFRt expression (**Supplementary Figure 2F**). We hypothesized that this may have been due to either AAV purity, or time of infection post-electroporation. To assess whether optimizing time of infection post-electroporation could yield successful integration, we performed a sample insertion in Jurkat cells, an immortalized T-lymphocyte line. Successful integration would yield a 1180 bp DNA fragment flanking the *TRAC* cut site, which we observed with AAV infection in Jurkat cells one-hour post-electroporation of RNP. Interestingly, we did not observe integration of Jurkat cells at four hours post-electroporation (**Supplementary Figure 2G**). Thus, we attempted to conduct a time-course experiment at a fixed MOI ( $1E6$ ) in primary T-cells in which we would infect with AAV immediately, 30 minutes, one hour, 2 hours, and 4 hours post-electroporation. We additionally utilized a new AAV batch with high purity. At all timepoints, we found successful integration in human T-cells as measured by expression of EGFRt and TCR by FACS analysis. As we observed integration at all timepoints irrespective of the time to addition, we concluded that AAV purity, indicated by isolated bands of AAV capsid proteins (VP1, 2 and 3) by SDS-PAGE was the limiting factor for integration (**Figure 5A, Supplementary Figure 2H**). While time to AAV

infection was not limited for successful integration, we observed the highest integration in primary human T-cells with immediate infection after electroporation.

We next sought to assess the stability of population EGFRt expression. We observed increased proliferation of TCR-positive control cells, in comparison to their knock-out counterparts in accordance with previously published works (Stenger et al., 2020). FACS analysis of knock-out revealed a shift in population TCR expression in which we observed only 18% TCR expression on Day 7, which increased to 48% on Day 13. This would be important to consider in the generation of alloCART133 as heterogeneous products could confound conclusions on the efficacy of the CAR, and putative toxicity. Thus, we validated the use of an immunomagnetic TCR-positive depletion kit which purified heterogeneous TCR-KO products from any remaining TCR<sup>+</sup> cells, as detected by flow cytometry. Therefore, using RNP electroporation, immediate infection and TCR-depletion, we successfully generated alloCART133 in three primary T-cell biological replicates (Leuk10, 12, 14 post TCR-depletion), in which we observed EGFRt expression ranging from 35% integration to 50%, indicating high yield, efficacious knock-in editing (**Figure 5C**).

### *3.2.3 Generation of an alloCART133 expansion protocol*

We next sought to establish a reliable expansion protocol for edited T-cells, particularly alloCART133. Akin to previous literature, expansion of alloCART133 has proven challenging (Depil et al., 2020). While editing has been successful, generating large enough quantities of edited T-cells for pre-clinical assessment required optimization. Thus,

we revisited the initial editing protocol to assess the efficiency of each step in the alloCART133 generation and expansion protocol. The initial protocol consisted of purifying CD3<sup>+</sup> T-cells, activating with soluble activator for three days, and then editing 1M T-cells in a single reaction with 2 µg of complexed Cpf1 RNP. All edited cells were then plated in a 24-well dish and infected with AAV at an MOI of 1E6 gc/cell in a volume of 500 µL of supplemented T-cell media and moved to a flask the next day. Cells would then be topped up the next day and expanded in a T75 flask for an additional seven days prior to immunomagnetic TCR-depletion, flow characterization and freezing. This initial expansion protocol rarely yielded more than 1M alloCART133<sup>+</sup> cells, from as many as 6M edited cells. To generate larger T-cell quantities, we first sought to ensure that we were expanding and editing only T-cell populations. Flow cytometric characterization pre- and post-CD3 immunomagnetic enrichment isolated for solely T-cell populations (pre-enrichment CD3<sup>+</sup> Leuk10 = 81.25%; post-enrichment CD3<sup>+</sup> Leuk10 98.65%), suggesting that the pre-editing product was pure (**Supplementary Figure 3A**). To increase final alloCART133 yields, we next sought to assess whether we could edit more cells per reaction with similar editing efficiency. In comparison to 1M cells per reaction, editing efficiency remained comparable at 3M cells with 2 µg of *TRAC*-targeting Cpf1 (**Supplementary Figure 3B**). While this ensured that we were editing more cells to increase yields, these early steps were not sufficient to increase final alloCART133 numbers as the pooled cells failed to expand post-edit. To optimize post-edit expansion, we sought to assess whether changing cell density could impact edited T-cell expansion. We did this by editing 3M T-cells and plating them in 24-wells immediately post-edit at either

a density of 0.5M cells or 1M cells. The next day, T-cells were spun down and resuspended in fresh media and moved to a 6-well dish or kept in a 24-well. After seven days of culturing, we found that plating cells at an initial density of 1M cells, and then replating in a 24-well yielded the highest quantity of pooled cells (19.2M), while plating in a 6-well yielded 11.62M. Plating at an initial density of 0.5M cells yielded lower total T-cell numbers across all expansion conditions (**Supplementary Figure 3C**). While this was promising, immunomagnetic depletion of TCR-positive cells post edit depleted 95% of cells, indicating that expanded T-cells were unedited. This was later confirmed by flow cytometric evaluation. Thus, we sought to improve the total editing efficiency of T-cells to yield higher final alloCART133 cells. To do so, we performed AAV infection in the original 24-well (1M) versus a 96-well round bottom dish at a density of 200,000 cells per well, in 50  $\mu$ L. Knock-in efficiency increased from 11.77% to 42.17% in the 96-well, likely due to increased contact of viral particles with cells in lower volumes, and spatial density (*data not shown*). However, despite optimization at all steps of allogeneic CAR-T generation, edited Leuk10 cells rarely expanded to high enough numbers for pre-clinical evaluation. Thus, we sought to assess whether PBMCs from different patient samples could edit and expand better than Leuk10. Editing in Leuk12, another leukapheresis product derived from a healthy donor, generated even higher knock-in efficiency and expansion. Pre-TCR-depleted products had 44% expression of EGFRt (CAR marker), and 3% TCR<sup>+</sup> cells, indicating 97% TCR KO cells. Post-depletion eliminated all TCR<sup>+</sup> cells and increased relative CAR frequency to 47%. Even more so, these cells expanded post-editing to generate 10M CAR<sup>+</sup> cells (20M cells) from 6M edited cells (*data not shown*). Thus, while

we observed better growth kinetics and editing with different strategies, the expansion of Leuk12 revealed that these differences were likely due to intrinsic PBMC product characteristics. Thus, we were able to define an optimized expansion protocol, as well as identify sample to sample variations in editing efficiency and yield.

#### 3.2.4 *In vitro* treatment of alloCART133 shows comparable efficacy to CART133

We next sought to assess the pre-clinical efficacy of alloCART133 by performing *in vitro* cytotoxicity and activation assays using a patient-derived GBM specimens expressing high levels of CD133; BT935. To test CAR specificity against CD133, we additionally performed this assay in HEK 293T (overexpression). After engineering these target cells with firefly luciferase and infrared red fluorescent protein (iRFP), we co-cultured control CAR (CAR CON), the autologous CAR (CART133), TRAC-KO cells and alloCART133 for 24 hours. Cytotoxicity, as measured by lower luminescence signal, was preferentially observed in CD133-targeting effector cells (CART133 and alloCART133) at various effector to target ratios (E:T) in BT935 using Leuk10 (**Figure 6A, Supplementary Figure 4A**) and Leuk12 edited cells (**Supplementary Figure 4B**). AlloCART133 showed relatively comparable cytotoxicity in BT935 in comparison to CART133. In contrast, no cytotoxicity was observed in HEK 293T confirming specificity of the CAR in alloCART133 and CART133 in Leuk10 cells (**Figure 6B, Supplementary Figure 4C**). These findings were assessed in two biological T-cell replicates, Leuk10 and Leuk12, confirming the replicability of comparable capacity of alloCART133 and CART133 irrespective of PBMC derivation.

We next performed activation assays by FACS characterization of CAR CON, CART133, *TRAC*-KO and alloCART133 after 24 hours of co-culturing with target cells at an E:T ratio of 1:1 using Leuk10 cells in CD133<sup>HIGH</sup> lines GBM8 and BT935, as well as negative control HEK 293T. To assess activation, we stained cells with the early activation marker CD69, as well as the activation/exhaustion marker PD-1 in CD4 and CD8 T-cell products. We observed significant and preferential activation of alloCART133 when co-cultured with CD133-expressing cells (BT935, GBM8), in comparison to non-targeting T-cell products (*TRAC*-KO and CAR CON)(**Figure 6C-J**). While CART133 showed more potent activation, alloCART133 showed lower basal and non-specific activation as measured by CD69 expression, and/or exhaustion, as measured by PD-1 expression in the absence of target cells relative to both CAR CON and CART133, particularly in the CD4 fractions (**Figure 6E, H-J**). While PD-1 is not a discriminate exhaustion marker alone, lower levels of PD-1 expression in alloCART133 may be indicative of reduced exhaustion. This may be due to reduced tonic signalling associated with traditional CAR-Ts that is mitigated in alloCART133 by control of CAR expression by the endogenous TCR promoter. Thus, the cumulation of these results suggested that alloCART133 showed *in vitro* preclinical efficacy against CD133-expressing GBMs, and lower basal activation relative to CART133.

### 3.2.5 *In vivo* treatment of alloCART133 shows moderate tumor control

While we observed differences in *in vitro* behaviour of alloCART133 in comparison to CART133, we sought to compare their pre-clinical efficacy in an intracranial, *in vivo* patient-derived xenograft of human GBM. Thus, we engrafted 1M BT935 expressing

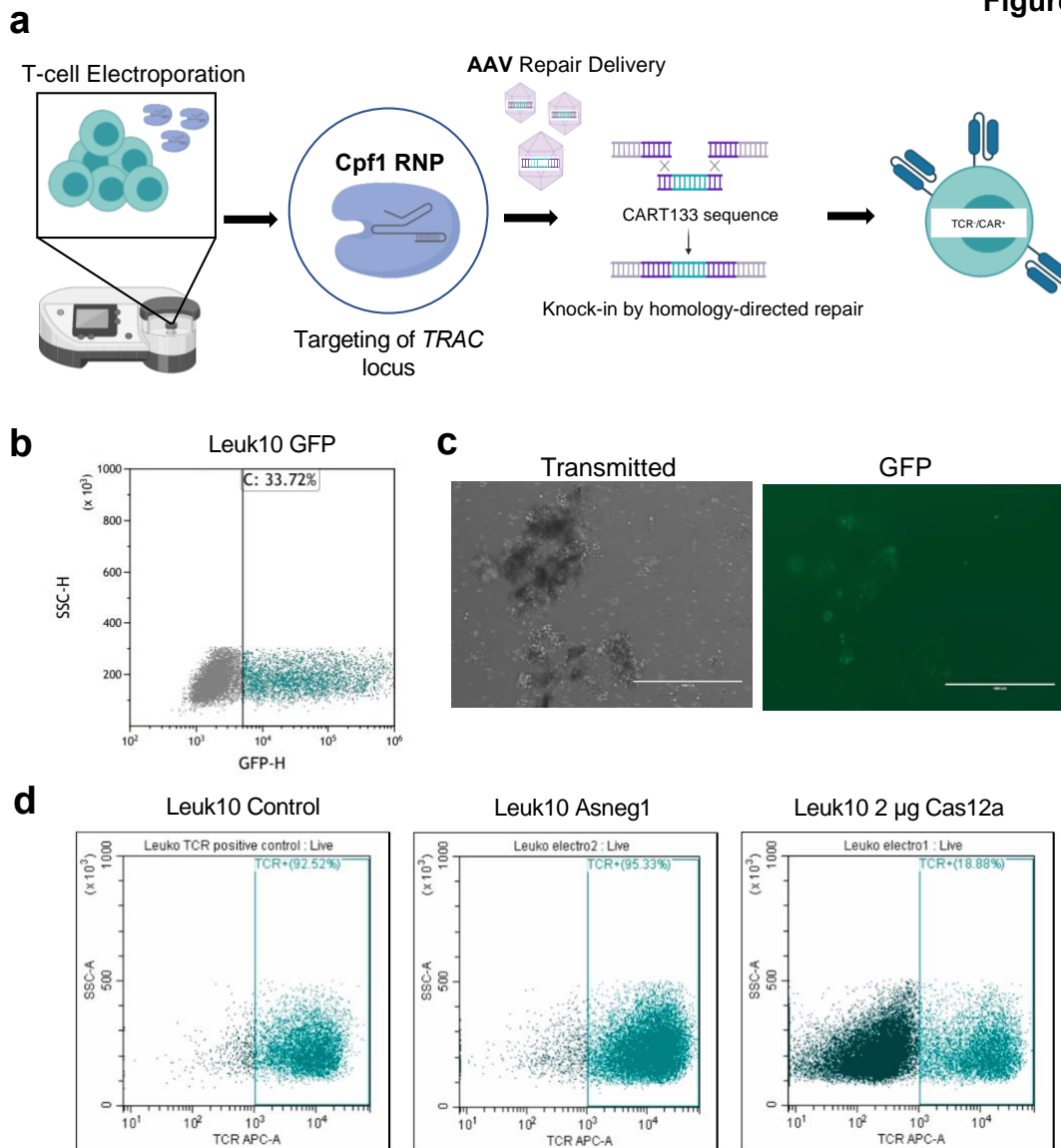
firefly luciferase in 8–12-week-old NOD/SCID/IL-2R $\gamma$ -null (NSG) for treatment (N=24). Upon confirming engraftment of BT935 using the *in vivo* imaging system (IVIS) to detect luminescence signal, we randomized mice based on basal tumor volume into four treatment cohorts: CAR CON, TRAC-KO, CART133 and alloCART133. We next treated mice intratumorally with two doses of 1M T-cells (CAR CON and TRAC-KO) or CAR-expressing cells (alloCART133 and CART133) over a two-week period. While the experiment has not reached endpoint to assess survival differences, weekly imaging by IVIS has currently revealed modest tumor control in alloCART133-treated mice, and more robust tumor control in CART133. As expected, mice bearing tumors treated with TRAC-KO cells harbour the largest tumor volume, followed by CAR CON, alloCART133 and CART133. As TRAC KO cells do not express the TCR, allogeneic effects may modestly reduce tumor volume as comparatively observed in CAR CON. This phenomenon may additionally be observed in CART133 (**Figure 6K**). However, activation kinetics observed in *in vitro* assays may explain the current changes in tumor kinetics. As CART133 showed rapid and robust activation, tumor control may be more robust earlier on in comparison to alloCART133. While alloCART133 showed activation, reduced constitutive signalling and exhaustion may allow for CAR persistence and long-term tumor control.

### 3.2.6 Short-term next steps

In the immediate future, we plan to collect *in vitro* activation, cytotoxicity and cytokine release data in BT935, GBM8 and HEK 293T. The initial set of experiments did not include TRAC-KO as a control, which was later deemed necessary as CAR CON was

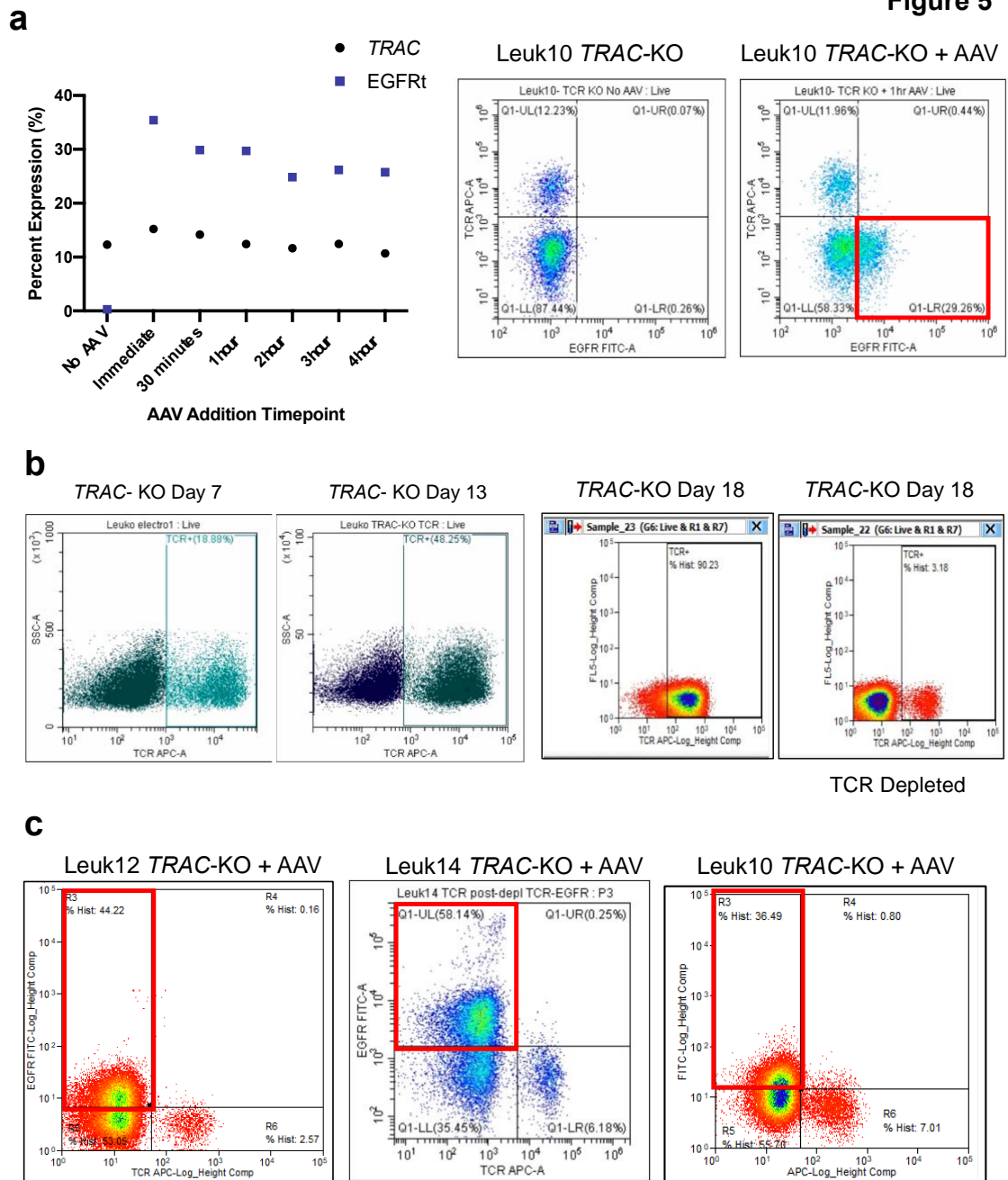
an inappropriate control for allogeneic CARs edited in a different manner. This data will also be extended *in vivo*, in which we plan to collect survival data and tumor burden data at endpoint for BT935. This will allow us to compare efficacy of alloCART133 to CART133. Xenograft studies will additionally be extended to a biological replicate (GBM8) to ensure that efficacy is “universal” and not mediated by tumor-specific factors.

**Figure 4**



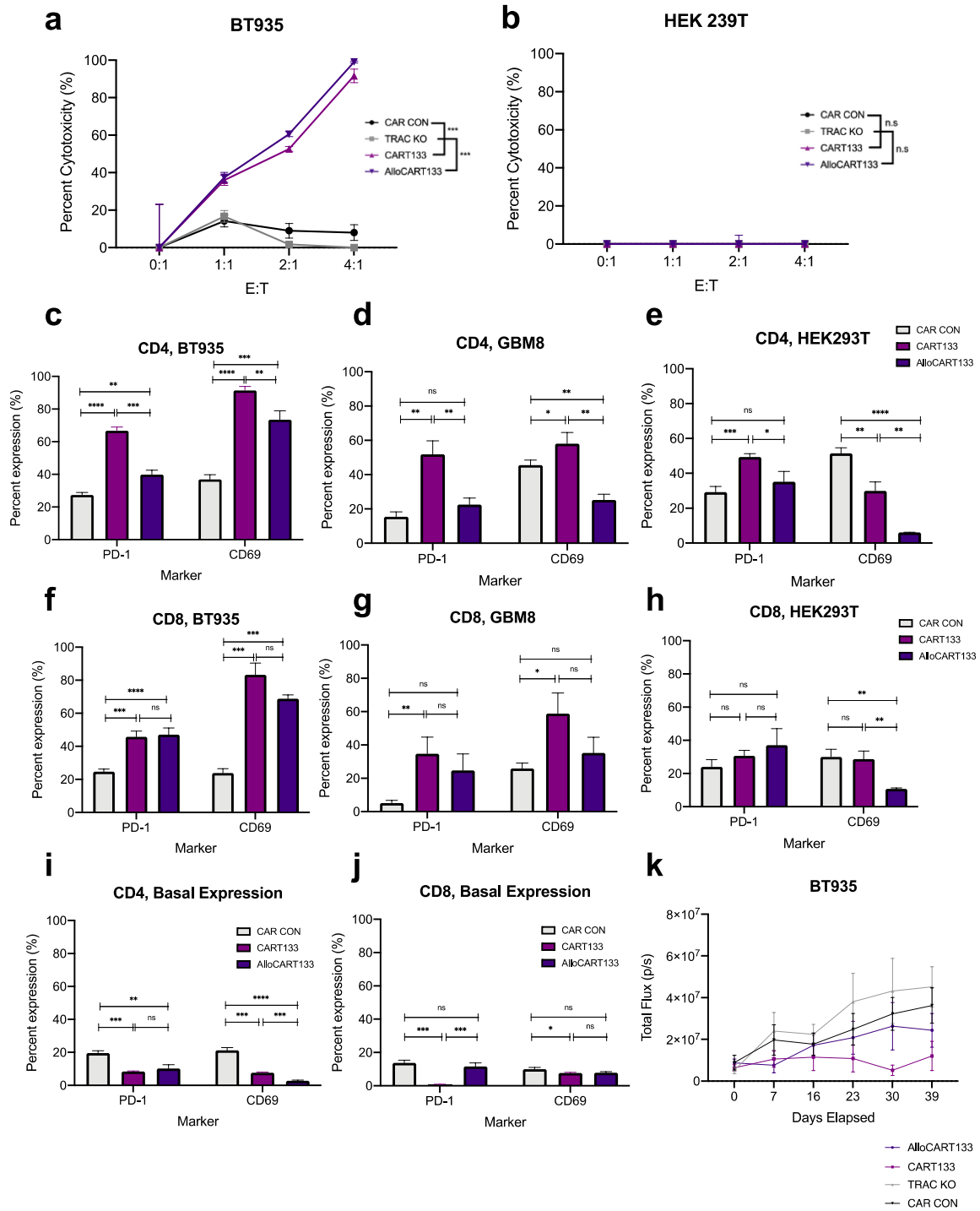
**Figure 4. Editing in primary T-cells reveals efficient TCR knockout by RNP electroporation.** (a) Schematic on KiKo editing strategy for generation of allogeneic CART133 in primary T-cells. Electroporation of TRAC-targeting Cpf1 generates a knock-out followed by knock-in of CART133 sequence by homology-directed repair upon AAV infection. (b-c) Electroporation is a viable transfection strategy in T-cells as shown by electroporation of GFP plasmid. (d) Electroporation of TRAC-targeting RNP successfully knock-out TCR in primary T-cells at 2  $\mu$ g of complexed, electroporated RNP in Leuk10 cells.

**Figure 5**



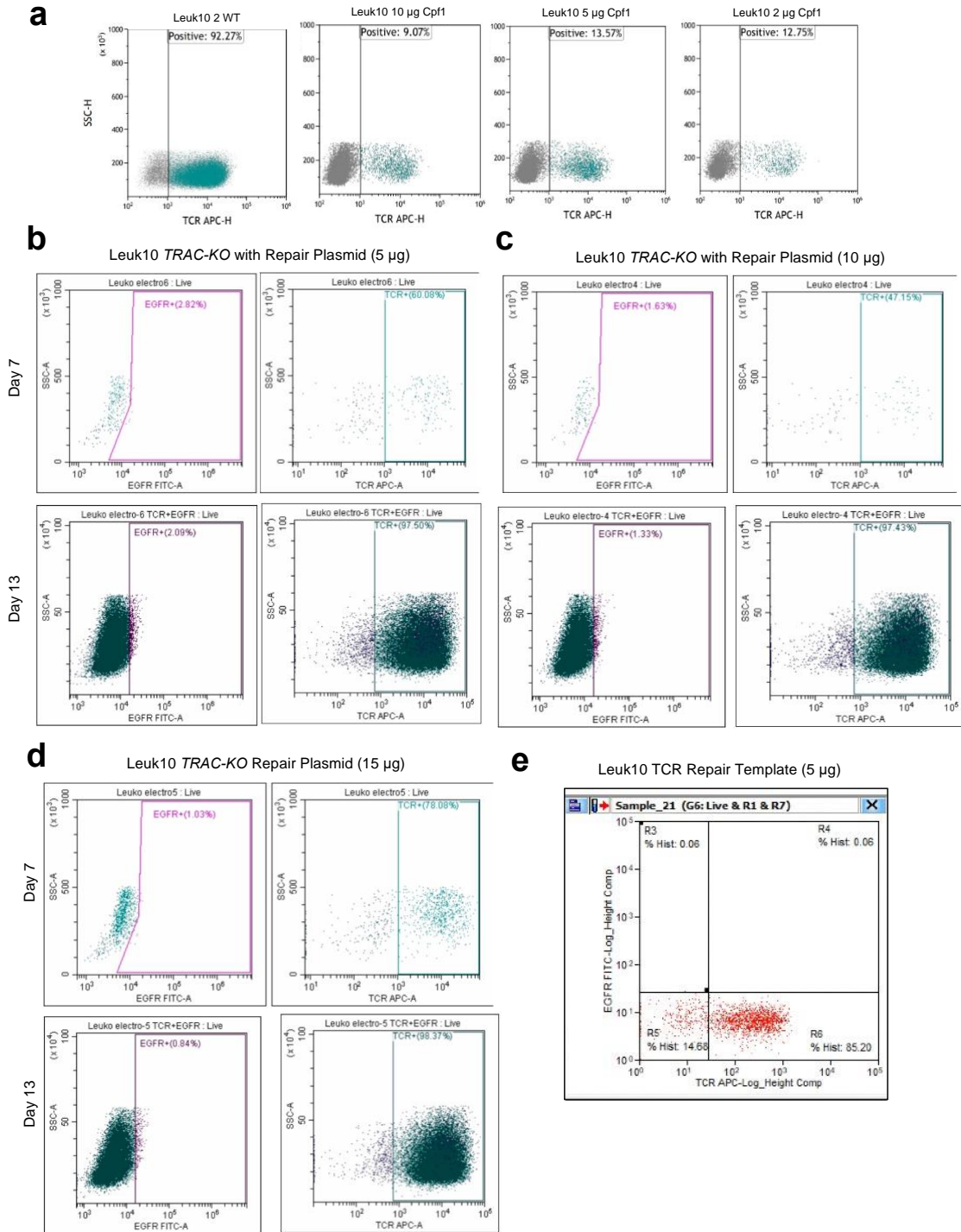
**Figure 5: CART133 knock-in successfully generated alloCART133 and requires TCR<sup>+</sup> cell depletion.** (a) Time-dependent infection of AAV-CART133 after RNP electroporation reveals successful knock-in at all timepoints as measured by EGFRt expression. (b) TCR<sup>+</sup> cells out-proliferate TCR-KO cells and require immunomagnetic depletion from knock-out pool. (c) KiKo strategy and TCR depletion reveals high efficiency editing in three biological primary T-cell replicates.

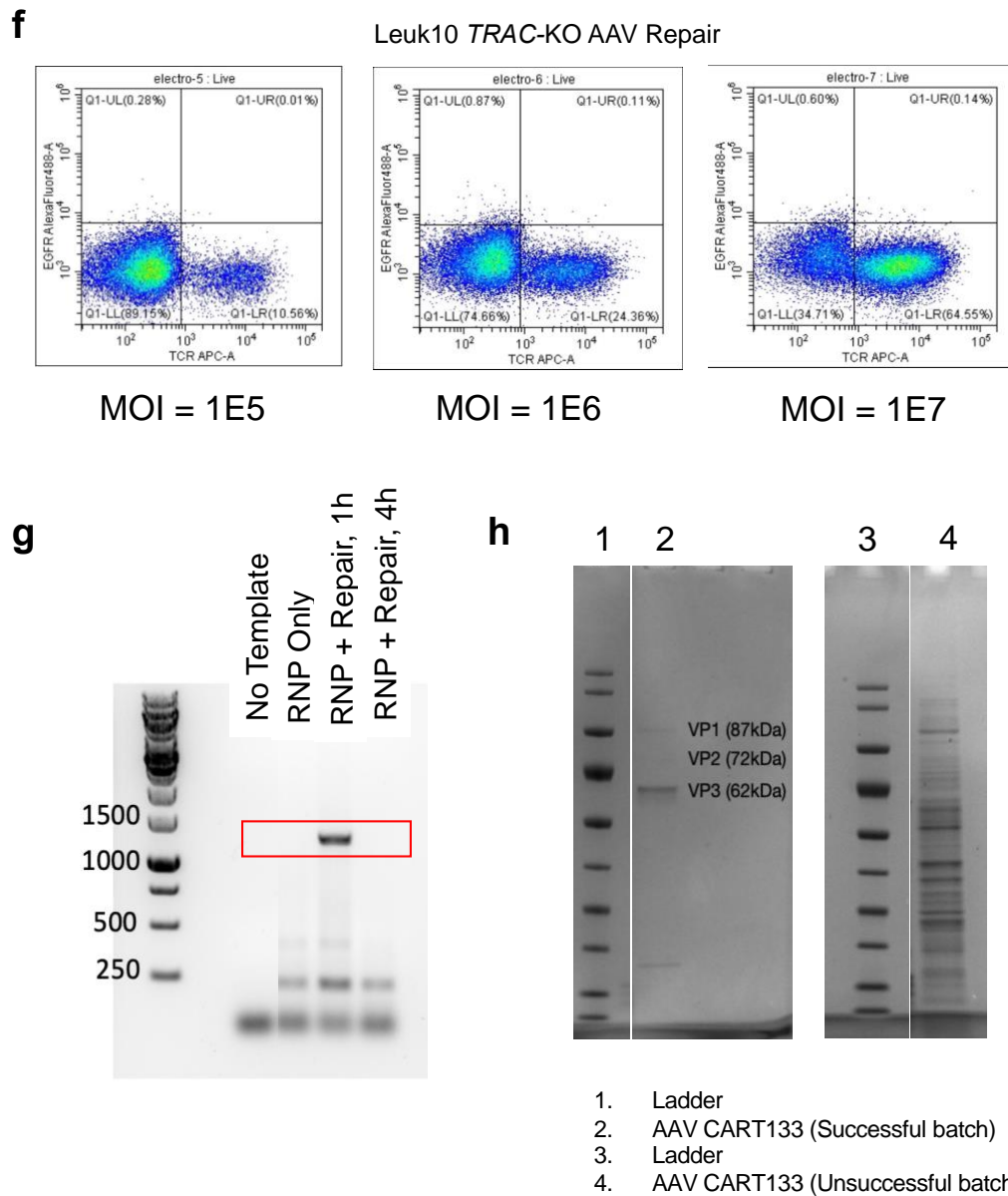
**Figure 6**



**Figure 6: AlloCART133 shows anti-tumor efficacy in vitro and in vivo in patient-derived GBM xenografts.** Cytotoxicity assay of (a) BT935 and (b) in Leuk10 edited cells reveals comparable CART133 and alloCART133 killing. Activation (CD69) and exhaustion (PD-1) marker expression of CD4<sup>+</sup> Leuk10-edited T-cells when co-cultured with CD133<sup>HIGH</sup> lines (c) BT935, (d) GBM8 and CD133<sup>-</sup> line (e) HEK 293T shows comparable phenotype of AlloCART133 to CART133 in the presence of CD133. Activation and exhaustion marker expression of CD8<sup>+</sup> Leuk10-edited T-cells when co-cultured with CD133<sup>HIGH</sup> lines (f) BT935, (g) GBM8 and CD133<sup>-</sup> line (h) HEK 293T shows comparable phenotype of AlloCART133 to CART133 in the presence of CD133. Activation and exhaustion marker expression of (i) CD4<sup>+</sup> and (j) CD8<sup>+</sup> basal Leuk10-edited T-cells shows lower basal activation and exhaustion of AlloCART133 in CD4<sup>+</sup> cells. (k) *In vivo* T-cell product treatment in BT935 reveals modest tumor control in mice treated with CART133 and alloCART133. Points represent mean of three technical replicates. Error bars represent standard error of the mean. \* $p \leq 0.05$ , \*\* $p \leq 0.001$ , \*\*\* $p \leq 0.0001$ ; \*\*\*\* $p \leq 0.00001$ ; multiple t-tests with Holm-Sidak correction.

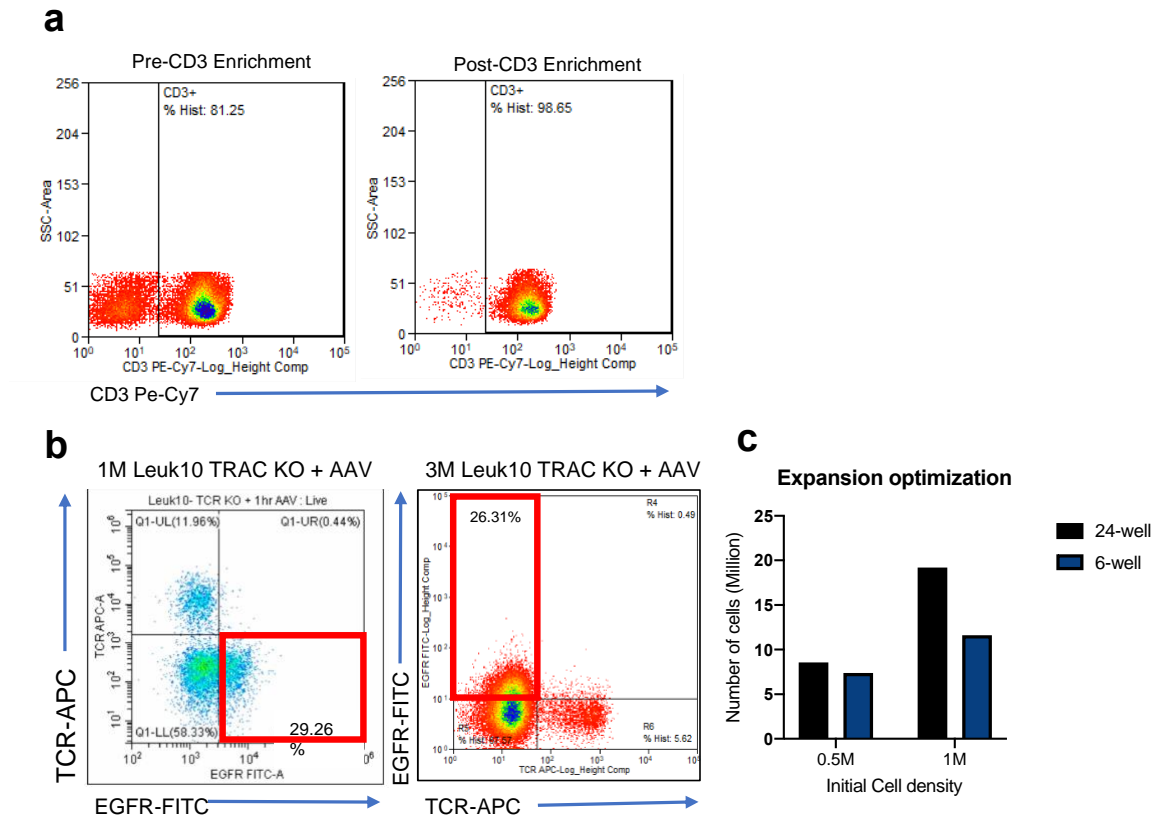
Supplementary Figure 2





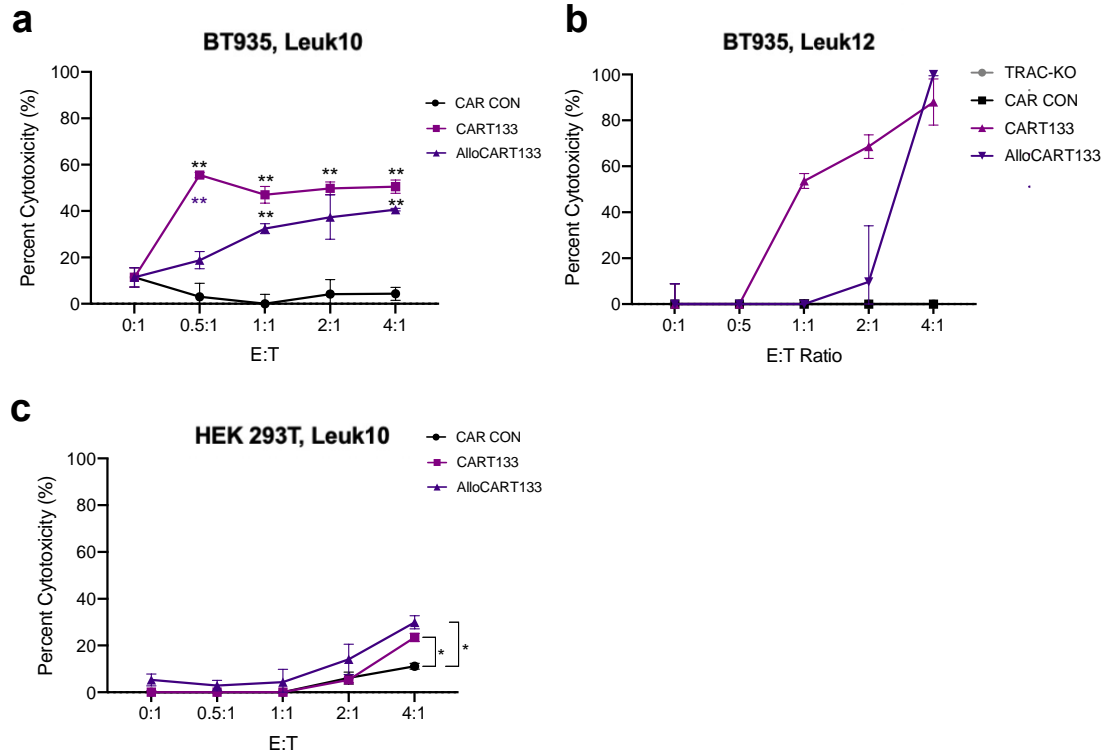
**Supplementary Figure 2.** (a) 2  $\mu$ g of TRAC-targeting RNP in Leuk10 cells is sufficient to efficiently knock-out TCR expression. (b-d) Co-electroporation of repair template containing CAR sequence in plasmid did not generate knock-in at 5, 10 and 15  $\mu$ g of plasmid. (e) Co-electroporation of a 5  $\mu$ g of isolated repair template proved toxic to T-cells and did not generate successful knock-in. (f) Infection of an impure AAV product at multiple MOIs (1E5, 1E6 and 1E7) did not successfully generate a knock-in in human T-cells. (g) Repair in Jurkat cells is only successful upon AAV infection one-hour post-electroporation. (h) AAV purity, measured by capsid protein band detection by SDS-PAGE revealed differences in knock-in capacity in human T-cells.

Supplementary Figure 3



**Supplementary Figure 3.** (a) CD3<sup>+</sup> enrichment prior to editing and expansion reveals pure T-cell population. (b) Electroporation of 3M T-cells with 2 μg of TRAC-targeting RNP shows comparable editing to 1M cells. (c) Plating unpurified edited T-cells at a cell density of 1M cells in a 6-well dish yields highest expansion rate.

Supplementary Figure 4



**Supplementary Figure 4.** Cytotoxicity assay of (a) Leuk10 and (b) Leuk12 edited T-cells in co-culture with BT935. (c) Cytotoxicity assay of HEK 293T with Leuk10 edited T-cells. Error bars represent standard error of the mean. \* $p \leq 0.05$ , \*\* $p \leq 0.001$ , \*\*\* $p \leq 0.0001$ ; \*\*\*\* $p \leq 0.00001$ ; multiple t-tests with Holm-Sidak correction.

## **CHAPTER 4: CONCLUSIONS AND FUTURE DIRECTIONS**

### **4.1 Discussion**

GBM is the most common primary malignant brain tumor in adults. Despite aggressive multi-modal treatment including surgery and chemoradiotherapy, GBM remains incurable. Poor prognosis and clinical outcome may be attributed to significant spatiotemporal ITH present at the genomic, epigenomic and transcriptomic levels. This may be attributed to a small population of chemo- and radio-resistant GSCs marked by the pentaspan glycoprotein CD133. The expression of CD133 has previously been shown to correlate with disease progression, metastasis, recurrence, and poor overall survival. Despite our understanding of its clinical and phenotypic outputs, little is currently known of the function of CD133, highlighting a pivotal gap in our understanding of GSC biology in current research.

To define the role of tumorigenic proteins, the study of PPIs and protein interaction networks in cancer presents as an avenue to define complex oncogenic phenotypes and processes, such as those associated with CD133. This led to the conception of the first project of this thesis, in which we aimed to interrogate the PPIs of CD133 by use of BioID. However, due to the current limitations of the use of BioID, we sought to use genetic engineering by CRISPR to generate an endogenously BioID-tagged CD133 in human GBMs.

While the biological function of CD133 has yet to be holistically defined, previous work from our lab has revealed that targeting GSCs by CD133 presents as a promising therapeutic strategy. In particular, the rational development of a CD133-targeting CAR-T

was able to eliminate tumor burden and significantly increase survival in our patient-derived models of human GBM (Vora et al., 2020). Even more so, we developed on the first patient-derived, pre-clinical models of “on-target, off-tumor effects” for antigens expressed also expressed in the human hematopoietic system (Salim et al., 2020).

However, as the next step in the path towards clinical development, CAR-T generation is currently limited as it is autologous, or patient-derived in nature. This presents a host of concerns including time to manufacturing, inconsistent products, and disease-related challenges such as qualitative and quantitative T-cell dysfunction. To circumvent these concerns, the use of allogeneic, or donor-derived CAR-Ts has begun to gain clinical traction for hematological malignancies. This thus led to the development of the second project, in which we sought to pre-clinically test the use of an allogeneic CD133 CAR-T in our model systems.

#### *4.1.1 Endogenous genomic knock-in of BioID*

In Chapter 2, we began to assess the use of an endogenous BioID system, in which we would knock-in a biotin ligase (miniTurboID) into the N- and C-terminus genomic loci of *PROM1*. We first assessed the array of CD133 expression in five patient-derived human GBM samples, in which we observed differential population-based expression, as well as localization (cell surface vs intracellular) by FACS analysis and immunoblotting of subcellular membranous and cytosolic fractions. Akin to previous literature, CD133 has previously been shown to localize cytoplasmically in plasma membrane-negative GBM cells (Brescia et al., 2013). An independent study previously showed that shuttling of CD133 may be dependent on environmental cues such as nutrient availability (Izumi et

al., 2019). However, these studies examined differences in CD133 cell-surface positivity from the same tumor specimens. Other studies have confirmed stable detection of CD133 lacking the epitope AC133 in GBM specimens, as observed in our patient-derived specimen BT241 (Campos et al., 2011). Though this study did not assess prognostic differences based on CD133 localization, cytoplasmic CD133 has been associated with poor outcome in hepatocellular carcinoma and clear renal cell carcinoma (Y. L. Chen et al., 2017; Saeednejad Zanjani et al., 2017). Alternatively, in other solid cancers such as triple negative breast cancer, hepatocellular carcinoma and colorectal adenocarcinoma, nuclear mislocalization of CD133 has been detected, and was associated with better overall prognosis (Cantile et al., 2013; Y. L. Chen et al., 2017; Y. M. Lee, Yeo, Seong, & Kim, 2018). These studies putatively highlight the array of CD133 function across cancers, and within GBM, and thus the need to develop a thorough understanding of its mechanism.

To edit GBM cells, we have assessed the use of a two-step strategy using electroporated RNP, followed by AAV-mediated delivery of an HDR template. Primary human cells such as patient-derived GBM specimens have been notoriously difficult to edit by conventional transfection methods. Though AAV has previously been used in GBM for CRISPR screening, we believe that we have shown the broader use of CRISPR technology and AAV infection as strategies for enabling PPI discovery (Chow et al., 2017). In working to generate an endogenous BioID-tagged CD133, we hope to characterize the utility of a biologically-relevant screening platform.

#### 4.1.2 *Generation of alloCART133 shows early pre-clinical efficacy*

In Chapter 3, we show the generation and pre-clinical validation of an allogeneic CAR-T product targeting CD133. Using a previously reported technique, we show that KiKo of CART133 at the endogenous TCR using CRISPR and AAV-mediated genomic engineering is a highly efficient technique in editing human T-cells (Dai et al., 2019). Of the work currently published on allogeneic CAR-Ts, some variability exists in locus of choice (*TRAC* or *TRBC* ( $\beta$  constant region)). In this work, targeting the *TRAC* was sufficient in knocking out the  $\alpha\beta$  TCR heterodimer. While targeting of the *TRBC* may present as an alternative strategy, a previous study found no differences in *TRAC* or *TRBC* knockout T-cells in expansion, specific lysis and T-cell phenotype (Torikai et al., 2012). Of more significance is the study of TCR KO on the development of GvHD. Interestingly, few studies in the literature have addressed the issue of GvHD and allorejection in pre-clinical models and primarily assessed in patients (Brudno et al., 2016; Y. Chen et al., 2017). In looking to studies on hematopoietic stem cell transplant, clinical manifestations of GvHD include hunched posture, reduced activity and weight loss. However, this may present as a challenge for use in cancer models as tumor-bearing mice show similar clinical symptoms (Jacus, Rahija, Davis, Throm, & Stewart, 2015). Thus, the need to develop a robust and reliable model system for evaluating and predicting clinical GvHD is still required.

Another consideration in the development of allogeneic CAR products that may be of more immunological significance is of allorejection or host elimination. To circumvent this issue, B<sub>2</sub>M has been targeted to knockout Class I MHC molecules to avoid host

rejection (X. Liu et al., 2017). However, this may mark allogeneic products for elimination by natural killer (NK) cells via “missing-self” induced lysis by binding of HLA-E to activating receptors such as CD94/NKG2C (Lauterbach, Wieten, Popeijus, Voorter, & Tilanus, 2015). However, B<sub>2</sub>M knock-out may be unnecessary in allogeneic CAR-Ts for intratumoral treatment as NK cells do not show high propensity for immune infiltration in the GBM TME (Yang, Han, Sughrue, Tihan, & Parsa, 2011). This however would require pre-clinical and clinical evaluation of sole TCR-KO allogeneic product persistence in the intracranial compartment. While the combined knock-outs in allogeneic products may require more thorough investigation, this work highlights the applicability of multiplexing. For instance, allogeneic CAR-Ts may benefit from combined knock-out of clinically relevant markers such as immune checkpoints including PD-1 (X. Wang et al., 2019), TIM-3 (Sakuishi et al., 2010), LAG-3 (Harris-Bookman et al., 2018), TIGIT (Lucca et al., 2020), MGAT3 (Ye et al., 2019), PDIA3 (Ye et al., 2019) and A2AR (Goswami et al., 2020). This may improve T-cell function in response to immunosuppressive factors in the TME, as CAR products for GBM have shown limited success in the clinic (Nabil Ahmed et al., 2015; Brown et al., 2016; O'Rourke et al., 2017).

#### **4.2 Future Directions**

To characterize the CD133 protein-protein interactome, we next plan to perform the miniTurboID integration in human GBM cells. In particular, we hope to perform these experiments in BT935 and BT241 to investigate PPIs associated with differential localization, and in human NSCs to interrogate disease-related PPIs. Upon integration, we

will validate tagging of BioID to CD133 by immunofluorescence, co-immunoprecipitation and western blotting to ensure appropriate localization and function. In addition, functional assays will be performed in comparison to wildtype cells to ensure that signalling and associated phenotypic output, namely sphere formation and proliferation, of CD133 is unaffected by tagging. Following validation of endogenous tagging, the BioID screen will be performed followed by proteomic analysis to identify putative PPIs, which will require subsequent validation by the aforementioned assays. While identification of PPIs presents opportunities for targeting, the primary goal of this study will be to describe novel CD133 PPIs in human GBM, as well as present the endogenous genomic knock-in of BioID as a validated discovery platform for use in primary cells.

To complete the pre-clinical assessment of alloCART133, we plan to extend assessment of *in vivo* efficacy to GBM8 as a biological replicate. We plan to collect survival data as well as differences in tumor burden for all *in vivo* cohorts to compare efficacy between CART133 and alloCART133. Upon defining pre-clinical efficacy, we will perform immunogenicity studies in immunocompetent mouse model of GBM. Using the chemically-induced mouse glioma line CT2A engineered to express human CD133, we will treat human T-cell products, including alloCART133 and CART133 to assess GvHD in mice. By treating intratumorally and intravenously by tail vein injection, we can additionally assess host elimination of CART133 and alloCART133 to define whether treatment modality can circumvent allorejection. By generating a robust gene editing

strategy in T-cells, we additionally hope to combine TCR-KO with the knock-out of other biologically relevant genes such as PD-1 to improve CAR efficacy in patients.

In conclusion, GBM presents an aggressive and incurable disease with poor patient prognosis. Using CD133 as a centralizing concept, the work of this thesis aimed to further our understanding of its role in GBM while optimizing targeting modalities against it. By working to uncover the mechanism(s) and interactions by which CD133 confers a tumorigenic phenotype, we hope to expand avenues for targeting and define its role in GBM. Simultaneously, by developing next-generation allogeneic immunotherapeutics, we hope to improve the accessibility of CAR-T therapy by use of “off-the-shelf” donor-derived products, while optimizing functionality with the aid of genomic editing to improve clinical outcomes in GBM.

## References

- Abd-Elghany, A. A., Naji, A. A., Alonazi, B., Aldosary, H., Alsufayan, M. A., Alnasser, M., . . . Mahmoud, M. Z. (2019). Radiological characteristics of glioblastoma multiforme using CT and MRI examination. *Journal of Radiation Research and Applied Sciences*, *12*(1), 289-293. doi:10.1080/16878507.2019.1655864
- Ahmed, N., Brawley, V., Hegde, M., Bielamowicz, K., Kalra, M., Landi, D., . . . Gottschalk, S. (2017). HER2-Specific Chimeric Antigen Receptor-Modified Virus-Specific T Cells for Progressive Glioblastoma: A Phase 1 Dose-Escalation Trial. *JAMA Oncol*, *3*(8), 1094-1101. doi:10.1001/jamaoncol.2017.0184
- Ahmed, N., Brawley, V., Hegde, M., Bielamowicz, K., Wakefield, A., Ghazi, A., . . . Hicks, J. (2015). Autologous HER2 CMV bispecific CAR T cells are safe and demonstrate clinical benefit for glioblastoma in a Phase I trial. *Journal for Immunotherapy of Cancer*, *3*(Suppl 2), O11-O11. doi:10.1186/2051-1426-3-S2-O11
- Alcantara Llaguno, S. R., Wang, Z., Sun, D., Chen, J., Xu, J., Kim, E., . . . Parada, L. F. (2015). Adult Lineage-Restricted CNS Progenitors Specify Distinct Glioblastoma Subtypes. *Cancer Cell*, *28*(4), 429-440. doi:10.1016/j.ccell.2015.09.007
- Aldape, K., Zadeh, G., Mansouri, S., Reifenberger, G., & von Deimling, A. (2015). Glioblastoma: pathology, molecular mechanisms and markers. *Acta Neuropathol*, *129*(6), 829-848. doi:10.1007/s00401-015-1432-1
- Alexander, B. M., & Cloughesy, T. F. (2017). Adult Glioblastoma. *Journal of Clinical Oncology*, *35*(21), 2402-2409. doi:10.1200/jco.2017.73.0119
- Arvanitis, C. D., Ferraro, G. B., & Jain, R. K. (2020). The blood-brain barrier and blood-tumour barrier in brain tumours and metastases. *Nat Rev Cancer*, *20*(1), 26-41. doi:10.1038/s41568-019-0205-x
- Bagley, S. J., Desai, A. S., Linette, G. P., June, C. H., & O'Rourke, D. M. (2018). CAR T-cell therapy for glioblastoma: recent clinical advances and future challenges. *Neuro Oncol*, *20*(11), 1429-1438. doi:10.1093/neuonc/noy032
- Bao, S., Wu, Q., Li, Z., Sathornsumetee, S., Wang, H., McLendon, R. E., . . . Rich, J. N. (2008). Targeting cancer stem cells through L1CAM suppresses glioma growth. *Cancer Res*, *68*(15), 6043-6048. doi:10.1158/0008-5472.CAN-08-1079
- Bao, S., Wu, Q., McLendon, R. E., Hao, Y., Shi, Q., Hjelmeland, A. B., . . . Rich, J. N. (2006). Glioma stem cells promote radioresistance by preferential activation of the DNA damage response. *Nature*, *444*(7120), 756-760. doi:10.1038/nature05236
- Barthel, F. P., Johnson, K. C., Varn, F. S., Moskalik, A. D., Tanner, G., Kocakavuk, E., . . . Consortium, G. (2019). Longitudinal molecular trajectories of diffuse glioma in adults. *Nature*, *576*(7785), 112-120. doi:10.1038/s41586-019-1775-1
- Bayik, D., Zhou, Y., Park, C., Hong, C., Vail, D., Silver, D. J., . . . Lathia, J. D. (2020). Myeloid-Derived Suppressor Cell Subsets Drive Glioblastoma Growth in a Sex-Specific Manner. *Cancer Discov*, *10*(8), 1210-1225. doi:10.1158/2159-8290.CD-19-1355
- Beier, D., Hau, P., Proescholdt, M., Lohmeier, A., Wischhusen, J., Oefner, P. J., . . . Beier, C. P. (2007). CD133(+) and CD133(-) glioblastoma-derived cancer stem

- cells show differential growth characteristics and molecular profiles. *Cancer Res*, 67(9), 4010-4015. doi:10.1158/0008-5472.CAN-06-4180
- Bielamowicz, K., Fousek, K., Byrd, T. T., Samaha, H., Mukherjee, M., Aware, N., . . . Ahmed, N. (2018). Trivalent CAR T cells overcome interpatient antigenic variability in glioblastoma. *Neuro Oncol*, 20(4), 506-518. doi:10.1093/neuonc/nox182
- Brennan, C. W., Verhaak, R. G., McKenna, A., Campos, B., Nounshmehr, H., Salama, S. R., . . . Network, T. R. (2013). The somatic genomic landscape of glioblastoma. *Cell*, 155(2), 462-477. doi:10.1016/j.cell.2013.09.034
- Brescia, P., Ortensi, B., Fornasari, L., Levi, D., Broggi, G., & Pelicci, G. (2013). CD133 is essential for glioblastoma stem cell maintenance. *Stem Cells*, 31(5), 857-869. doi:10.1002/stem.1317
- Brooks, W. H., Roszman, T. L., Mahaley, M. S., & Woosley, R. E. (1977). Immunobiology of primary intracranial tumours. II. Analysis of lymphocyte subpopulations in patients with primary brain tumours. *Clin Exp Immunol*, 29(1), 61-66. Retrieved from <https://www.ncbi.nlm.nih.gov/pubmed/330067>
- Brown, C. E., Alizadeh, D., Starr, R., Weng, L., Wagner, J. R., Naranjo, A., . . . Badie, B. (2016). Regression of Glioblastoma after Chimeric Antigen Receptor T-Cell Therapy. *N Engl J Med*, 375(26), 2561-2569. doi:10.1056/NEJMoa1610497
- Brown, C. E., Badie, B., Barish, M. E., Weng, L., Ostberg, J. R., Chang, W. C., . . . Jensen, M. C. (2015). Bioactivity and Safety of IL13Ralpha2-Redirected Chimeric Antigen Receptor CD8+ T Cells in Patients with Recurrent Glioblastoma. *Clin Cancer Res*, 21(18), 4062-4072. doi:10.1158/1078-0432.CCR-15-0428
- Brudno, J. N., & Kochenderfer, J. N. (2016). Toxicities of chimeric antigen receptor T cells: recognition and management. *Blood*, 127(26), 3321-3330. doi:10.1182/blood-2016-04-703751
- Brudno, J. N., Somerville, R. P., Shi, V., Rose, J. J., Halverson, D. C., Fowler, D. H., . . . Kochenderfer, J. N. (2016). Allogeneic T Cells That Express an Anti-CD19 Chimeric Antigen Receptor Induce Remissions of B-Cell Malignancies That Progress After Allogeneic Hematopoietic Stem-Cell Transplantation Without Causing Graft-Versus-Host Disease. *J Clin Oncol*, 34(10), 1112-1121. doi:10.1200/JCO.2015.64.5929
- Campos, B., Zeng, L., Daotrong, P. H., Eckstein, V., Unterberg, A., Mairbaur, H., & Herold-Mende, C. (2011). Expression and regulation of AC133 and CD133 in glioblastoma. *Glia*, 59(12), 1974-1986. doi:10.1002/glia.21239
- Cancer Genome Atlas Research, N. (2008). Comprehensive genomic characterization defines human glioblastoma genes and core pathways. *Nature*, 455(7216), 1061-1068. doi:10.1038/nature07385
- Cantile, M., Collina, F., D'Aiuto, M., Rinaldo, M., Pirozzi, G., Borsellino, C., . . . Di Bonito, M. (2013). Nuclear localization of cancer stem cell marker CD133 in triple-negative breast cancer: a case report. *Tumori*, 99(5), e245-250. doi:10.1700/1377.15325

- Capper, D., Jones, D. T. W., Sill, M., Hovestadt, V., Schrimpf, D., Sturm, D., . . . Pfister, S. M. (2018). DNA methylation-based classification of central nervous system tumours. *Nature*, *555*(7697), 469-474. doi:10.1038/nature26000
- Ceccarelli, M., Barthel, F. P., Malta, T. M., Sabedot, T. S., Salama, S. R., Murray, B. A., . . . Verhaak, R. G. (2016). Molecular Profiling Reveals Biologically Discrete Subsets and Pathways of Progression in Diffuse Glioma. *Cell*, *164*(3), 550-563. doi:10.1016/j.cell.2015.12.028
- Chamberlain, M. C. (2008). Bevacizumab plus irinotecan in recurrent glioblastoma. *J Clin Oncol*, *26*(6), 1012-1013; author reply 1013. doi:10.1200/JCO.2007.15.1605
- Chamberlain, M. C., & Raizer, J. (2009). Antiangiogenic therapy for high-grade gliomas. *CNS Neurol Disord Drug Targets*, *8*(3), 184-194. doi:10.2174/187152709788680706
- Chang, C. H., Horton, J., Schoenfeld, D., Salazer, O., Perez-Tamayo, R., Kramer, S., . . . Tsukada, Y. (1983). Comparison of postoperative radiotherapy and combined postoperative radiotherapy and chemotherapy in the multidisciplinary management of malignant gliomas. A joint Radiation Therapy Oncology Group and Eastern Cooperative Oncology Group study. *Cancer*, *52*(6), 997-1007. doi:10.1002/1097-0142(19830915)52:6<997::aid-cnrcr2820520612>3.0.co;2-2
- Chen, R., Nishimura, M. C., Bumbaca, S. M., Kharbanda, S., Forrest, W. F., Kasman, I. M., . . . Phillips, H. S. (2010). A hierarchy of self-renewing tumor-initiating cell types in glioblastoma. *Cancer Cell*, *17*(4), 362-375. doi:10.1016/j.ccr.2009.12.049
- Chen, Y., Cheng, Y., Suo, P., Yan, C., Wang, Y., Chen, Y., . . . Huang, X. (2017). Donor-derived CD19-targeted T cell infusion induces minimal residual disease-negative remission in relapsed B-cell acute lymphoblastic leukaemia with no response to donor lymphocyte infusions after haploidentical haematopoietic stem cell transplantation. *Br J Haematol*, *179*(4), 598-605. doi:10.1111/bjh.14923
- Chen, Y. L., Lin, P. Y., Ming, Y. Z., Huang, W. C., Chen, R. F., Chen, P. M., & Chu, P. Y. (2017). The effects of the location of cancer stem cell marker CD133 on the prognosis of hepatocellular carcinoma patients. *BMC Cancer*, *17*(1), 474. doi:10.1186/s12885-017-3460-9
- Choe, J. H., Watchmaker, P. B., Simic, M. S., Gilbert, R. D., Li, A. W., Krasnow, N. A., . . . Lim, W. A. (2021). SynNotch-CAR T cells overcome challenges of specificity, heterogeneity, and persistence in treating glioblastoma. *Sci Transl Med*, *13*(591). doi:10.1126/scitranslmed.abe7378
- Choi, B. D., Yu, X., Castano, A. P., Bouffard, A. A., Schmidts, A., Larson, R. C., . . . Maus, M. V. (2019). CAR-T cells secreting BiTEs circumvent antigen escape without detectable toxicity. *Nat Biotechnol*, *37*(9), 1049-1058. doi:10.1038/s41587-019-0192-1
- Choi, B. D., Yu, X., Castano, A. P., Darr, H., Henderson, D. B., Bouffard, A. A., . . . Maus, M. V. (2019). CRISPR-Cas9 disruption of PD-1 enhances activity of universal EGFRvIII CAR T cells in a preclinical model of human glioblastoma. *J Immunother Cancer*, *7*(1), 304. doi:10.1186/s40425-019-0806-7
- Chongsathidkiet, P., Jackson, C., Koyama, S., Loebel, F., Cui, X., Farber, S. H., . . . Fecci, P. E. (2018). Sequestration of T cells in bone marrow in the setting of

- glioblastoma and other intracranial tumors. *Nat Med*, 24(9), 1459-1468.  
doi:10.1038/s41591-018-0135-2
- Chow, R. D., Guzman, C. D., Wang, G., Schmidt, F., Youngblood, M. W., Ye, L., . . . Chen, S. (2017). AAV-mediated direct in vivo CRISPR screen identifies functional suppressors in glioblastoma. *Nat Neurosci*, 20(10), 1329-1341.  
doi:10.1038/nn.4620
- Colwell, N., Larion, M., Giles, A. J., Seldomridge, A. N., Sizdahkhani, S., Gilbert, M. R., & Park, D. M. (2017). Hypoxia in the glioblastoma microenvironment: shaping the phenotype of cancer stem-like cells. *Neuro Oncol*, 19(7), 887-896.  
doi:10.1093/neuonc/now258
- Corbeil, D., Joester, A., Fargeas, C. A., Jaszai, J., Garwood, J., Hellwig, A., . . . Huttner, W. B. (2009). Expression of distinct splice variants of the stem cell marker prominin-1 (CD133) in glial cells. *Glia*, 57(8), 860-874. doi:10.1002/glia.20812
- Couturier, C. P., Ayyadhury, S., Le, P. U., Nadaf, J., Monlong, J., Riva, G., . . . Petrecca, K. (2020). Single-cell RNA-seq reveals that glioblastoma recapitulates a normal neurodevelopmental hierarchy. *Nat Commun*, 11(1), 3406. doi:10.1038/s41467-020-17186-5
- Crespo, I., Vital, A. L., Nieto, A. B., Rebelo, O., Tao, H., Lopes, M. C., . . . Tabernero, M. D. (2011). Detailed characterization of alterations of chromosomes 7, 9, and 10 in glioblastomas as assessed by single-nucleotide polymorphism arrays. *J Mol Diagn*, 13(6), 634-647. doi:10.1016/j.jmoldx.2011.06.003
- Cugurra, A., Mamuladze, T., Rustenhoven, J., Dykstra, T., Beroshvili, G., Greenberg, Z. J., . . . Kipnis, J. (2021). Skull and vertebral bone marrow are myeloid cell reservoirs for the meninges and CNS parenchyma. *Science*, eabf7844.  
doi:10.1126/science.abf7844
- D'Alessio, A., Proietti, G., Sica, G., & Scicchitano, B. M. (2019). Pathological and Molecular Features of Glioblastoma and Its Peritumoral Tissue. *Cancers (Basel)*, 11(4). doi:10.3390/cancers11040469
- Dai, X., Park, J. J., Du, Y., Kim, H. R., Wang, G., Errami, Y., & Chen, S. (2019). One-step generation of modular CAR-T cells with AAV-Cpf1. *Nat Methods*, 16(3), 247-254. doi:10.1038/s41592-019-0329-7
- Dalerba, P., Cho, R. W., & Clarke, M. F. (2007). Cancer stem cells: models and concepts. *Annu Rev Med*, 58, 267-284. doi:10.1146/annurev.med.58.062105.204854
- Depil, S., Duchateau, P., Grupp, S. A., Mufti, G., & Poirot, L. (2020). 'Off-the-shelf' allogeneic CAR T cells: development and challenges. *Nat Rev Drug Discov*. doi:10.1038/s41573-019-0051-2
- Dix, A. R., Brooks, W. H., Roszman, T. L., & Morford, L. A. (1999). Immune defects observed in patients with primary malignant brain tumors. *J Neuroimmunol*, 100(1-2), 216-232. doi:10.1016/s0165-5728(99)00203-9
- Du, X. J., Li, X. M., Cai, L. B., Sun, J. C., Wang, S. Y., Wang, X. C., . . . Wu, S. X. (2019). Efficacy and safety of nimotuzumab in addition to radiotherapy and temozolomide for cerebral glioblastoma: a phase II multicenter clinical trial. *J Cancer*, 10(14), 3214-3223. doi:10.7150/jca.30123

- Eckel-Passow, J. E., Lachance, D. H., Molinaro, A. M., Walsh, K. M., Decker, P. A., Sicotte, H., . . . Jenkins, R. B. (2015). Glioma Groups Based on 1p/19q, IDH, and TERT Promoter Mutations in Tumors. *N Engl J Med*, *372*(26), 2499-2508. doi:10.1056/NEJMoa1407279
- Eyquem, J., Mansilla-Soto, J., Giavridis, T., van der Stegen, S. J., Hamieh, M., Cunanan, K. M., . . . Sadelain, M. (2017). Targeting a CAR to the TRAC locus with CRISPR/Cas9 enhances tumour rejection. *Nature*, *543*(7643), 113-117. doi:10.1038/nature21405
- Fargeas, C. A., Huttner, W. B., & Corbeil, D. (2007). Nomenclature of prominin-1 (CD133) splice variants - an update. *Tissue Antigens*, *69*(6), 602-606. doi:10.1111/j.1399-0039.2007.00825.x
- Fargeas, C. A., Joester, A., Missol-Kolka, E., Hellwig, A., Huttner, W. B., & Corbeil, D. (2004). Identification of novel Prominin-1/CD133 splice variants with alternative C-termini and their expression in epididymis and testis. *J Cell Sci*, *117*(Pt 18), 4301-4311. doi:10.1242/jcs.01315
- Fernandes, C., Costa, A., Osorio, L., Lago, R. C., Linhares, P., Carvalho, B., & Caeiro, C. (2017). Current Standards of Care in Glioblastoma Therapy. In S. De Vleeschouwer (Ed.), *Glioblastoma*. Brisbane (AU).
- Fodde, R., & Brabletz, T. (2007). Wnt/beta-catenin signaling in cancer stemness and malignant behavior. *Curr Opin Cell Biol*, *19*(2), 150-158. doi:10.1016/j.ceb.2007.02.007
- Fraietta, J. A., Lacey, S. F., Orlando, E. J., Pruteanu-Malinici, I., Gohil, M., Lundh, S., . . . Melenhorst, J. J. (2018). Determinants of response and resistance to CD19 chimeric antigen receptor (CAR) T cell therapy of chronic lymphocytic leukemia. *Nat Med*, *24*(5), 563-571. doi:10.1038/s41591-018-0010-1
- Francis, J. M., Zhang, C. Z., Maire, C. L., Jung, J., Manzo, V. E., Adalsteinsson, V. A., . . . Ligon, K. L. (2014). EGFR variant heterogeneity in glioblastoma resolved through single-nucleus sequencing. *Cancer Discov*, *4*(8), 956-971. doi:10.1158/2159-8290.CD-13-0879
- Freije, W. A., Castro-Vargas, F. E., Fang, Z., Horvath, S., Cloughesy, T., Liao, L. M., . . . Nelson, S. F. (2004). Gene expression profiling of gliomas strongly predicts survival. *Cancer Res*, *64*(18), 6503-6510. doi:10.1158/0008-5472.CAN-04-0452
- Friedman, H. S., Prados, M. D., Wen, P. Y., Mikkelsen, T., Schiff, D., Abrey, L. E., . . . Cloughesy, T. (2009). Bevacizumab alone and in combination with irinotecan in recurrent glioblastoma. *J Clin Oncol*, *27*(28), 4733-4740. doi:10.1200/JCO.2008.19.8721
- Friedmann-Morvinski, D., Bushong, E. A., Ke, E., Soda, Y., Marumoto, T., Singer, O., . . . Verma, I. M. (2012). Dedifferentiation of neurons and astrocytes by oncogenes can induce gliomas in mice. *Science*, *338*(6110), 1080-1084. doi:10.1126/science.1226929
- Galli, R., Binda, E., Orfanelli, U., Cipelletti, B., Gritti, A., De Vitis, S., . . . Vescovi, A. (2004). Isolation and characterization of tumorigenic, stem-like neural precursors from human glioblastoma. *Cancer Res*, *64*(19), 7011-7021. doi:10.1158/0008-5472.CAN-04-1364

- Gangoso, E., Southgate, B., Bradley, L., Rus, S., Galvez-Cancino, F., McGivern, N., . . . Pollard, S. M. (2021). Glioblastomas acquire myeloid-affiliated transcriptional programs via epigenetic immunoeediting to elicit immune evasion. *Cell*, *184*(9), 2454-2470 e2426. doi:10.1016/j.cell.2021.03.023
- Gibson, T. J., Seiler, M., & Veitia, R. A. (2013). The transience of transient overexpression. *Nat Methods*, *10*(8), 715-721. doi:10.1038/nmeth.2534
- Gopisetty, G., Xu, J., Sampath, D., Colman, H., & Puduvalli, V. K. (2013). Epigenetic regulation of CD133/PROM1 expression in glioma stem cells by Sp1/myc and promoter methylation. *Oncogene*, *32*(26), 3119-3129. doi:10.1038/onc.2012.331
- Gorsi, H. S., Khanna, P. C., Tumblin, M., Yeh-Nayre, L., Milburn, M., Elster, J. D., & Crawford, J. R. (2018). Single-agent bevacizumab in the treatment of recurrent or refractory pediatric low-grade glioma: A single institutional experience. *Pediatr Blood Cancer*, *65*(9), e27234. doi:10.1002/pbc.27234
- Goswami, S., Walle, T., Cornish, A. E., Basu, S., Anandhan, S., Fernandez, I., . . . Sharma, P. (2020). Immune profiling of human tumors identifies CD73 as a combinatorial target in glioblastoma. *Nat Med*, *26*(1), 39-46. doi:10.1038/s41591-019-0694-x
- Green, S. B., Byar, D. P., Walker, M. D., Pistenmaa, D. A., Alexander, E., Jr., Batzdorf, U., . . . Strike, T. A. (1983). Comparisons of carmustine, procarbazine, and high-dose methylprednisolone as additions to surgery and radiotherapy for the treatment of malignant glioma. *Cancer Treat Rep*, *67*(2), 121-132.
- Grossman, S. A., O'Neill, A., Grunnet, M., Mehta, M., Pearlman, J. L., Wagner, H., . . . Eastern Cooperative Oncology, G. (2003). Phase III study comparing three cycles of infusional carmustine and cisplatin followed by radiation therapy with radiation therapy and concurrent carmustine in patients with newly diagnosed supratentorial glioblastoma multiforme: Eastern Cooperative Oncology Group Trial 2394. *J Clin Oncol*, *21*(8), 1485-1491. doi:10.1200/JCO.2003.10.035
- Grossman, S. A., Ye, X., Lesser, G., Sloan, A., Carraway, H., Desideri, S., . . . Consortium, N. C. (2011). Immunosuppression in patients with high-grade gliomas treated with radiation and temozolomide. *Clin Cancer Res*, *17*(16), 5473-5480. doi:10.1158/1078-0432.CCR-11-0774
- Gupta, A., & Dwivedi, T. (2017). A Simplified Overview of World Health Organization Classification Update of Central Nervous System Tumors 2016. *J Neurosci Rural Pract*, *8*(4), 629-641. doi:10.4103/jnrp.jnrp\_168\_17
- Gwynne, W. D., Shakeel, M. S., Girgis-Gabardo, A., Kim, K. H., Ford, E., Dvorkin-Gheva, A., . . . Hassell, J. A. (2020). Antagonists of the serotonin receptor 5A target human breast tumor initiating cells. *BMC Cancer*, *20*(1), 724. doi:10.1186/s12885-020-07193-6
- Hara, T., Chanoch-Myers, R., Mathewson, N. D., Myskiw, C., Atta, L., Bussema, L., . . . Tirosh, I. (2021). Interactions between cancer cells and immune cells drive transitions to mesenchymal-like states in glioblastoma. *Cancer Cell*. doi:<https://doi.org/10.1016/j.ccell.2021.05.002>
- Harris-Bookman, S., Mathios, D., Martin, A. M., Xia, Y., Kim, E., Xu, H., . . . Lim, M. (2018). Expression of LAG-3 and efficacy of combination treatment with anti-

- LAG-3 and anti-PD-1 monoclonal antibodies in glioblastoma. *Int J Cancer*, 143(12), 3201-3208. doi:10.1002/ijc.31661
- Hassaneen, W., Levine, N. B., Suki, D., Salaskar, A. L., de Moura Lima, A., McCutcheon, I. E., . . . Sawaya, R. (2011). Multiple craniotomies in the management of multifocal and multicentric glioblastoma. Clinical article. *J Neurosurg*, 114(3), 576-584. doi:10.3171/2010.6.JNS091326
- Hasselbalch, B., Lassen, U., Hansen, S., Holmberg, M., Sorensen, M., Kosteljanetz, M., . . . Poulsen, H. S. (2010). Cetuximab, bevacizumab, and irinotecan for patients with primary glioblastoma and progression after radiation therapy and temozolomide: a phase II trial. *Neuro Oncol*, 12(5), 508-516. doi:10.1093/neuonc/nop063
- Hau, E., Shen, H., Clark, C., Graham, P. H., Koh, E. S., & K, L. M. (2016). The evolving roles and controversies of radiotherapy in the treatment of glioblastoma. *J Med Radiat Sci*, 63(2), 114-123. doi:10.1002/jmrs.149
- Hegi, M. E., Diserens, A. C., Gorlia, T., Hamou, M. F., de Tribolet, N., Weller, M., . . . Stupp, R. (2005). MGMT gene silencing and benefit from temozolomide in glioblastoma. *N Engl J Med*, 352(10), 997-1003. doi:10.1056/NEJMoa043331
- Heimberger, A. B., Hlatky, R., Suki, D., Yang, D., Weinberg, J., Gilbert, M., . . . Aldape, K. (2005). Prognostic effect of epidermal growth factor receptor and EGFRvIII in glioblastoma multiforme patients. *Clin Cancer Res*, 11(4), 1462-1466. doi:10.1158/1078-0432.CCR-04-1737
- Huang, J., Liu, F., Liu, Z., Tang, H., Wu, H., Gong, Q., & Chen, J. (2017). Immune Checkpoint in Glioblastoma: Promising and Challenging. *Front Pharmacol*, 8, 242. doi:10.3389/fphar.2017.00242
- Huang, M., Zhang, D., Wu, J. Y., Xing, K., Yeo, E., Li, C., . . . Fan, Y. (2020). Wnt-mediated endothelial transformation into mesenchymal stem cell-like cells induces chemoresistance in glioblastoma. *Sci Transl Med*, 12(532). doi:10.1126/scitranslmed.aay7522
- Ito, H., Nakashima, H., & Chiocca, E. A. (2019). Molecular responses to immune checkpoint blockade in glioblastoma. *Nat Med*, 25(3), 359-361. doi:10.1038/s41591-019-0385-7
- Izumi, H., Li, Y., Shibaki, M., Mori, D., Yasunami, M., Sato, S., . . . Nakagawara, A. (2019). Recycling endosomal CD133 functions as an inhibitor of autophagy at the pericentrosomal region. *Sci Rep*, 9(1), 2236. doi:10.1038/s41598-019-39229-8
- Jacques, T. S., Swales, A., Brzozowski, M. J., Henriquez, N. V., Linehan, J. M., Mirzadeh, Z., . . . Brandner, S. (2010). Combinations of genetic mutations in the adult neural stem cell compartment determine brain tumour phenotypes. *EMBO J*, 29(1), 222-235. doi:10.1038/emboj.2009.327
- Jacus, M. O., Rahija, R. J., Davis, A. D., Thom, S. L., & Stewart, C. F. (2015). Observational Evaluations of Mice during Cerebral Microdialysis for Pediatric Brain Tumor Research. *J Am Assoc Lab Anim Sci*, 54(3), 304-310. Retrieved from <https://www.ncbi.nlm.nih.gov/pubmed/26045457>

- Johnson, B. E., Mazor, T., Hong, C., Barnes, M., Aihara, K., McLean, C. Y., . . . Costello, J. F. (2014). Mutational analysis reveals the origin and therapy-driven evolution of recurrent glioma. *Science*, *343*(6167), 189-193. doi:10.1126/science.1239947
- Jones, P. A., & Baylin, S. B. (2007). The epigenomics of cancer. *Cell*, *128*(4), 683-692. doi:10.1016/j.cell.2007.01.029
- Joo, K. M., Kim, S. Y., Jin, X., Song, S. Y., Kong, D. S., Lee, J. I., . . . Nam, D. H. (2008). Clinical and biological implications of CD133-positive and CD133-negative cells in glioblastomas. *Lab Invest*, *88*(8), 808-815. doi:10.1038/labinvest.2008.57
- Kania, G., Corbeil, D., Fuchs, J., Tarasov, K. V., Blyszczuk, P., Huttner, W. B., . . . Wobus, A. M. (2005). Somatic stem cell marker prominin-1/CD133 is expressed in embryonic stem cell-derived progenitors. *Stem Cells*, *23*(6), 791-804. doi:10.1634/stemcells.2004-0232
- Kim, D. I., & Roux, K. J. (2016). Filling the Void: Proximity-Based Labeling of Proteins in Living Cells. *Trends Cell Biol*, *26*(11), 804-817. doi:10.1016/j.tcb.2016.09.004
- Kim, H., Zheng, S., Amini, S. S., Virk, S. M., Mikkelsen, T., Brat, D. J., . . . Verhaak, R. G. (2015). Whole-genome and multisector exome sequencing of primary and post-treatment glioblastoma reveals patterns of tumor evolution. *Genome Res*, *25*(3), 316-327. doi:10.1101/gr.180612.114
- Kim, J., Lee, I. H., Cho, H. J., Park, C. K., Jung, Y. S., Kim, Y., . . . Nam, D. H. (2015). Spatiotemporal Evolution of the Primary Glioblastoma Genome. *Cancer Cell*, *28*(3), 318-328. doi:10.1016/j.ccell.2015.07.013
- Kwoczek, J., Riese, S. B., Tischer, S., Bak, S., Lahrberg, J., Oelke, M., . . . Eiz-Vesper, B. (2018). Cord blood-derived T cells allow the generation of a more naive tumor-reactive cytotoxic T-cell phenotype. *Transfusion*, *58*(1), 88-99. doi:10.1111/trf.14365
- Labun, K., Montague, T. G., Krause, M., Torres Cleuren, Y. N., Tjeldnes, H., & Valen, E. (2019). CHOPCHOP v3: expanding the CRISPR web toolbox beyond genome editing. *Nucleic Acids Res*, *47*(W1), W171-W174. doi:10.1093/nar/gkz365
- Lan, X., Jorg, D. J., Cavalli, F. M. G., Richards, L. M., Nguyen, L. V., Vanner, R. J., . . . Dirks, P. B. (2017). Fate mapping of human glioblastoma reveals an invariant stem cell hierarchy. *Nature*, *549*(7671), 227-232. doi:10.1038/nature23666
- Lapidot, T., Sirard, C., Vormoor, J., Murdoch, B., Hoang, T., Caceres-Cortes, J., . . . Dick, J. E. (1994). A cell initiating human acute myeloid leukaemia after transplantation into SCID mice. *Nature*, *367*(6464), 645-648. doi:10.1038/367645a0
- Lathia, J. D., Gallagher, J., Heddleston, J. M., Wang, J., Eyler, C. E., Macswords, J., . . . Rich, J. N. (2010). Integrin alpha 6 regulates glioblastoma stem cells. *Cell Stem Cell*, *6*(5), 421-432. doi:10.1016/j.stem.2010.02.018
- Lauterbach, N., Wieten, L., Popeijus, H. E., Voorter, C. E., & Tilanus, M. G. (2015). HLA-E regulates NKG2C+ natural killer cell function through presentation of a restricted peptide repertoire. *Hum Immunol*, *76*(8), 578-586. doi:10.1016/j.humimm.2015.09.003

- Lee, J. H., Lee, J. E., Kahng, J. Y., Kim, S. H., Park, J. S., Yoon, S. J., . . . Lee, J. H. (2018). Human glioblastoma arises from subventricular zone cells with low-level driver mutations. *Nature*, *560*(7717), 243-247. doi:10.1038/s41586-018-0389-3
- Lee, M. Y., Ryu, J. M., Lee, S. H., Park, J. H., & Han, H. J. (2010). Lipid rafts play an important role for maintenance of embryonic stem cell self-renewal. *J Lipid Res*, *51*(8), 2082-2089. doi:10.1194/jlr.M001545
- Lee, Y. M., Yeo, M. K., Seong, I. O., & Kim, K. H. (2018). Nuclear Expression of CD133 Is Associated with Good Prognosis in Patients with Colorectal Adenocarcinoma. *Anticancer Res*, *38*(8), 4819-4826. doi:10.21873/anticancerres.12792
- Li, Z., Ivanov, A. A., Su, R., Gonzalez-Pecchi, V., Qi, Q., Liu, S., . . . Fu, H. (2017). The OncoPPi network of cancer-focused protein-protein interactions to inform biological insights and therapeutic strategies. *Nat Commun*, *8*, 14356. doi:10.1038/ncomms14356
- Li, Z., Liu, G., Tong, Y., Zhang, M., Xu, Y., Qin, L., . . . He, J. (2015). Comprehensive analysis of the T-cell receptor beta chain gene in rhesus monkey by high throughput sequencing. *Sci Rep*, *5*, 10092. doi:10.1038/srep10092
- Lim, M., Ye, X., Piotrowski, A. F., Desai, A. S., Ahluwalia, M. S., Walbert, T., . . . Grossman, S. A. (2020). Updated safety phase I trial of anti-LAG-3 alone and in combination with anti-PD-1 in patients with recurrent GBM. *Journal of Clinical Oncology*, *38*(15\_suppl), 2512-2512. doi:10.1200/JCO.2020.38.15\_suppl.2512
- Liu, C., Sage, J. C., Miller, M. R., Verhaak, R. G., Hippenmeyer, S., Vogel, H., . . . Zong, H. (2011). Mosaic analysis with double markers reveals tumor cell of origin in glioma. *Cell*, *146*(2), 209-221. doi:10.1016/j.cell.2011.06.014
- Liu, G., Yuan, X., Zeng, Z., Tunici, P., Ng, H., Abdulkadir, I. R., . . . Yu, J. S. (2006). Analysis of gene expression and chemoresistance of CD133+ cancer stem cells in glioblastoma. *Mol Cancer*, *5*, 67. doi:10.1186/1476-4598-5-67
- Liu, P., Cheng, H., Roberts, T. M., & Zhao, J. J. (2009). Targeting the phosphoinositide 3-kinase pathway in cancer. *Nat Rev Drug Discov*, *8*(8), 627-644. doi:10.1038/nrd2926
- Liu, X., Zhang, Y., Cheng, C., Cheng, A. W., Zhang, X., Li, N., . . . Wang, H. (2017). CRISPR-Cas9-mediated multiplex gene editing in CAR-T cells. *Cell Res*, *27*(1), 154-157. doi:10.1038/cr.2016.142
- Liu, Z., Han, H., He, X., Li, S., Wu, C., Yu, C., & Wang, S. (2016). Expression of the galectin-9-Tim-3 pathway in glioma tissues is associated with the clinical manifestations of glioma. *Oncol Lett*, *11*(3), 1829-1834. doi:10.3892/ol.2016.4142
- Lombardi, G., Barresi, V., Indraccolo, S., Simbolo, M., Fassan, M., Mandruzato, S., . . . Zagonel, V. (2020). Pembrolizumab Activity in Recurrent High-Grade Gliomas with Partial or Complete Loss of Mismatch Repair Protein Expression: A Monocentric, Observational and Prospective Pilot Study. *Cancers (Basel)*, *12*(8). doi:10.3390/cancers12082283
- Lombardi, G., Pambuku, A., Bellu, L., Farina, M., Della Puppa, A., Denaro, L., & Zagonel, V. (2017). Effectiveness of antiangiogenic drugs in glioblastoma

- patients: A systematic review and meta-analysis of randomized clinical trials. *Crit Rev Oncol Hematol*, 111, 94-102. doi:10.1016/j.critrevonc.2017.01.018
- Long, A. H., Haso, W. M., Shern, J. F., Wanhainen, K. M., Murgai, M., Ingaramo, M., . . . Mackall, C. L. (2015). 4-1BB costimulation ameliorates T cell exhaustion induced by tonic signaling of chimeric antigen receptors. *Nat Med*, 21(6), 581-590. doi:10.1038/nm.3838
- Loregian, A., & Palu, G. (2005). Disruption of protein-protein interactions: towards new targets for chemotherapy. *J Cell Physiol*, 204(3), 750-762. doi:10.1002/jcp.20356
- Louis, D. N., Ohgaki, H., Wiestler, O. D., Cavenee, W. K., Burger, P. C., Jouvet, A., . . . Kleihues, P. (2007). The 2007 WHO classification of tumours of the central nervous system. *Acta Neuropathol*, 114(2), 97-109. doi:10.1007/s00401-007-0243-4
- Louis, D. N., Perry, A., Reifenberger, G., von Deimling, A., Figarella-Branger, D., Cavenee, W. K., . . . Ellison, D. W. (2016). The 2016 World Health Organization Classification of Tumors of the Central Nervous System: a summary. *Acta Neuropathologica*, 131(6), 803-820. doi:10.1007/s00401-016-1545-1
- Louis, D. N., Perry, A., Wesseling, P., Brat, D. J., Cree, I. A., Figarella-Branger, D., . . . Ellison, D. W. (2021). The 2021 WHO Classification of Tumors of the Central Nervous System: a summary. *Neuro Oncol*. doi:10.1093/neuonc/noab106
- Louveau, A., Smirnov, I., Keyes, T. J., Eccles, J. D., Rouhani, S. J., Peske, J. D., . . . Kipnis, J. (2015). Structural and functional features of central nervous system lymphatic vessels. *Nature*, 523(7560), 337-341. doi:10.1038/nature14432
- Lu, H., Zhou, Q., He, J., Jiang, Z., Peng, C., Tong, R., & Shi, J. (2020). Recent advances in the development of protein-protein interactions modulators: mechanisms and clinical trials. *Signal Transduct Target Ther*, 5(1), 213. doi:10.1038/s41392-020-00315-3
- Lu, V. M., Akinduro, O. O., & Daniels, D. J. (2020). H3K27M mutation in adult cerebellar glioblastoma. *J Clin Neurosci*, 71, 316-317. doi:10.1016/j.jocn.2019.11.016
- Lucca, L. E., Lerner, B. A., Park, C., DeBartolo, D., Harnett, B., Kumar, V. P., . . . Pitt, D. (2020). Differential expression of the T-cell inhibitor TIGIT in glioblastoma and MS. *Neurol Neuroimmunol Neuroinflamm*, 7(3). doi:10.1212/NXI.0000000000000712
- Lynn, R. C., Weber, E. W., Sotillo, E., Gennert, D., Xu, P., Good, Z., . . . Mackall, C. L. (2019). c-Jun overexpression in CAR T cells induces exhaustion resistance. *Nature*, 576(7786), 293-300. doi:10.1038/s41586-019-1805-z
- MacLeod G, Bozek DA, Rajakulendran N, Monteiro V, Ahmadi M, Steinhart Z, Kushida MM, . . . , Angers S. (2019) Genome-Wide CRISPR-Cas9 Screens Expose Genetic Vulnerabilities and Mechanisms of Temozolomide Sensitivity in Glioblastoma Stem Cells. *Cell Rep*, 27(3):971-986.e9. doi: 10.1016/j.celrep.2019.03.047.
- Mak, A. B., Nixon, A. M., Kittanakom, S., Stewart, J. M., Chen, G. I., Curak, J., . . . Moffat, J. (2012). Regulation of CD133 by HDAC6 promotes beta-catenin

- signaling to suppress cancer cell differentiation. *Cell Rep*, 2(4), 951-963.  
doi:10.1016/j.celrep.2012.09.016
- Mak, A.B., Pehar, M., Nixon, A.M., Williams, R.A., Uetrecht, A.C., Puglielli, L., Moffat, J. (2014). Post-translational regulation of CD133 by ATase1/ATase2-mediated lysine acetylation. *J Mol Biol*, 426(11):2175-82. doi: 10.1016/j.jmb.2014.02.012.
- Manoranjan, B., Chokshi, C., Venugopal, C., Subapanditha, M., Savage, N., Tatari, N., . . . Singh, S. K. (2020). A CD133-AKT-Wnt signaling axis drives glioblastoma brain tumor-initiating cells. *Oncogene*, 39(7), 1590-1599. doi:10.1038/s41388-019-1086-x
- Mateo, C., Moreno, E., Amour, K., Lombardero, J., Harris, W., & Pérez, R. (1997). Humanization of a mouse monoclonal antibody that blocks the epidermal growth factor receptor: recovery of antagonistic activity. *Immunotechnology*, 3(1), 71-81. doi:10.1016/s1380-2933(97)00065-1
- Maude, S. L., Teachey, D. T., Porter, D. L., & Grupp, S. A. (2015). CD19-targeted chimeric antigen receptor T-cell therapy for acute lymphoblastic leukemia. *Blood*, 125(26), 4017-4023. doi:10.1182/blood-2014-12-580068
- Maw, M. A., Corbeil, D., Koch, J., Hellwig, A., Wilson-Wheeler, J. C., Bridges, R. J., . . . Röper, K. (2000). A frameshift mutation in prominin (mouse)-like 1 causes human retinal degeneration. *Human molecular genetics*, 9(1), 27-34.
- May, D. G., & Roux, K. J. (2019). BioID: A Method to Generate a History of Protein Associations. *Methods Mol Biol*, 2008, 83-95. doi:10.1007/978-1-4939-9537-0\_7
- Meyer, M., Reimand, J., Lan, X., Head, R., Zhu, X., Kushida, M., . . . Dirks, P. B. (2015). Single cell-derived clonal analysis of human glioblastoma links functional and genomic heterogeneity. *Proc Natl Acad Sci U S A*, 112(3), 851-856. doi:10.1073/pnas.1320611111
- Migliorini, D., Dietrich, P. Y., Stupp, R., Linette, G. P., Posey, A. D., Jr., & June, C. H. (2018). CAR T-Cell Therapies in Glioblastoma: A First Look. *Clin Cancer Res*, 24(3), 535-540. doi:10.1158/1078-0432.CCR-17-2871
- Miller, A. M., Shah, R. H., Pentsova, E. I., Pourmaleki, M., Briggs, S., Distefano, N., . . . Mellinghoff, I. K. (2019). Tracking tumour evolution in glioma through liquid biopsies of cerebrospinal fluid. *Nature*, 565(7741), 654-658. doi:10.1038/s41586-019-0882-3
- Miraglia, S., Godfrey, W., Yin, A. H., Atkins, K., Warnke, R., Holden, J. T., . . . Buck, D. W. (1997). A novel five-transmembrane hematopoietic stem cell antigen: isolation, characterization, and molecular cloning. *Blood*, 90(12), 5013-5021. Retrieved from <https://www.ncbi.nlm.nih.gov/pubmed/9389721>
- Mirchia, K., & Richardson, T. E. (2020). Beyond IDH-Mutation: Emerging Molecular Diagnostic and Prognostic Features in Adult Diffuse Gliomas. *Cancers (Basel)*, 12(7). doi:10.3390/cancers12071817
- Mirzaei, R., Sarkar, S., & Yong, V. W. (2017). T Cell Exhaustion in Glioblastoma: Intricacies of Immune Checkpoints. *Trends Immunol*, 38(2), 104-115. doi:10.1016/j.it.2016.11.005

- Mohanty, R., Chowdhury, C. R., Arega, S., Sen, P., Ganguly, P., & Ganguly, N. (2019). CAR T cell therapy: A new era for cancer treatment (Review). *Oncol Rep*, *42*(6), 2183-2195. doi:10.3892/or.2019.7335
- Mohme, M., Schliffke, S., Maire, C. L., Runger, A., Glau, L., Mende, K. C., . . . Lamszus, K. (2018). Immunophenotyping of Newly Diagnosed and Recurrent Glioblastoma Defines Distinct Immune Exhaustion Profiles in Peripheral and Tumor-infiltrating Lymphocytes. *Clin Cancer Res*, *24*(17), 4187-4200. doi:10.1158/1078-0432.CCR-17-2617
- Monteiro, A. R., Hill, R., Pilkington, G. J., & Madureira, P. A. (2017). The Role of Hypoxia in Glioblastoma Invasion. *Cells*, *6*(4). doi:10.3390/cells6040045
- Moreira, S., Seo, C., Gordon, V., Xing, S., Wu, R., Polena, E., . . . Doble, B. W. (2018). Endogenous BioID elucidates TCF7L1 interactome modulation upon GSK-3 inhibition in mouse ESCs. *bioRxiv*, 431023. doi:10.1101/431023
- Neftel, C., Laffy, J., Filbin, M. G., Hara, T., Shore, M. E., Rahme, G. J., . . . Suva, M. L. (2019). An Integrative Model of Cellular States, Plasticity, and Genetics for Glioblastoma. *Cell*, *178*(4), 835-849 e821. doi:10.1016/j.cell.2019.06.024
- Noushmehr, H., Weisenberger, D. J., Diefes, K., Phillips, H. S., Pujara, K., Berman, B. P., . . . Cancer Genome Atlas Research, N. (2010). Identification of a CpG island methylator phenotype that defines a distinct subgroup of glioma. *Cancer Cell*, *17*(5), 510-522. doi:10.1016/j.ccr.2010.03.017
- O'Donnell, J. S., Teng, M. W. L., & Smyth, M. J. (2019). Cancer immunoediting and resistance to T cell-based immunotherapy. *Nat Rev Clin Oncol*, *16*(3), 151-167. doi:10.1038/s41571-018-0142-8
- O'Rourke, D. M., Nasrallah, M. P., Desai, A., Melenhorst, J. J., Mansfield, K., Morrisette, J. J. D., . . . Maus, M. V. (2017). A single dose of peripherally infused EGFRvIII-directed CAR T cells mediates antigen loss and induces adaptive resistance in patients with recurrent glioblastoma. *Sci Transl Med*, *9*(399). doi:10.1126/scitranslmed.aaa0984
- Ochocka, N., Segit, P., Walentynowicz, K. A., Wojnicki, K., Cyranowski, S., Swatler, J., . . . Kaminska, B. (2021). Single-cell RNA sequencing reveals functional heterogeneity of glioma-associated brain macrophages. *Nat Commun*, *12*(1), 1151. doi:10.1038/s41467-021-21407-w
- Ogden, A. T., Waziri, A. E., Lochhead, R. A., Fusco, D., Lopez, K., Ellis, J. A., . . . Bruce, J. N. (2008). Identification of A2B5+CD133- tumor-initiating cells in adult human gliomas. *Neurosurgery*, *62*(2), 505-514; discussion 514-505. doi:10.1227/01.neu.0000316019.28421.95
- Ohgaki, H., Dessen, P., Jourde, B., Horstmann, S., Nishikawa, T., Di Patre, P. L., . . . Kleihues, P. (2004). Genetic pathways to glioblastoma: a population-based study. *Cancer Res*, *64*(19), 6892-6899. doi:10.1158/0008-5472.CAN-04-1337
- Ohgaki, H., & Kleihues, P. (2013). The definition of primary and secondary glioblastoma. *Clin Cancer Res*, *19*(4), 764-772. doi:10.1158/1078-0432.CCR-12-3002
- Okada, Y., Hurwitz, E. E., Esposito, J. M., Brower, M. A., Nutt, C. L., & Louis, D. N. (2003). Selection pressures of TP53 mutation and microenvironmental location influence epidermal growth factor receptor gene amplification in human

- glioblastomas. *Cancer Res*, 63(2), 413-416. Retrieved from <https://www.ncbi.nlm.nih.gov/pubmed/12543796>
- Ostrom, Q. T., Patil, N., Cioffi, G., Waite, K., Kruchko, C., & Barnholtz-Sloan, J. S. (2020). CBTRUS Statistical Report: Primary Brain and Other Central Nervous System Tumors Diagnosed in the United States in 2013-2017. *Neuro Oncol*, 22(12 Suppl 2), iv1-iv96. doi:10.1093/neuonc/noaa200
- Ott, M., Tomaszowski, K. H., Marisetty, A., Kong, L. Y., Wei, J., Duna, M., . . . Heimberger, A. B. (2020). Profiling of patients with glioma reveals the dominant immunosuppressive axis is refractory to immune function restoration. *JCI Insight*, 5(17). doi:10.1172/jci.insight.134386
- Ozdemir-Kaynak, E., Qutub, A. A., & Yesil-Celiktas, O. (2018). Advances in Glioblastoma Multiforme Treatment: New Models for Nanoparticle Therapy. *Front Physiol*, 9, 170. doi:10.3389/fphys.2018.00170
- Pardoll, D. M. (2012). The blockade of immune checkpoints in cancer immunotherapy. *Nat Rev Cancer*, 12(4), 252-264. doi:10.1038/nrc3239
- Parsons, D. W., Jones, S., Zhang, X., Lin, J. C., Leary, R. J., Angenendt, P., . . . Kinzler, K. W. (2008). An integrated genomic analysis of human glioblastoma multiforme. *Science*, 321(5897), 1807-1812. doi:10.1126/science.1164382
- Patel, A. P., Tirosh, I., Trombetta, J. J., Shalek, A. K., Gillespie, S. M., Wakimoto, H., . . . Bernstein, B. E. (2014). Single-cell RNA-seq highlights intratumoral heterogeneity in primary glioblastoma. *Science*, 344(6190), 1396-1401. doi:10.1126/science.1254257
- Patil, C. G., Yi, A., Elramsisy, A., Hu, J., Mukherjee, D., Irvin, D. K., . . . Nuno, M. (2012). Prognosis of patients with multifocal glioblastoma: a case-control study. *J Neurosurg*, 117(4), 705-711. doi:10.3171/2012.7.JNS12147
- Phillips, H. S., Kharbanda, S., Chen, R., Forrester, W. F., Soriano, R. H., Wu, T. D., . . . Aldape, K. (2006). Molecular subclasses of high-grade glioma predict prognosis, delineate a pattern of disease progression, and resemble stages in neurogenesis. *Cancer Cell*, 9(3), 157-173. doi:10.1016/j.ccr.2006.02.019
- Prager, B. C., Bhargava, S., Mahadev, V., Hubert, C. G., & Rich, J. N. (2020). Glioblastoma Stem Cells: Driving Resilience through Chaos. *Trends Cancer*, 6(3), 223-235. doi:10.1016/j.trecan.2020.01.009
- Puchalski, R. B., Shah, N., Miller, J., Dalley, R., Nomura, S. R., Yoon, J. G., . . . Foltz, G. D. (2018). An anatomic transcriptional atlas of human glioblastoma. *Science*, 360(6389), 660-663. doi:10.1126/science.aaf2666
- Qazi, M. A., Vora, P., Venugopal, C., Sidhu, S. S., Moffat, J., Swanton, C., & Singh, S. K. (2017). Intratumoral heterogeneity: pathways to treatment resistance and relapse in human glioblastoma. *Ann Oncol*, 28(7), 1448-1456. doi:10.1093/annonc/mdx169
- Ravi, V. M., Will, P., Kueckelhaus, J., Sun, N., Joseph, K., Salié, H., . . . Heiland, D. H. (2021). Spatiotemporal heterogeneity of glioblastoma is dictated by microenvironmental interference. *bioRxiv*, 2021.2002.2016.431475. doi:10.1101/2021.02.16.431475

- Razavi, S. M., Lee, K. E., Jin, B. E., Aujla, P. S., Gholamin, S., & Li, G. (2016). Immune Evasion Strategies of Glioblastoma. *Front Surg*, *3*, 11. doi:10.3389/fsurg.2016.00011
- Reardon, D. A., Brandes, A. A., Omuro, A., Mulholland, P., Lim, M., Wick, A., . . . Weller, M. (2020). Effect of Nivolumab vs Bevacizumab in Patients With Recurrent Glioblastoma: The CheckMate 143 Phase 3 Randomized Clinical Trial. *JAMA Oncol*, *6*(7), 1003-1010. doi:10.1001/jamaoncol.2020.1024
- Rees, J. H., Smirniotopoulos, J. G., Jones, R. V., & Wong, K. (1996). Glioblastoma multiforme: radiologic-pathologic correlation. *Radiographics*, *16*(6), 1413-1438; quiz 1462-1413. doi:10.1148/radiographics.16.6.8946545
- Reinartz, R., Wang, S., Kebir, S., Silver, D. J., Wieland, A., Zheng, T., . . . Scheffler, B. (2017). Functional Subclone Profiling for Prediction of Treatment-Induced Intratumor Population Shifts and Discovery of Rational Drug Combinations in Human Glioblastoma. *Clin Cancer Res*, *23*(2), 562-574. doi:10.1158/1078-0432.CCR-15-2089
- Ren, J., Liu, X., Fang, C., Jiang, S., June, C. H., & Zhao, Y. (2017). Multiplex Genome Editing to Generate Universal CAR T Cells Resistant to PD1 Inhibition. *Clin Cancer Res*, *23*(9), 2255-2266. doi:10.1158/1078-0432.CCR-16-1300
- Reynolds, B. A., & Weiss, S. (1992). Generation of neurons and astrocytes from isolated cells of the adult mammalian central nervous system. *Science*, *255*(5052), 1707-1710. doi:10.1126/science.1553558
- Ricci-Vitiani, L., Pallini, R., Biffoni, M., Todaro, M., Invernici, G., Cenci, T., . . . De Maria, R. (2010). Tumour vascularization via endothelial differentiation of glioblastoma stem-like cells. *Nature*, *468*(7325), 824-828. doi:10.1038/nature09557
- Richards, L. M., Whitley, O. K. N., MacLeod, G., Cavalli, F. M. G., Coutinho, F. J., Jaramillo, J. E., . . . Pugh, T. J. (2021). Gradient of Developmental and Injury Response transcriptional states defines functional vulnerabilities underpinning glioblastoma heterogeneity. *Nature Cancer*, *2*(2), 157-173. doi:10.1038/s43018-020-00154-9
- Rigbolt, K. T., Prokhorova, T. A., Akimov, V., Henningsen, J., Johansen, P. T., Kratchmarova, I., . . . Blagoev, B. (2011). System-wide temporal characterization of the proteome and phosphoproteome of human embryonic stem cell differentiation. *Sci Signal*, *4*(164), rs3. doi:10.1126/scisignal.2001570
- Saeednejad Zanjani, L., Madjd, Z., Abolhasani, M., Andersson, Y., Rasti, A., Shariftabrizi, A., & Asgari, M. (2017). Cytoplasmic expression of CD133 stemness marker is associated with tumor aggressiveness in clear cell renal cell carcinoma. *Exp Mol Pathol*, *103*(2), 218-228. doi:10.1016/j.yexmp.2017.10.001
- Sahebjam, S., Forsyth, P. A., Tran, N. D., Arrington, J. A., Macaulay, R., Etame, A. B., . . . Yu, H. M. (2021). Hypofractionated stereotactic re-irradiation with pembrolizumab and bevacizumab in patients with recurrent high-grade gliomas: results from a phase I study. *Neuro Oncol*, *23*(4), 677-686. doi:10.1093/neuonc/noaa260

- Sakuishi, K., Apetoh, L., Sullivan, J. M., Blazar, B. R., Kuchroo, V. K., & Anderson, A. C. (2010). Targeting Tim-3 and PD-1 pathways to reverse T cell exhaustion and restore anti-tumor immunity. *J Exp Med*, *207*(10), 2187-2194. doi:10.1084/jem.20100643
- Salim, S. K., Xu, J., Wong, N., Venugopal, C., Hope, K. J., & Singh, S. K. (2020). Assessing the Safety of a Cell-Based Immunotherapy for Brain Cancers Using a Humanized Model of Hematopoiesis. *STAR Protocols*, *1*(3), 100124. doi:<https://doi.org/10.1016/j.xpro.2020.100124>
- Sanai, N., Polley, M. Y., McDermott, M. W., Parsa, A. T., & Berger, M. S. (2011). An extent of resection threshold for newly diagnosed glioblastomas. *J Neurosurg*, *115*(1), 3-8. doi:10.3171/2011.2.JNS10998
- Sanli, A. M., Turkoglu, E., Dolgun, H., & Sekerci, Z. (2010). Unusual manifestations of primary Glioblastoma Multiforme: A report of three cases. *Surg Neurol Int*, *1*, 87. doi:10.4103/2152-7806.74146
- Shapiro, W. R., Green, S. B., Burger, P. C., Mahaley, M. S., Jr., Selker, R. G., VanGilder, J. C., . . . et al. (1989). Randomized trial of three chemotherapy regimens and two radiotherapy regimens and two radiotherapy regimens in postoperative treatment of malignant glioma. Brain Tumor Cooperative Group Trial 8001. *J Neurosurg*, *71*(1), 1-9. doi:10.3171/jns.1989.71.1.0001
- Sheng, K. L., Kang, L., Pridham, K. J., Dunkenberger, L. E., Sheng, Z., & Varghese, R. T. (2020). An integrated approach to biomarker discovery reveals gene signatures highly predictive of cancer progression. *Sci Rep*, *10*(1), 21246. doi:10.1038/s41598-020-78126-3
- Shiromizu, C. M., & Jancic, C. C. (2018). gammadelta T Lymphocytes: An Effector Cell in Autoimmunity and Infection. *Front Immunol*, *9*, 2389. doi:10.3389/fimmu.2018.02389
- Shlush, L. I., Zandi, S., Mitchell, A., Chen, W. C., Brandwein, J. M., Gupta, V., . . . Dick, J. E. (2014). Identification of pre-leukaemic haematopoietic stem cells in acute leukaemia. *Nature*, *506*(7488), 328-333. doi:10.1038/nature13038
- Shmelkov, S. V., Jun, L., St Clair, R., McGarrigle, D., Derderian, C. A., Usenko, J. K., . . . Rafii, S. (2004). Alternative promoters regulate transcription of the gene that encodes stem cell surface protein AC133. *Blood*, *103*(6), 2055-2061. doi:10.1182/blood-2003-06-1881
- Singh, D., Chan, J. M., Zoppoli, P., Niola, F., Sullivan, R., Castano, A., . . . Iavarone, A. (2012). Transforming fusions of FGFR and TACC genes in human glioblastoma. *Science*, *337*(6099), 1231-1235. doi:10.1126/science.1220834
- Singh, S. K., Clarke, I. D., Terasaki, M., Bonn, V. E., Hawkins, C., Squire, J., & Dirks, P. B. (2003). Identification of a cancer stem cell in human brain tumors. *Cancer Res*, *63*(18), 5821-5828. Retrieved from <https://www.ncbi.nlm.nih.gov/pubmed/14522905>
- Singh, S. K., Hawkins, C., Clarke, I. D., Squire, J. A., Bayani, J., Hide, T., . . . Dirks, P. B. (2004). Identification of human brain tumour initiating cells. *Nature*, *432*(7015), 396-401. doi:10.1038/nature03128

- Skaga, E., Kuleskiy, E., Fayzullin, A., Sandberg, C. J., Potdar, S., Kyttala, A., . . . Vik-Mo, E. O. (2019). Intertumoral heterogeneity in patient-specific drug sensitivities in treatment-naive glioblastoma. *BMC Cancer*, *19*(1), 628. doi:10.1186/s12885-019-5861-4
- Snuderl, M., Fazlollahi, L., Le, L. P., Nitta, M., Zhelyazkova, B. H., Davidson, C. J., . . . Iafrate, A. J. (2011). Mosaic amplification of multiple receptor tyrosine kinase genes in glioblastoma. *Cancer Cell*, *20*(6), 810-817. doi:10.1016/j.ccr.2011.11.005
- Sompallae, R., Hofmann, O., Maher, C. A., Gedye, C., Behren, A., Vitezic, M., . . . Hide, W. (2013). A comprehensive promoter landscape identifies a novel promoter for CD133 in restricted tissues, cancers, and stem cells. *Front Genet*, *4*, 209. doi:10.3389/fgene.2013.00209
- Son, M. J., Woolard, K., Nam, D. H., Lee, J., & Fine, H. A. (2009). SSEA-1 is an enrichment marker for tumor-initiating cells in human glioblastoma. *Cell Stem Cell*, *4*(5), 440-452. doi:10.1016/j.stem.2009.03.003
- Sottoriva, A., Spiteri, I., Piccirillo, S. G., Touloumis, A., Collins, V. P., Marioni, J. C., . . . Tavaré, S. (2013). Intratumor heterogeneity in human glioblastoma reflects cancer evolutionary dynamics. *Proc Natl Acad Sci U S A*, *110*(10), 4009-4014. doi:10.1073/pnas.1219747110
- Sousa, F., Moura, R. P., Moreira, E., Martins, C., & Sarmiento, B. (2018). Therapeutic Monoclonal Antibodies Delivery for the Glioblastoma Treatment. *Adv Protein Chem Struct Biol*, *112*, 61-80. doi:10.1016/bs.apcsb.2018.03.001
- Stadtmauer, E. A., Fraietta, J. A., Davis, M. M., Cohen, A. D., Weber, K. L., Lancaster, E., . . . June, C. H. (2020). CRISPR-engineered T cells in patients with refractory cancer. *Science*, *367*(6481). doi:10.1126/science.aba7365
- Stenger, D., Stief, T. A., Kaeuferle, T., Willier, S., Rataj, F., Schober, K., . . . Feuchtinger, T. (2020). Endogenous TCR promotes in vivo persistence of CD19-CAR-T cells compared to a CRISPR/Cas9-mediated TCR knockout CAR. *Blood*, *136*(12), 1407-1418. doi:10.1182/blood.2020005185
- Stommel, J. M., Kimmelman, A. C., Ying, H., Nabioullin, R., Ponugoti, A. H., Wiedemeyer, R., . . . DePinho, R. A. (2007). Coactivation of receptor tyrosine kinases affects the response of tumor cells to targeted therapies. *Science*, *318*(5848), 287-290. doi:10.1126/science.1142946
- Stupp, R., Dietrich, P. Y., Ostermann Kraljevic, S., Pica, A., Maillard, I., Maeder, P., . . . Leyvraz, S. (2002). Promising survival for patients with newly diagnosed glioblastoma multiforme treated with concomitant radiation plus temozolomide followed by adjuvant temozolomide. *J Clin Oncol*, *20*(5), 1375-1382. doi:10.1200/JCO.2002.20.5.1375
- Stupp, R., Mason, W. P., van den Bent, M. J., Weller, M., Fisher, B., Taphoorn, M. J., . . . National Cancer Institute of Canada Clinical Trials, G. (2005). Radiotherapy plus concomitant and adjuvant temozolomide for glioblastoma. *N Engl J Med*, *352*(10), 987-996. doi:10.1056/NEJMoa043330
- Stupp, R., Taillibert, S., Kanner, A., Read, W., Steinberg, D., Lhermitte, B., . . . Ram, Z. (2017). Effect of Tumor-Treating Fields Plus Maintenance Temozolomide vs

- Maintenance Temozolomide Alone on Survival in Patients With Glioblastoma: A Randomized Clinical Trial. *JAMA*, 318(23), 2306-2316.  
doi:10.1001/jama.2017.18718
- Sturm, D., Witt, H., Hovestadt, V., Khuong-Quang, D. A., Jones, D. T., Konermann, C., . . . Pfister, S. M. (2012). Hotspot mutations in H3F3A and IDH1 define distinct epigenetic and biological subgroups of glioblastoma. *Cancer Cell*, 22(4), 425-437.  
doi:10.1016/j.ccr.2012.08.024
- Suva, M. L., Rheinbay, E., Gillespie, S. M., Patel, A. P., Wakimoto, H., Rabkin, S. D., . . . Bernstein, B. E. (2014). Reconstructing and reprogramming the tumor-propagating potential of glioblastoma stem-like cells. *Cell*, 157(3), 580-594.  
doi:10.1016/j.cell.2014.02.030
- Tabu, K., Sasai, K., Kimura, T., Wang, L., Aoyanagi, E., Kohsaka, S., . . . Tanaka, S. (2008). Promoter hypomethylation regulates CD133 expression in human gliomas. *Cell Res*, 18(10), 1037-1046. doi:10.1038/cr.2008.270
- Torikai, H., Reik, A., Liu, P. Q., Zhou, Y., Zhang, L., Maiti, S., . . . Cooper, L. J. (2012). A foundation for universal T-cell based immunotherapy: T cells engineered to express a CD19-specific chimeric-antigen-receptor and eliminate expression of endogenous TCR. *Blood*, 119(24), 5697-5705. doi:10.1182/blood-2012-01-405365
- Touat, M., Li, Y. Y., Boynton, A. N., Spurr, L. F., Iorgulescu, J. B., Bohrsen, C. L., . . . Ligon, K. L. (2020). Mechanisms and therapeutic implications of hypermutation in gliomas. *Nature*, 580(7804), 517-523. doi:10.1038/s41586-020-2209-9
- Uchida, N., Buck, D. W., He, D., Reitsma, M. J., Masek, M., Phan, T. V., . . . Weissman, I. L. (2000). Direct isolation of human central nervous system stem cells. *Proc Natl Acad Sci U S A*, 97(26), 14720-14725. doi:10.1073/pnas.97.26.14720
- Vandemoortele, G., De Sutter, D., Moliere, A., Pauwels, J., Gevaert, K., & Eyckerman, S. (2019). A Well-Controlled BioID Design for Endogenous Bait Proteins. *J Proteome Res*, 18(1), 95-106. doi:10.1021/acs.jproteome.8b00367
- Varnaite, R., & MacNeill, S. A. (2016). Meet the neighbors: Mapping local protein interactomes by proximity-dependent labeling with BioID. *Proteomics*, 16(19), 2503-2518. doi:10.1002/pmic.201600123
- Venerando, A., Girardi, C., Ruzzene, M., & Pinna, L. A. (2013). Pyrvinium pamoate does not activate protein kinase CK1, but promotes Akt/PKB down-regulation and GSK3 activation. *Biochem J*, 452(1), 131-137. doi:10.1042/BJ20121140
- Venugopal, C., Hallett, R., Vora, P., Manoranjan, B., Mahendram, S., Qazi, M. A., . . . Singh, S. K. (2015). Pyrvinium Targets CD133 in Human Glioblastoma Brain Tumor-Initiating Cells. *Clin Cancer Res*, 21(23), 5324-5337. doi:10.1158/1078-0432.CCR-14-3147
- Verhaak, R. G., Hoadley, K. A., Purdom, E., Wang, V., Qi, Y., Wilkerson, M. D., . . . Cancer Genome Atlas Research, N. (2010). Integrated genomic analysis identifies clinically relevant subtypes of glioblastoma characterized by abnormalities in PDGFRA, IDH1, EGFR, and NF1. *Cancer Cell*, 17(1), 98-110.  
doi:10.1016/j.ccr.2009.12.020

- Vigneswaran, K., Neill, S., & Hadjipanayis, C. G. (2015). Beyond the World Health Organization grading of infiltrating gliomas: advances in the molecular genetics of glioma classification. *Ann Transl Med*, 3(7), 95. doi:10.3978/j.issn.2305-5839.2015.03.57
- Vora, P., Venugopal, C., Salim, S. K., Tatari, N., Bakhshinyan, D., Singh, M., . . . Singh, S. (2020). The Rational Development of CD133-Targeting Immunotherapies for Glioblastoma. *Cell Stem Cell*, 26(6), 832-844 e836. doi:10.1016/j.stem.2020.04.008
- Wang, H., Zhou, H., Xu, J., Lu, Y., Ji, X., Yao, Y., . . . Wan, J. (2021). Different T-cell subsets in glioblastoma multiforme and targeted immunotherapy. *Cancer Lett*, 496, 134-143. doi:10.1016/j.canlet.2020.09.028
- Wang, J., Cazzato, E., Ladewig, E., Frattini, V., Rosenbloom, D. I., Zairis, S., . . . Rabadan, R. (2016). Clonal evolution of glioblastoma under therapy. *Nat Genet*, 48(7), 768-776. doi:10.1038/ng.3590
- Wang, J., Sanmamed, M. F., Datar, I., Su, T. T., Ji, L., Sun, J., . . . Chen, L. (2019). Fibrinogen-like Protein 1 Is a Major Immune Inhibitory Ligand of LAG-3. *Cell*, 176(1-2), 334-347 e312. doi:10.1016/j.cell.2018.11.010
- Wang, Q., Hu, B., Hu, X., Kim, H., Squatrito, M., Scarpace, L., . . . Verhaak, R. G. W. (2017). Tumor Evolution of Glioma-Intrinsic Gene Expression Subtypes Associates with Immunological Changes in the Microenvironment. *Cancer Cell*, 32(1), 42-56 e46. doi:10.1016/j.ccell.2017.06.003
- Wang, X., Guo, G., Guan, H., Yu, Y., Lu, J., & Yu, J. (2019). Challenges and potential of PD-1/PD-L1 checkpoint blockade immunotherapy for glioblastoma. *J Exp Clin Cancer Res*, 38(1), 87. doi:10.1186/s13046-019-1085-3
- Wangaryattawanich, P., Hatami, M., Wang, J., Thomas, G., Flanders, A., Kirby, J., . . . Colen, R. R. (2015). Multicenter imaging outcomes study of The Cancer Genome Atlas glioblastoma patient cohort: imaging predictors of overall and progression-free survival. *Neuro Oncol*, 17(11), 1525-1537. doi:10.1093/neuonc/nov117
- Webber, B. R., Lonetree, C. L., Kluesner, M. G., Johnson, M. J., Pomeroy, E. J., Diers, M. D., . . . Moriarity, B. S. (2019). Highly efficient multiplex human T cell engineering without double-strand breaks using Cas9 base editors. *Nat Commun*, 10(1), 5222. doi:10.1038/s41467-019-13007-6
- Wei, Y., Jiang, Y., Zou, F., Liu, Y., Wang, S., Xu, N., . . . Jiang, J. (2013). Activation of PI3K/Akt pathway by CD133-p85 interaction promotes tumorigenic capacity of glioma stem cells. *Proc Natl Acad Sci U S A*, 110(17), 6829-6834. doi:10.1073/pnas.1217002110
- Wick, W., Weller, M., van den Bent, M., Sanson, M., Weiler, M., von Deimling, A., . . . Reifenberger, G. (2014). MGMT testing--the challenges for biomarker-based glioma treatment. *Nat Rev Neurol*, 10(7), 372-385. doi:10.1038/nrneurol.2014.100
- Willingham, S. B., Volkmer, J. P., Gentles, A. J., Sahoo, D., Dalerba, P., Mitra, S. S., . . . Weissman, I. L. (2012). The CD47-signal regulatory protein alpha (SIRPα) interaction is a therapeutic target for human solid tumors. *Proc Natl Acad Sci U S A*, 109(17), 6662-6667. doi:10.1073/pnas.1121623109

- Woroniecka, K., Chongsathidkiet, P., Rhodin, K., Kemeny, H., Dechant, C., Farber, S. H., . . . Fecci, P. E. (2018). T-Cell Exhaustion Signatures Vary with Tumor Type and Are Severe in Glioblastoma. *Clin Cancer Res*, *24*(17), 4175-4186. doi:10.1158/1078-0432.CCR-17-1846
- Woroniecka, K. I., Rhodin, K. E., Chongsathidkiet, P., Keith, K. A., & Fecci, P. E. (2018). T-cell Dysfunction in Glioblastoma: Applying a New Framework. *Clin Cancer Res*, *24*(16), 3792-3802. doi:10.1158/1078-0432.CCR-18-0047
- Yamazaki, S., Iwama, A., Takayanagi, S., Morita, Y., Eto, K., Ema, H., & Nakauchi, H. (2006). Cytokine signals modulated via lipid rafts mimic niche signals and induce hibernation in hematopoietic stem cells. *EMBO J*, *25*(15), 3515-3523. doi:10.1038/sj.emboj.7601236
- Yan, H., Parsons, D. W., Jin, G., McLendon, R., Rasheed, B. A., Yuan, W., . . . Bigner, D. D. (2009). IDH1 and IDH2 mutations in gliomas. *N Engl J Med*, *360*(8), 765-773. doi:10.1056/NEJMoa0808710
- Yan, X., Ma, L., Yi, D., Yoon, J. G., Diercks, A., Foltz, G., . . . Tian, Q. (2011). A CD133-related gene expression signature identifies an aggressive glioblastoma subtype with excessive mutations. *Proc Natl Acad Sci U S A*, *108*(4), 1591-1596. doi:10.1073/pnas.1018696108
- Yang, I., Han, S. J., Sughrue, M. E., Tihan, T., & Parsa, A. T. (2011). Immune cell infiltrate differences in pilocytic astrocytoma and glioblastoma: evidence of distinct immunological microenvironments that reflect tumor biology. *J Neurosurg*, *115*(3), 505-511. doi:10.3171/2011.4.JNS101172
- Ye, L., Park, J. J., Dong, M. B., Yang, Q., Chow, R. D., Peng, L., . . . Chen, S. (2019). In vivo CRISPR screening in CD8 T cells with AAV-Sleeping Beauty hybrid vectors identifies membrane targets for improving immunotherapy for glioblastoma. *Nat Biotechnol*, *37*(11), 1302-1313. doi:10.1038/s41587-019-0246-4
- Young, R. M., Jamshidi, A., Davis, G., & Sherman, J. H. (2015). Current trends in the surgical management and treatment of adult glioblastoma. *Ann Transl Med*, *3*(9), 121. doi:10.3978/j.issn.2305-5839.2015.05.10
- Zeng, J., See, A. P., Phallen, J., Jackson, C. M., Belcaid, Z., Ruzevick, J., . . . Lim, M. (2013). Anti-PD-1 blockade and stereotactic radiation produce long-term survival in mice with intracranial gliomas. *Int J Radiat Oncol Biol Phys*, *86*(2), 343-349. doi:10.1016/j.ijrobp.2012.12.025
- Zeppernick, F., Ahmadi, R., Campos, B., Dictus, C., Helmke, B. M., Becker, N., . . . Herold-Mende, C. C. (2008). Stem cell marker CD133 affects clinical outcome in glioma patients. *Clin Cancer Res*, *14*(1), 123-129. doi:10.1158/1078-0432.CCR-07-0932
- Zhang, J., Stevens, M. F., & Bradshaw, T. D. (2012). Temozolomide: mechanisms of action, repair and resistance. *Curr Mol Pharmacol*, *5*(1), 102-114. doi:10.2174/1874467211205010102
- Zhang, Y., Cruickshanks, N., Pahuski, M., Yuan, F., Dutta, A., Schiff, D., . . . Abounader, R. (2017). Noncoding RNAs in Glioblastoma. In S. De Vleeschouwer (Ed.), *Glioblastoma*. Brisbane (AU).

Zou, C., Zhao, P., Xiao, Z., Han, X., Fu, F., & Fu, L. (2017). gammadelta T cells in cancer immunotherapy. *Oncotarget*, 8(5), 8900-8909.  
doi:10.18632/oncotarget.13051

## Appendix: Academic Achievements

### Published Works

1. Vora P, Venugopal C, **Salim SK**, Tatari N, Bakhshinyan D, Singh M, Seyfrid M, Upreti D, Rentas S, Wong N, Williams R, Qazi MA, Chokshi C, Ding A, Subapanditha MK, Savage N, Mahendram S, Ford E, Adile AA, McKenna D, McFarlane N, Huynh V, Wylie RG, Pan J, Bramson J, Hope K, Moffat J, Singh SK. (2020). The rational development of CD133-targeting immunotherapies for glioblastoma. *Cell Stem Cell* S1934-5909, 30147-30148.
2. Bakhshinyan D, Savage N, **Salim, SK**, Venugopal, C, & Singh SK. (2021). The Strange Case of Jekyll and Hyde: Parallels Between Neural Stem Cells and Glioblastoma-Initiating Cells. *Frontiers in oncology*, 10, 603738. <https://doi.org/10.3389/fonc.2020.603738>
3. Tatari N, Maich WT, **Salim SK**, Mckenna D, Venugopal C, Singh SK (2020). Preclinical Testing of CAR T Cells in a Patient-Derived Xenograft Model of Glioblastoma. *STAR Protocols*, 1(3):100174. doi: 10.1016/j.xpro.2020.100174.
4. **Salim SK**, Xu J, Wong N, Venugopal C, Hope KJ, Singh S (2020)K. Assessing the Safety of a Cell-Based Immunotherapy for Brain Cancers Using a Humanized Model of Hematopoiesis. *STAR Protocols*, 1(3):100124. doi: 10.1016/j.xpro.2020.100124.

### Published Book Chapters

1. **Salim SK**, Savage N, Maich W, Venugopal C, Singh SK (2021). Intratumoral heterogeneity associated with glioblastoma drug response and resistance. Glioblastoma Resistance to Chemotherapy: Molecular Mechanisms and Innovative Reversal Strategies. *Elsevier. In Press*.

### Manuscripts Under Review and In Preparation

1. Qazi MA, **Salim SK**, Brown KR, Savage N, Mickolajewicz N, Han H, Subapanditha MK, Bakhshinyan D, Nixon A, Vora P, Desmond K, Chokshi C, Singh M, Khoo A, Macklin A, Tatari N, Winegarden N, Richards L, Pugh T, Bock N, Mansouri A, Venugopal C, Kislinger T, Goyal S, Moffat J, Singh SK. (2021) Characterization of the minimal residual disease state reveals distinct evolutionary trajectories of human glioblastoma. *Manuscript in Preparation*
2. Chokshi C, Brakel BA, Tatari N, Savage N, **Salim SK**, Venugopal C, Singh SK. Advances in immunotherapy for adult glioblastoma. *Under Review at Cancers*.

3. Seyfrid, M., Maich, W., Shaikh, M., Tatari, N., Upreti, D., Piyasena, D., Subapanditha, M., Savage, N., McKenna, D., Kuhlmann, L., Khoo, A., **Salim, S.**, Basse-archibong, B., Gwynne, W., Chokshi, C., Brown, K., Murtaza, N., Bakhshinyan, D., Vora, P., Venugopal, C., Moffat, J. & Singh, SK. (2021) Hitting more birds with one stone: CD70 as an actionable immunotherapeutic target in recurrent glioblastoma. *bioRxiv*, 2021.2006.2002.446670. *Under Review at Journal for ImmunoTherapy of Cancer*.

#### **Scientific Meetings: Oral Presentations (\*Presenter)**

1. **Salim SK\***, Wei J, Dimitrov V, Chen K, Venugopal C, Vora P, Moffat J, Singh SK (2020). Systematic Generation of Allogeneic Immune-targeting Modalities for Glioblastoma. New York Academy of Sciences' Frontiers in Immunotherapy.

#### **Scientific Meetings: Poster Presentations**

1. **Salim SK**, Wei J, Dimitrov V, Chen K, Venugopal C, Vora P, Moffat J, Singh SK (2020). Systematic Generation of Allogeneic Immune-targeting Modalities for Glioblastoma. American Association for Cancer Research AACR Virtual Special Conference on Tumor Immunology and Immunotherapy.
2. **Salim SK**, Wei J, Dimitrov V, Chen K, Venugopal C, Vora P, Moffat J, Singh SK (2020). Systematic Generation of Allogeneic Immune-targeting Modalities for Glioblastoma. Biochemistry and Biomedical Sciences Research Symposium.
3. **Salim SK**, Wei J, Gwynne WD, Ford E, Maich WT, Venugopal C, Moffat J, Singh SK (2021). **Deciphering protein-protein interactions by** endogenous tagging of CD133. Biochemistry and Biomedical Sciences Research Symposium.

#### **Scholarships & Awards**

1. **MITACS Accelerate** (\$26,000)  
McMaster University, 2019-2020
2. **BioCanRx Summit for Cancer Immunotherapy, Runner-up Oral Presentation**  
Victoria, BC, 2019
3. **BioCanRx Summit for Cancer Immunotherapy, Travel Award** (\$1200)  
Victoria, BC, 2019
4. **Biochemistry and Biomedical Sciences, Travel Award** (\$500)

McMaster University, 2019

5. **Canada Graduate Scholarships-Master's (CGS-M)**(\$17,500)  
McMaster University, 2020-2021
6. **Biochemistry Entrance Scholarship** (\$1000)  
McMaster University, 2019
7. **Biochemistry and Biomedical Sciences Research Symposium, Top Poster Prize**  
McMaster University, 2021

### Coverage

1. “Humanizing” preclinical toxicity studies: A novel approach to assessing the safety of brain tumour-targeted immunotherapies. OICR The Rising Stars Quarterly (2021), by Rebecca Burchett. <https://mailchi.mp/5181daa5c317/rising-stars-quarterly-star-mentors-patient-partners-and-tumour-targeting-radioligands-4578776>

### Scholarly Activities

1. *Session Co-Chair*, Session 2B: Driving the commercialization the translation and commercialization of cancer innovations in Ontario  
OICR Translational Research Conference, 2021
2. *Terry Fox Research Institute New Frontiers Grant*, 2020 (Secondary to Dr. Sheila K. Singh)
3. *Nature Communications* Research Article, 2020 (Secondary to Dr. Sheila K. Singh)
4. *Cell Stem Cell* Research Article, 2020 (Secondary to Dr. Sheila K. Singh)